1-1-2011

The impact of folate deficiency on the base excision repair pathway: Analysis of enzyme coordination in response to dna damage and imbalanced repair

Amanda Pilling
Wayne State University,

THE IMPACT OF FOLATE DEFICIENCY ON THE BASE EXCISION REPAIR PATHWAY: ANALYSIS OF ENZYME COORDINATION IN RESPONSE TO DNA DAMAGE AND IMBALANCED REPAIR

by

AMANDA B. PILLING

DISSERTATION

Submitted to the Graduate School

of Wayne State University,

Detroit, MI

in partial fulfillment of the requirements

for the degree of

DOCTOR OF PHILOSOPHY

2011

MAJOR: NUTRITION AND FOOD SCIENCE

Approved by:

_____

Advisor   Date

_____

_____

_____

DEDICATION

This manuscript is dedicated in loving honor of my parents

whose solid foundation and continued encouragement

gives me the strength to pursue greatness.

ACKNOWLEDGEMENTS

My first and most earnest acknowledgement goes to my PhD advisor and committee chair, Dr. Ahmad R. Heydari. Through his mentoring and insight I learned the fundamentals of research and how to effectively communicate results. Invaluable were his patience and compassion during the challenges of my graduate career, which made it possible to be where I am today.

Many thanks to my committee members Drs. Diane Cabelof, Kequan Zhou, and Malathy Shekhar who provided me with new concepts and ideas to explore in my project. Sincere acknowledgement to former lab mate and colleague, Archana Unnikrishnan who's tireless work ethic inspired me daily. Our friendship allowed us to share many ideas about our respective research as well as provide moral support throughout our time in the lab. I would also like to acknowledge Dr. Tom Prychitko who was always a positive influence during difficult times. So many others who provided technical support in the lab including Fadi Ackall, Deepa Kushwaha, Hiral Patel, Faten, Lisa Lucente, Safa Beydoun, Sukayna Ismail, and Mahbuba Choudhury.

TABLE OF CONTENTS

LIST OF FIGURES

CHAPTER 1: BACKGROUND AND SIGNIFICANCE

Nutrition and Health

The importance of nutrition and health has been a fundamental component of medicine since the time of Greek physician Hippocrates in 4th century B.C. who advised taking 'functional foods'; using nutrition as medicine. Traditional Chinese medicine dating back more than 2000 years utilizes animal and plant based minerals and herbs to promote good health and prevent disease. Practitioners used empirical evidence and knowledge to treat ailments and disease through changing ones diet and lifestyle.

In today's era of medicine disease phenotypes include complex, multi-factorial syndromes including cardiovascular disease, diabetes, obesity, and cancer. The increasing incidence of these conditions and the observation of their occurrence in developed countries where a highly processed diet and sedentary lifestyle predominate, leads one to accept that these environmental changes are intimately associated with onset of these diseases. Since food is something we take in routinely over the course of our lifetime, it becomes the most important environmental impact to human health. Food components interact with tissues, cells, micro- and macromolecules within our body resulting in various biochemical reactions. This understanding of the link between nutrition and health is continually explored in modern medicine using powerful molecular approaches to decipher nutrient interactions.

Current research in the field of health and disease focuses on promoting health, disease prevention, and determining molecular patterns in response to changes in the diet. Nutrigenomics is the study of how genes and gene products interact with dietary components to alter disease phenotype and how genetic variations effect how dietary components are metabolized. This looks at how individual differences in the genome can impact susceptibility to diet. Establishing individual dietary requirements is used currently to modify disease risk. Focus on dietary

intervention to reduce the risk of cardiovascular disease in the U.S. has included implementation of the DASH diet (Dietary Approaches to Stop Hypertension) which recommends higher intake of fruits and vegetables and reducing intake of saturated fat to lower LDL cholesterol [1]. Prospective studies evaluating dietary patterns to reduce the risk of type II diabetes as well as progression of the disease found that high intake of fruits and vegetables, whole grains, fish and poultry with decreased consumption of processed foods, sugar-sweetened beverages and red meat were found to lower disease risk and complications [2, 3].

Bioactive or functional foods are defined as having positive effects on functions in the body, improving the state of health and/or reducing disease risk [4]. Powerful molecular approaches can determine nutrient activities at a molecular level and provide information on nutritional bioefficacy. Genome wide association studies (GWAS) have located genes associated with many diseases. Many studies have investigated the changes in gene expression in response to various nutrient profiles giving insight into the complexity of gene-nutrient interaction. However, genetics alone cannot explain the various phenotypes observed in the chronic diseases such as cancer. Adding to the complexity is the contribution of epigenetic changes, the extra-genetic alterations such as DNA methylation, histone modifications, and non-coding RNA functions that alter gene expression without changing the DNA sequence [5], [6], [7]. Emerging data show a direct influence of dietary factors and micronutrients on gene expression, DNA methylation, and chromatin remodeling [8].

The study of proteomics in conjunction with nutrigenomics assesses how the genome is expressed in response to diet [9]. The identification and quantification of bioactive proteins is fundamental to determine action of nutrients on molecular mechanisms. Integrating data from these sources; genetic, epigenetic, and proteomic, allows a systems biology approach to

nutritional intervention. This information can potentially create valid personalized medicine where risk of disease is calculated based on genetic profiles, environmental factors and other variables and tailoring treatment based on this information [10].

At the forefront of research involving diet impact and disease is that of nutrient interaction with cancer. Due to a large aging population and increasing exposure to various environmental insults, the incidence of cancer is projected to increase in most developed countries. The World Cancer Research Fund and American Institute of Cancer Research evaluation of the available epidemiological evidence on food, nutrition and physical activity clearly support the suggestion that cancer incidence and mortality are potentially preventable by modification of the diet and incorporating physical activity into one's lifestyle (WCRF/AICR 2007). Epidemiological evidence and supporting in vivo animal studies have implicated bioactive food components in altering pathways in cancer including apoptosis, cell cycle control, differentiation, inflammation and angiogenesis [11]. There is currently increasing interest of how nutrients modify gene interaction depending on individual genetic variation, such as single nucleotide polymorphisms or SNPs, and how this influences disease risk and prognosis. Functional SNPs can be found in gene promoter regions potentially altering gene expression profiles and subsequently effecting protein abundance in response to bioactive food components.

Epigenetic changes, which alter gene expression without a change in DNA sequence, are also mechanisms of nutrient regulation. Studies demonstrate intake of a methyl-deficient diet leads to methylation profiles consistent with neoplastic transformation [12]. The ability to characterize DNA methylation profiles or histone modifications will impact the ability to determine how diet impacts the differential epigenetic effects in normal versus cancer cells [13]. The overall impact of genetic and epigenetic changes can be monitored by looking at

transcription status, or transcriptomics in response to dietary factors. Genome-wide analysis and microarray technologies can gather a large amount of data and be applied to the biological system as a whole or to targeted cellular processes.

Folate and Cancer

Folate, a water soluble B vitamin, has been studied extensively in relation to cancer, due to its crucial role in DNA synthesis and repair. Folate deficiency has been linked to several visceral cancers showing an inverse relationship between higher consumption of foods containing folate and reduced relative risk of cancer. Epidemiological studies assess folate status either by food frequency questionnaires where total folate intake is from food and supplements, or folate status can be measured by circulating biomarkers such as plasma folate. When looking at breast cancer risk with folate status, a number of studies have suggested and inverse correlation, however these analyses are complex [14]. The Nurses Health Study determined that women taking folic acid-containing multivitamins for 15 years or more had a 75% risk reduction in developing colorectal cancer [15].

The exact mechanism of how folate deficiency mediates onset and progression of cancer remains to be determined. The role of folate in one-carbon metabolism provides clues into the potential pathways that could initiate genomic instability and epigenetic alterations. Reduced dietary folate reduces the substrates available for one-carbon transfer reactions. Within this pathway, folic acid is converted to tetrahydrofolate metabolites to be used in one-carbon transfer reactions. In nucleotide synthesis 5,10-methyltetrahydrofolate is the methyl donor for the non-reversible methylation of dUMP to dTMP. 5,10-methyleneTHF can also enter de novo purine biosynthesis by addition of a formyl group [16]. In this respect folic acid and its conversion to 5,10-methylTHF is critical in maintaining the nucleotide pool for DNA synthesis and repair.

To maintain proper methylation, folic acid provides the substrate for remethylation of homocysteine to methionine ensuring adequate SAM levels for methylation in most biological reactions. In the methionine cycle, 5-methylTHF transfers one methyl group to homocysteine to synthesize methionine, activating S-adenosyl methionine (SAM) required for methylation of CpG sites found in gene promoter regions. The effect of folate status on DNA methylation has been studied extensively as one mechanism of carcinogenesis. Epigenetic regulation of gene expression is the other half of the story in terms of genome alterations involved in cancer initiation and progression. Global hypomethylation of onco-genes and site-specific hypermethylation of gene promoters are common features in tumorigenesis [17]. Hypomethylation can occur globally, where the entire genome is affected, or regional hypomethylation within the CpG sites of gene promoter regions. Both forms of hypomethylation are thought to induce oncogene activation, whereas regional hypermethylation of gene promoter regions is associated with transcriptional silencing of tumor suppressor genes [18]. The impact of folate deficiency on methylation status is observed in rodent models where prolonged folate deficiency resulted in global DNA hypomethylation in liver [19], [20]. In human studies, global DNA hypomethylation was seen in women made folate deficient [21], [22] and increases in homocysteine levels, an indication of reduced methionine conversion, are routinely observed in individuals with low folate status. In glioma patients, low methylation status confers poor prognosis due to activation of certain oncogenes and poor response to treatment with the alkylating agent TMZ due to increased activity of the MGMT enzyme. Folate supplementation was demonstrated to increase DNA methylation and improve sensitivity to TMZ [23]. The modification of DNA methylation is one of the major mechanisms studied in tumorigenesis.

Folate is involved in the production of thymidine through conversion of dUMP to dTMP by thymidylate synthase and production of purines by addition of a formyl group to 5,10 methylene THF. Since these DNA precursors are critical to repair of DNA, reduced folate can compromise DNA repair fidelity. Reduced conversion of dUMP to dTMP results in increased uracil misincorporation and accumulation of uracil in DNA. Uracil misincorporation is repaired by the base excision repair pathway (BER) involving a series of coordinated enzymatic steps to repair small, non-helix distorting lesions. The attempt to repair the misincorporated uracil by glycosylase removal in conditions of limited folate sets the stage for futile repair resulting in strand breaks, chromosomal aberrations and malignant transformation [24], [25]. Folate status is associated with uracil misincorporation, strand breaks and genomic instability in humans. In folate deficient individuals, uracil levels and micronuclei frequency are increased eight and three fold respectively [25].

Folate Deficiency and Base Excision Repair

The condition of folate deficiency has been shown to compromise base excision repair in both in vitro and in vivo studies [26], [27], [28], [29]. BER is a critical repair pathway responsible for repair of most endogenous base lesions, abasic sites, and single-strand breaks [30], [31] including most lesions generated by reactive oxygen species (ROS) and lesions generated by environmental agents and their metabolic intermediates [32]. The initial step in BER is recognition of the damaged base by a specific glycosylase, which cleaves the N-glycosyl bond between the sugar and the base forming an abasic site. There are about 10 known human glycosylases with overlapping substrate specificities [33] able to recognize more than one type of DNA damage. The monofunctional glycosylases possess only glycosylase activity and require an additional enzyme- an AP-endonuclease (APE1) for the incision of the sugar residue leaving

behind a 5'dRP [34]. The bifunctional glycosylases possess both glycosylase and AP lyase activity, and can excise the base and create a 3' incision upstream of the AP site. APE1has the ability to remove 3' obstructive groups, allowing *β-pol* to polymerase to replace the excised nucleotide and remove the 5'dRP moiety followed by ligation of the repaired fragment by LIG-3 in the short-patch pathway. Additional proteins are involved in the repair process including XRCC1, a platform protein, which recruits and coordinates proteins in the BER process [35] and PARP1 which binds to SSBs preventing degradation while recruiting the BER protein complex [36], [37]. The rate-limiting step in the BER pathway is performed by *β-pol* which possesses nucleotidyl transferase activity and dRP lyase activity [38], [39]. The dRP-lyase activity is critical, as persistence of dRP groups proves lethal in cells engineered with β-pol lacking the 8kDa dRPase domain [40]. *β-pol* null cells are hypersensitive to the alkylating agent MMS due to failure to remove the cytotoxic 5'-dRP group induced by initiation of the repair pathway. Since no other proteins can efficiently remove the 5'-dRP group, it's removal is the rate-limiting step during BER [41].

An important study done in our lab demonstrated imbalanced BER in folate deficient (FD) mice, where UDG expression and activity were induced in response to increased uracil misincorporation however, *β-pol* failed to be upregulated in the FD condition resulting in failure to complete repair and accumulation of toxic repair intermediates [42]. Work done in Balb/c mice, a strain shown to induce colorectal cancers with FD alone, shows increased dUTP:dTTP ratios, double-strand breaks [43]and decreased apoptosis as possible mechanisms of higher susceptibility to colon tumors when these animals are made folate deficient [44].

In line with FD and colorectal cancer is evidence supporting an inverse correlation between dietary folate intake and relative risk of colon cancer. These studies suggest a 20-40%

reduction in the risk of colorectal cancer or adenomas in subjects with the highest folate status compared to those with low folate status [45], [46]. Recently, however, evidence has emerged providing conflicting views on folic acid protection in colorectal carcinogenesis. A population study from Sweden reported high plasma folate concentrations are associated with increased risk of colorectal cancer [47] and the Aspirin/Folate Polyp Prevention study reported that folic acid supplementation at 1mg/day for 6 years significantly increased the recurrence of advanced colorectal adenomas by 67% in subjects with history of colorectal adenomas [48]. This paradox between folic acid's effect in carcinogenesis stems from its role in providing precursors for DNA synthesis and repair. Depending on the timing of folate intervention in the carcinogenesis process, initiated cancer cells can utilize accelerated DNA synthesis to promote growth and drive oncogenic progression. Mutations in Ras genes, found in 30% of all cancers, are frequently found in lung cancer adenocarcinoma in association with upregulated DHFR and TS [49] for DNA synthesis, giving rise to the concept of folate scavenging to drive cell growth and proliferation in cancer cells.

The concern that folate is demonstrating dual effects on cancer initiation and progression is of utmost importance especially in the U.S where mandatory folate fortification was introduced in 1998 proving a daily average intake of 100-200ug folic acid [50, 51]. However the actual increased intake turned out to be higher than anticipated. Analysis of cancer statistics suggest that the mandatory fortification has resulted in an increased risk of colon cancer [52]. Studies done to address this issue have shown that folate supplementation at 8 mg/kg in AOM-treated rats promoted progression of ACF and crypts per focus in the colons of these animals [53]. In $Apc^{+/-} Msh^{-/-}$ mice, which develop intestinal neoplasms spontaneously without carcinogen induction, demonstrated suppression of adenomas if folate supplementation was

given before onset of neoplasia but supplementation of folic acid after establishment of intestinal neoplastic foci caused tumor-promoting effects [54].

Our lab investigated the impact of folate deficiency on BER and carcinogenesis in mice treated with the chemical carcinogen 1,2-dimethylhydrazine (DMH). In our study the animals were put on folate deficient (0mg/kg) or folate adequate (2mg/kg) diet before treatment with DMH. After six weekly i.p. DMH injections, animals were maintained on the respective diet for an additional 6 weeks at which time the animals were sacrificed. The colons were excised and examined for number of aberrant crypt foci (ACF), the earliest precursor of colorectal cancer observed in humans [55]. Both wild-type C57/Bl6 and *β-pol* haploinsufficient mice were used in this study to determine the impact of reduced BER capacity in these conditions. Analysis of the number of ACF per mouse is shown in Fig 1. FD or *β-pol* haploinsufficiency alone failed to induce ACF in these animals. However, treatment with DMH induced ACF formation significantly in wild-type FD animals. Surprisingly the knockout FD animals showed reduced number of ACF, about 50% less than the wild-type counterparts.

When comparing the ACF progression in animals maintained on the FD diet 6 weeks after last DMH treatment to animals maintained on respective diet for 40 weeks after DMH treatment, the number of ACF is reduced in the FD animals (Fig 2A) however the number of crypts per focus is increased (Fig 2B) indicating advanced progression of neoplasm after 40 wks on a folate deficient diet in the wild-type animals. Colons stained with methylene blue display observed ACF and mucosa alterations as described above (Fig 2A). Pathological analysis of liver in wild-type and *β-pol*$^{+/-}$ mice maintained on respective diet for 40 weeks after final DMH treatment show visible tumor at time of sacrifice (Fig 3). Visible tumors were observed grossly in 50% of the FD WT DMH treated animals, where no tumor was observed in the FA wild-type

treated animals. All of the FA *β-pol*^{+/-} DMH-treated animals showed visible tumor and confirmed by H&E staining, where the FD knockout counterparts showed no tumor at 40 weeks post-DMH treatment. In the knockout animals, where *β-pol* mRNA expression is 50% reduced compared to wild-type and protein is several fold less (data not shown), FD appears to be conferring protection as indicated by reduced colon ACF formation and lack of tumor burden in liver at 40 weeks post-treatment.

Further investigation into gene expression in response to FD and DMH-treatment in the wild-type and knockout animals was done by microarray analysis of mucosal mRNA. Initial look at differentially expressed genes via scatter plot demonstrated extensive differential expression in the FD *β-pol*^{+/-} DMH-treated animals compared to the wild-type counterparts (data not shown). Hierarchal clustering of the microarray expression data was performed using the DAVID biological function database to group data based on biological pathway. The heat maps generated were based on intensity of gene expression from the raw data, using colors to identify those genes upregulated in red or down-regulated, in blue. Neutral or no change in gene expression is indicated by yellow. As shown in Fig 4, genes in the pro-apoptotic pathway were upregulated in the FD *β-pol*^{+/-} animals and down-regulated in the FD wild-type. Expression of DNA repair genes were down-regulated in the FD *β-pol*^{+/-} animals, while the opposite was observed in the FD wild-type animals showing upregulated expression of DNA repair genes in these animals. To confirm the finding of increased apoptotic signaling in the FD *β-pol*^{+/-} treated animals, pathological analysis using the TUNEL assay was performed on the colons of wild-type and knockout animals treated with DMH. As shown in Fig 5 the number of positively stained apoptotic cells per crypt was significantly higher in the FD *β-pol*^{+/-} condition compared to the FD wild-type. This data is consistent with the ACF data indicating increased apoptosis eliminates

cells with excessive DNA damage from progressing to malignant transformation. Proliferation indices were measured by Brdu staining of the colons of the DMH-treated knockout animals (Fig 6).

This data demonstrates diminished proliferation in the FD *β-pol*^{+/-} condition providing further evidence of FD inducing mechanisms to prevent propagation of an initiated cell population into oncogenic progression. In this way, the excessive DNA damage incurred in response to FD and DMH with inherent loss of *β-pol* induces apoptosis and inhibits DNA repair mechanisms to prevent erroneous repair and genomic instability leading to tumorigenesis.

Defective DNA repair is associated with many human hereditary diseases including NER (Xeroderma pigmentosum, Cockayne syndrome), DNA strand break repair (Ataxia telangectasia), mismatch repair (hereditary non-polyposis colon cancer) [34]. While there is no disease phenotype linked to BER deficiency, cancer susceptibility is accelerated when DNA repair is defective. Since it has been demonstrated that folate has the ability to modulate DNA repair within the base excision repair pathway and shown to impact tumorigenesis in our study in mice, it is imperative to determine the level of this regulation and elucidate the mechanisms of folate's role in DNA repair.

In this study, I first investigate the impact of folate deficiency on DNA methylation alterations in the promoter regions of key genes in the BER pathway. I then look at DNA repair mechanisms in response to folate deficiency and exposure to carcinogen and how the mechanism of damage and repair progresses after long-term carcinogen exposure. This data reveals loss of DNA repair capabilities under folate deficiency with loss of apoptosis signaling potentially giving rise to clonogenic selection of cells with a mutator phenotype.

Figure 1 *ACF formation in colon of β-pol$^{+/-}$ mice consuming a folate deficient diet.* WT and β-pol$^{+/-}$ received either a FA diet or FD diet and subjected to either no treatment (control) or i.p. treatment with DMH for 6 weeks at 30 mg/kg body weight (DMH treated). After sacrifice colons were processed in 10% neutral buffered formalin and stained with methylene blue. Colons were analyzed under light microscopy to visualize the number of ACF per mouse colon (ACF/mouse). Bars with different letters indicate significant differences at $P < 0.05$.
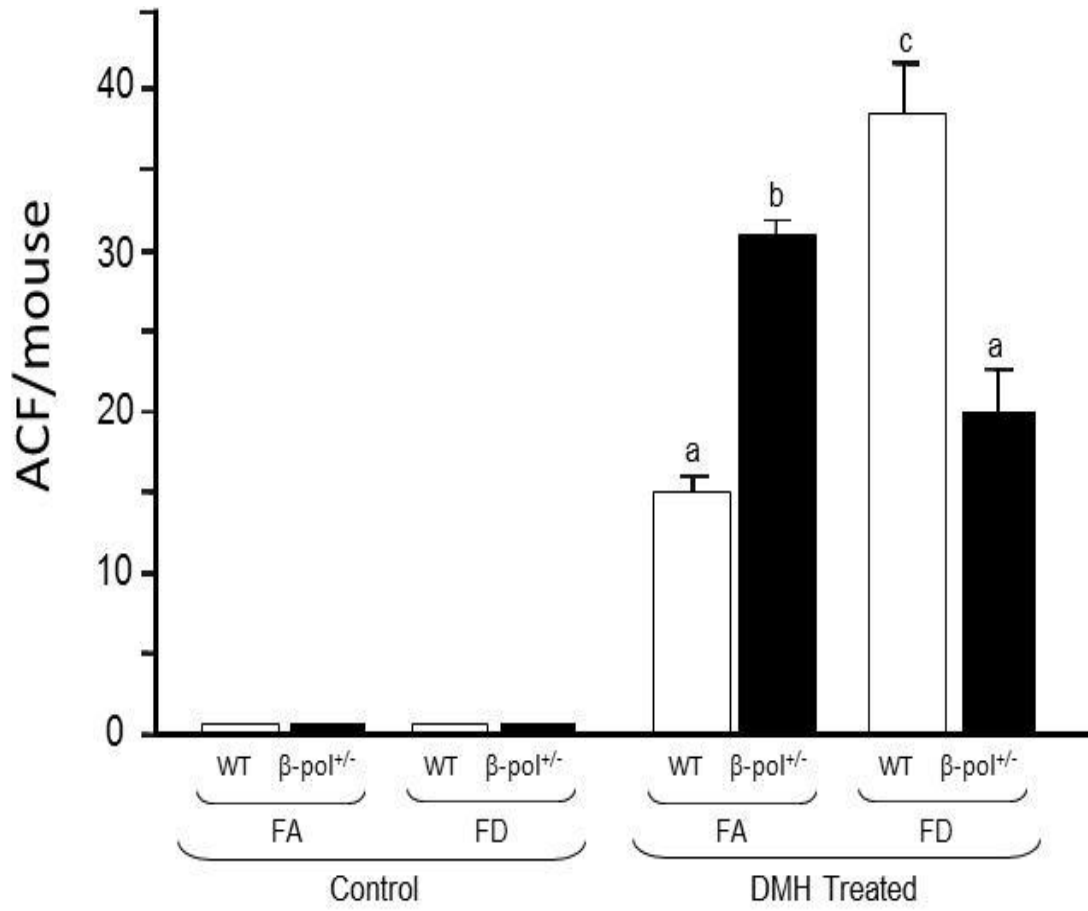
Figure 1

Figure 2 *Impact of long term feeding on ACF formation and Crypts Multiplicity.* Comparison of ACF formation and crypt multiplicity in mice fed either a FA or FD diet at 6 weeks versus 40 weeks post DMH treatment. Panel **A: (I)** Normal colonic crypts, (**II**) ACF formation in FD environment 6 weeks post DMH, (**III)** ACF formation in mice fed FA diet 40 weeks post DMH, and (**IV)** number of ACF of mice fed a FD diet 40 weeks post DMH treatment. Arrows depict area of aberrant crypt formation. Panel **B:** Relative number of ACF/mouse in mice fed either a FA or FD diet 6 weeks or 40 weeks post DMH treatment, respectively. Panel **C:** Number of aberrant crypts per focus in mice fed either a FA or FD diet 6 weeks or 40 weeks post DMH treatment, respectively. Bars with different letters indicate significant differences at *P* < 0.05.
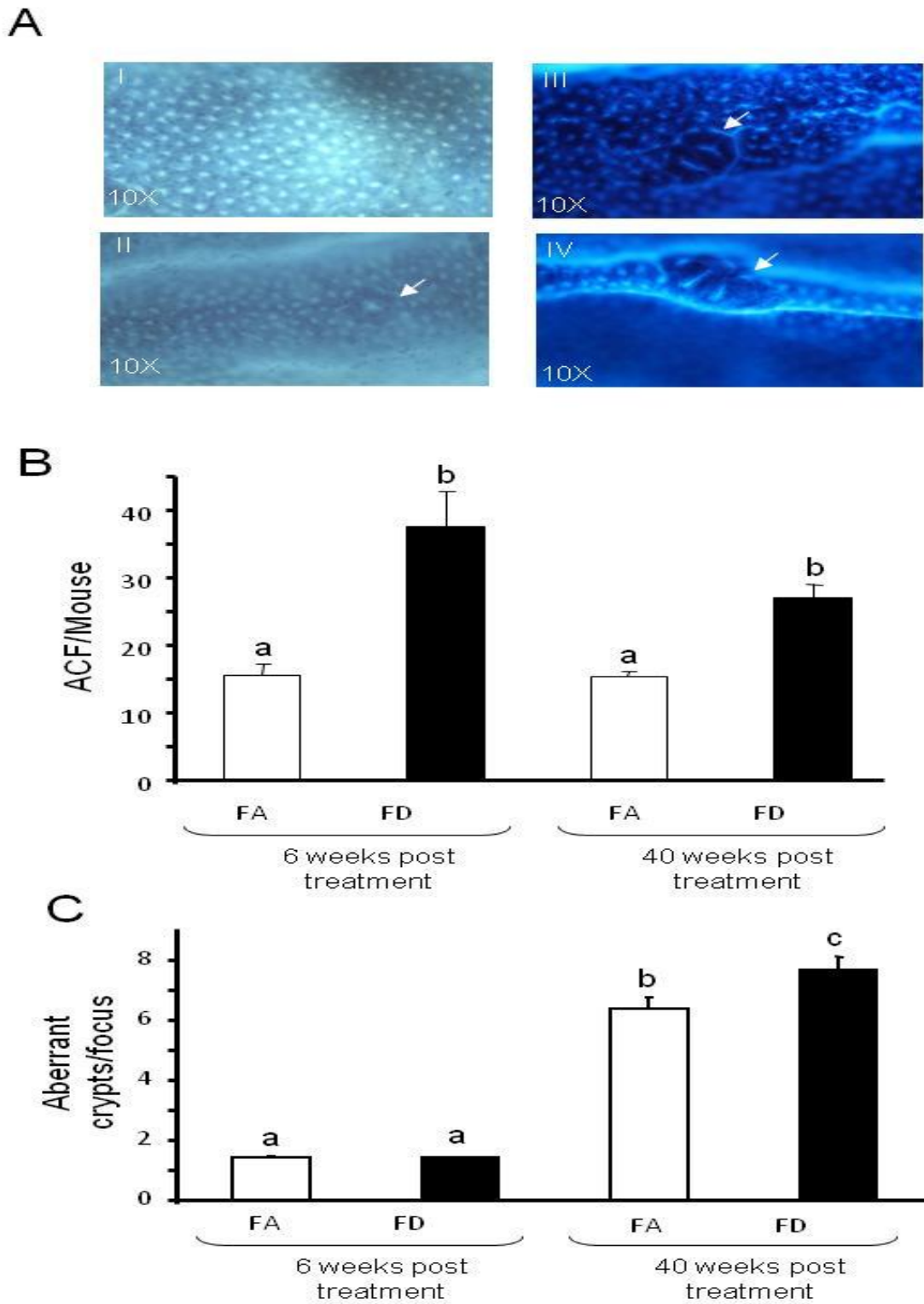
Figure 1

Figure 3 *Impact of β-pol⁺ᐟ⁻ and folate deficiency on induction of tumors in livers of DMH-treated mice.* The mice were sacrificed 40 weeks after last treatment of DMH and examined grossly. H&E micrographs showing tumor formation in liver sections from (**I**) WT FA, (**II**) WT FD, (**III**) FA β-pol⁺ᐟ⁻ and (**IV**) FD β-pol⁺ᐟ⁻ mice treated with DMH. The % value represents the percent of mice with visible liver tumor formation. All wild-type animals fed the FD diet showed liver tumors through H&E analysis.

Figure 3
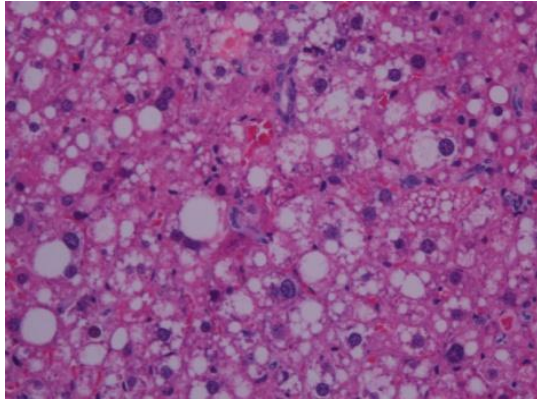
FA WT DMH, 0% visible tumor
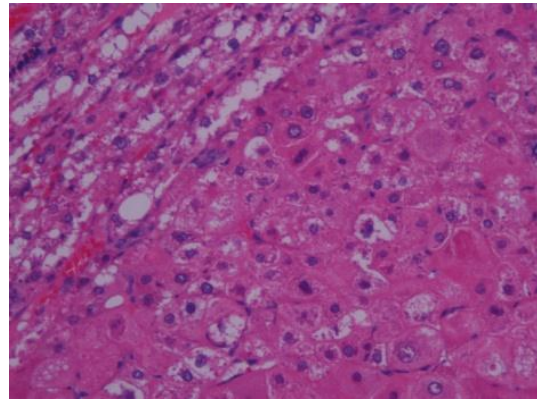
FD WT DMH, 50% visible tumor
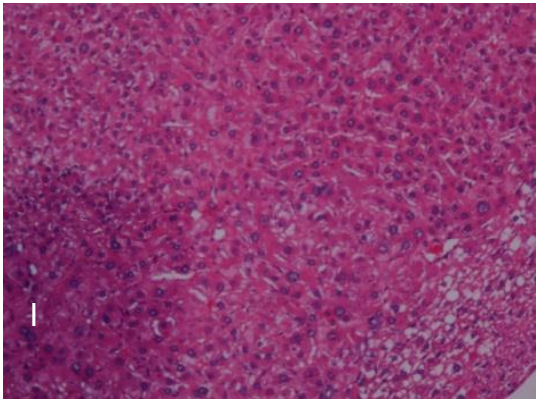
FA β-pol$^{+/-}$ DMH, 100% visible tumor
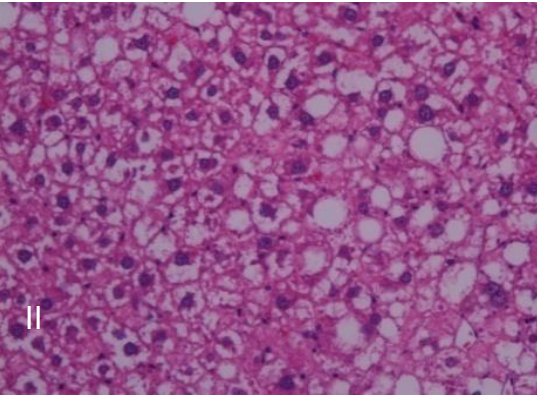
FD β-pol$^{+/-}$ DMH, 0% visible tumor

Figure 4 H*eat map representation of microarray data for pro-apoptotic and DNA repair differentially expressed genes.* Hierarchal Clustering analysis was performed using GeneSpringGX V10 (Agilent Technologies) software, and the parameters were set for centroid linkage which calculates the euclidean distance between the respective centroids of two clusters. A heat map in quadruple (A, B, C, and D) for each condition representing pro-apoptotic and DNA repair genes are shown.

Figure 4
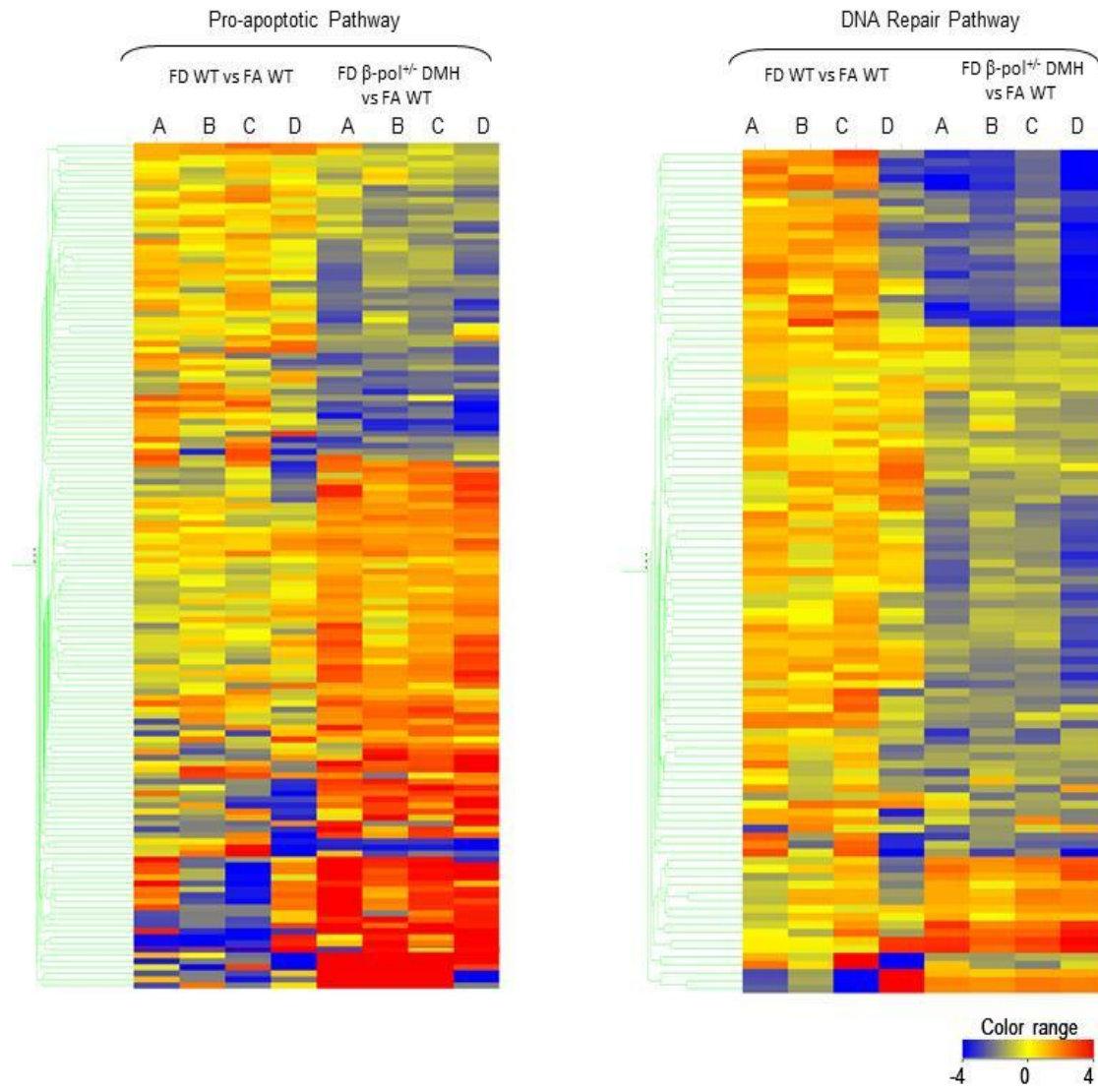
Figure 5 *Impact of* β-pol$^{+/-}$ *and folate deficiency on apoptotic activity and proliferation indices in colonocytes*. **A**. Representative photomicrographs showing TUNEL-positive staining in cells (*brown*) of colonic mucosa. (**I**) WT FA, (**II**) WT FD, (**III**) FA β-pol$^{+/-}$ and (**IV**) FD β-pol$^{+/-}$ mice treated with DMH. **B**. Tally of the TUNEL-positive apoptotic cells. WT and β-pol$^{+/-}$ were fed either a FA or FD diet and subjected to DMH treatment. Colons were excised after sacrifice and fixed in 10% neutral buffered formalin, paraffin embedded and sections stained for TUNEL positive and percent apoptotic cells were calculated as described in methods. Means without a common letter differ, *P* < 0.01. **C**. Representative photomicrographs showing H&E of colonic mucosa. (**I**) FA β-pol$^{+/-}$ and (**II**) FD β-pol$^{+/-}$ mice treated with DMH. Representative micrographs showing BrdU staining *(brown)* of colonic mucosa. (**III**) FA β-pol$^{+/-}$ and (**IV**) FD β-pol$^{+/-}$ mice treated with DMH. Proliferation Analysis: β-pol haploinsufficient mice were treated as described in materials and methods. Briefly, 2 hours prior to sacrifice mice were injected i.p. with BrdU (2.16mg/kg body weight). Colon segments were fixed in 10% formalin and embedded in paraffin. BrdU incorporation was detected by immunostaining as described in materials and methods. **D**. Enumeration of positive proliferation expressed as number of positive cells per crypt. * indicate differences at P<0.01.

Figure 5

A

I FA WT DMH

II FD WT DMH

III FA β-pol+/- DMH

IV FD β-pol+/- DMH

C

I FA β-pol+/- DMH

II FD β-pol+/- DMH

III FA β-pol+/- DMH

IV FD β-pol+/- DMH

B

Apoptotic body per crypt

WT   β-pol+/-   WT   β-pol+/-

FA   FD

DMH Treated

D

Percent Cell Proliferation

FA β-pol+/-   FD β-pol+/-

DMH Treated
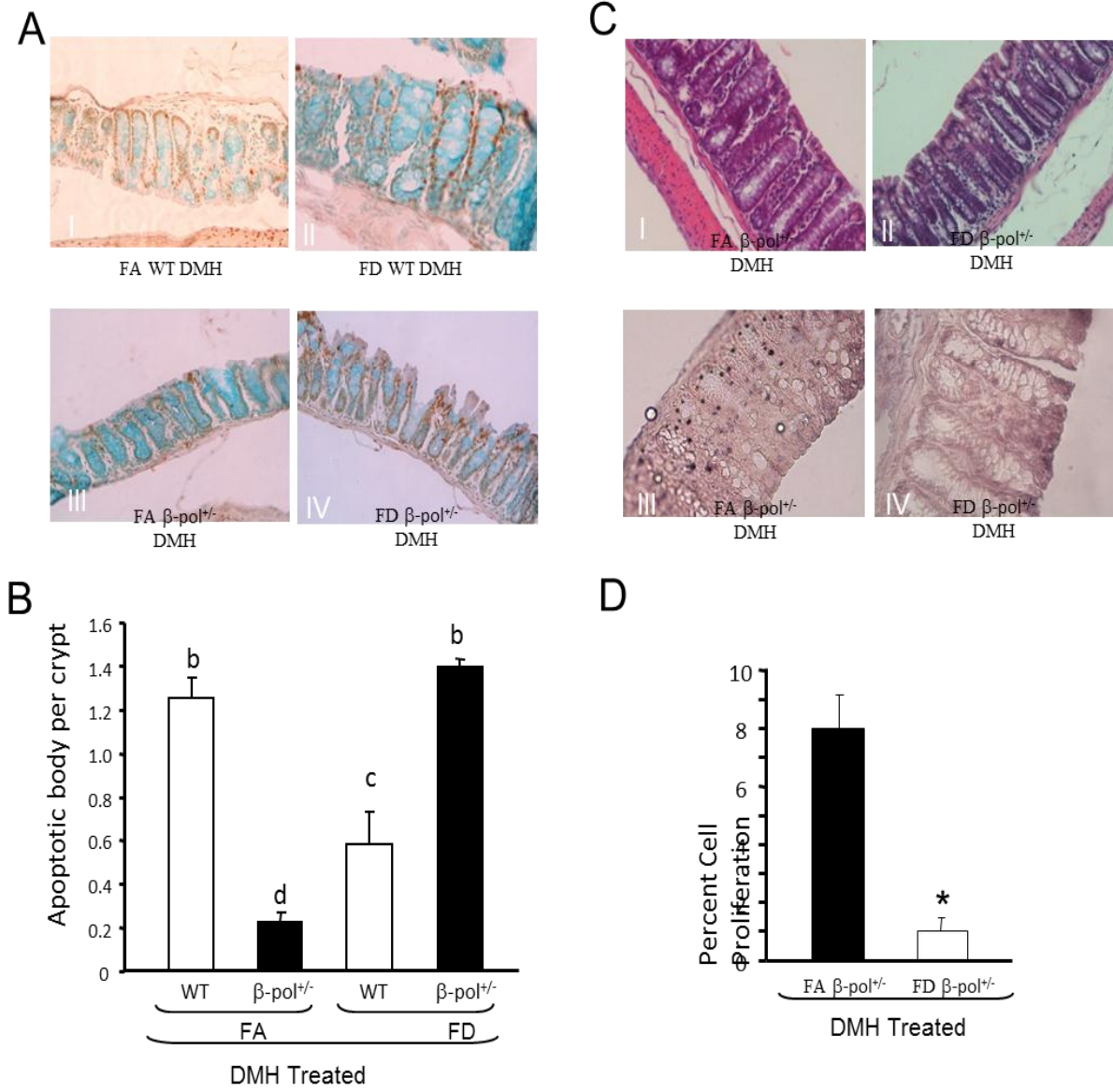
CHAPTER 2: FOLATE DEFICIENCY AND REGULATION OF PROMOTER REGION METHYLATION IN BER GENES

Introduction

Folic acid has been implicated to play a significant role in the pathogenesis of today's multi-factorial diseases including cardiovascular disease, neurodegenerative disorders and cancer [56-58]. The association between folic acid intake and cancer has been demonstrated in epidemiological studies showing diets high in fruits and vegetables relate to a decreased risk of cancer. Folates, water-soluble B vitamins, are found in high concentrations in green, leafy vegetables and are critical for one-carbon cellular metabolism. In the majority of human studies, data indicates that individuals who consume the largest amounts of folate-containing foods have a reduced relative risk of developing colon polyps or cancer [45, 46, 59].

Folate deficiency (FD) is associated with the development of several epithelial cancers including cancer of the lung, cervix, breast, brain, colon and liver with strongest association in colon [56]. Folate deficiency has been shown to increase DNA damage [26, 60] and chromosomal aberrations [25, 61] resulting in carcinogenic transformation. The mechanism by which FD increases the incidence of cancer is not completely understood. Several proposed mechanisms include the pathways by which folate functions in cellular one-carbon transfers to maintain DNA stability. Dietary folates play a critical role in maintaining DNA stability through providing sufficient nucleotide synthesis allowing high DNA replication fidelity and upholding epigenetic control throughout the genome. Intracellularly, folic acid is converted to tetrahydrofolate metabolites to be used in one-carbon transfer reactions. In nucleotide synthesis 5,10-methyltetrahydrofolate is the methyl donor for the non-reversible methylation of dUMP to dTMP. 5,10-methyleneTHF can also enter de novo purine biosynthesis by addition of a formyl

group [16]. In this respect folic acid and its conversion to 5,10-methylTHF is critical in maintaining the nucleotide pool for DNA synthesis and repair. To maintain proper methylation, folic acid provides the substrate for remethylation of homocysteine to methionine ensuring adequate SAM levels for methylation in most biological reactions. In the methionine cycle, 5-methylTHF transfers one methyl group to homocysteine to synthesize methionine, activating S-adenosyl methionine (SAM) required for methylation of DNA (Fig 6).

Folate deficiency by reduced folic acid intake establishes an environment conducive to loss of DNA integrity and epigenetic dysregulation. Limited folate causes reduced thymidine synthesis increasing the dUTP/dTTP pools [43] and increasing uracil misincorporation into DNA [62]. The resulting U:A mispairs are potentially mutagenic causing futile repair and strand breaks. Also, decreased synthesis of the purines, adenosine and guanosine inhibit normal DNA repair. Disruption of remethylation of homocysteine and transsulfuration pathway during folate deficiency can also result in accumulation of homocysteine leading to increased induction of oxidative stress and further compromise biological methylation reactions. Reduced folate status also plays a role in epigenetics, altering methylation status of the genome and consequently altering gene expression. Changes in methylation patterns have been observed in many types of cancer and include global hypomethylation which can potentially activate oncogenes as well as regional hypermethylation resulting in silencing of tumor- suppressor genes and DNA repair genes [17]. The hypomethylation of repeat sequences and non-coding DNA increases genomic instability by promoting chromosomal rearrangements [63]. These epigenetic alterations are preneoplastic, occurring early in the carcinogenic process and can set the stage for neoplasia [64].

The BER pathway is a damage-inducible pathway that repairs small non-helix distorting lesions such as uracil misincorporation, oxidative damages such as 8-oxoGuanine, and single-strand breaks. It is estimated that the BER pathway is responsible for repair of as many as one million nucleotides per cell per day [65] rendering functional BER and complete resolution of repair imperative for maintaining genomic stability. As shown by our lab and others, FD compromises the BER pathway by initiating repair without complete resolution of the damage resulting in accumulation of toxic repair intermediates such as single-strand breaks [42]. Unresolved repair intermediates can lead to double strand breaks, chromosomal aberrations and overall loss of genome integrity. Based on our findings of reduced BER capacity in the FD condition and determining that dysregulation of repair coordination occurs at the level of β *polymerase*, we wanted to investigate the mechanism of *β-pol* expression. Therefore, the objective of this study was to determine the level of gene expression of key enzymes in the BER pathway and establish if the mechanism of gene regulation is due to epigenetic factors, i.e. methylation of promoter regions.

Materials and Methods

Animals

Experiments were performed in young (3-4 months of age), wild-type C57Bl/6 specific pathogen free mice in accordance with National Institutes of Health (NIH) guidelines for the care and use of laboratory animals. The animals were maintained in an SPF facility under 12 hour light/dark cycle with ad libitum access to food and water. The animals were randomly assigned to two dietary groups and fed AIN93G-purified isoenergetic diets (Dyets, Inc., Lehigh Valley, PA). The control group received folate adequate diet containing 2mg/kg folic acid. The experimental group received a folate deficient diet containing 0mg/kg folic acid. 1% succinyl sulfathiazole

was added to all diets and diets were stored at -20 deg C. The diet regiment was maintained for eight weeks and animals' food intake and body weight were monitored twice weekly for signs of toxicity. The animals were anesthetized by CO_2 and sacrificed by cervical dislocation. Tissues harvested at time of sacrifice were flash frozen and stored in liquid nitrogen. The animal protocol was approved by the Wayne State University Animal Investigation Committee.

Folate Assay

Serum folate levels were measured using the SimulTRAC-SNB radioassay kit for vitamin B_{12} (^{57}Co) and folate (^{125}I) per the manufacturer's protocol (ICN Diagnostics, Orangeburg, NY). Blood was collected at time of sacrifice and allowed to clot at room temperature for 60 min. Samples were centrifuged, and serum was collected for immediate analysis of serum folate levels. Standards provided in the kit were used to generate a standard curve for determination of sample folate values. Radioactivity was measured by a γ-counter, and values were calculated as described by the manufacturer for both serum folate and serum B_{12}.

Isolation of Genomic DNA

Gravity Tip Column Extraction of DNA—DNA for methylation analysis of the promoter was isolated using Qiagen (Valencia, CA) gravity tip columns as described in the manufacturer's protocol. DNA was isolated from Brain, Spleen & Liver from folate added & folate deficient control and 2NP treated mice. This method generates large fragments of DNA (up to 150 kb) while minimizing shearing.

Analysis of 8-OHdG levels- Genomic DNA was isolated with the NaI DNA extractor kit (Wako chemicals, Inc.,Richmond, VA) [66]. This technique, which uses NaI instead of phenol, minimizes DNA oxidation that occurs during DNA isolation [66, 67]. 30μg of DNA was hydrolyzed using nuclease P1 and calf alkaline phosphatase. The levels of both 8-OHdG and

2dG in the DNA hydrolysates were quantified using a HPLC-EC detection system with a polar mobile phase as described previously [68, 69]. The level of DNA oxidation is expressed as the ratio of 8-OHdG to 2dG.

Detection of relative uracil levels- 4 ug DNA from liver was isolated as described [70] and blocked with methoxyamine for 2 hr at 37 deg C, treated with 0.2 units of UDG (New England Biolabs) for 15 minutes at 37 deg C. DNA is then probed with 2mM biotinylated ARP (Dojindo Molecular Technologies, MD) for 15 minutes at 37 deg C. DNA is then immobilized on nitrocellulose membrane, the membrane washed in 5X SCC and baked at 80 deg C for 30 minutes then incubated with HRP-containing hybridization buffer for 45 minutes. After washing, the membrane is incubated in ECL (Thermoscientific, Rockford, IL) for 5 minutes and then visualized and exposed using Bio-Rad ChemiImaging system. The data are expressed as integrated density value (IDV) of the band per microgram of DNA loaded.

Bisulphite treatment of DNA

For the investigation of DNA methylation pattern of the promoter regions of *β-pol* and *Ung* genes, bisulfite conversion method was used. Bisulfite reaction occurs between cytosine and sodium bisulfite, as a result unmethylated cytosine is deaminated to uracil while methylated cytosine remains unchanged. Genomic DNA normalized to 2 μg was used for the bisulfite treatment and the assay was performed as described by the manufacturer's protocol (Zymo Research, Orange, CA).

PCR Amplification of Bisulfite treated DNA

PCR amplification of the bisulfite treated DNA was done as uracil is converted to thymidine during the amplification of the bisulfite DNA. Primers were designed for the CpG islands present in the upstream of the exon-1 of the *β-pol* promoter. The methylated primers were designed for

the two separate fragments consisting of 146bp and 200bp (MethPrimer, San Francisco, CA). For *Ung*, methylated primers were designed for the 260 bp CpG rich region of the promoter P_B. p53 gene has highly abundant CpG region between exon7 and exon8, thus p53 gene was used as a positive control and methylated primers were designed for bp region. PCR amplification for the CpG rich region of each gene was carried out using MethPrimer's as described by the manufacturer's protocol (Promega, Madison, WI).

Subcloning of the methylated genes

The amplified genes were subcloned in bacteria. After subcloning the amplified fragment was sequenced with greater reliability and only one allele is sequenced per clone. Briefly, the amplified gene was analyzed on agarose gel and purified using gel extraction kit (Qiagen, Valencia, CA). Ligation of the purified DNA into pGEMT easy vector was done using 8ng purified DNA, pGEMT easy vector and T4 DNA ligase. (Promega Madison, WI). A ligation with the negative control having no insert DNA at 4°C overnight was done concurrently according to the manufacturers described protocol (Promega, Madison, WI)). The ligated product was then transformed into *JM109 E.coli* Competent Cells and transformation was done according to manufacturers protocol (Promega Madison, WI)). Transformed cells were plated on LB agar plates containing 100μg/ml ampicillin and IPTG/X-gal and incubated overnight at 37°C. The pGEMT Easy Vector has Amp^r gene and lac-Z gene for the selection of the transformed plasmid DNA. The selective plates had blue and white colonies, white colonies indicating insertion of the plasmid DNA by disrupting the lacZ gene and blue colonies indicating lack of the DNA insert. Thus, white colonies were selected for the plasmid isolation.

Plasmid Isolation & Sequence Analysis

After the overnight incubation, five white colonies from each plate were picked and grown in LB broth with 100µg/ml of ampicillin at 37°C overnight in incubated shaker. Plasmid DNA was isolated using Perfectprep Plasmid Mini kit (Eppendorf, Westbury, KY) and manufacturer's protocol was followed. The isolated plasmid DNA was then sequenced by M13 forward primer using ABI Prism 3700 sequencer (Applied biosystems, Foster City, CA). Sequences were analyzed for the change in methylation pattern in CpG rich area of the promoter region of β-pol and Ung genes in folate deficient and folate adequate animals.

Gene expression Analysis

The mRNA expression level of genes involved in BER pathway namely, Ung, Ogg1, APE1/Ref-1, *β-pol*, Xrrc1 and lig-1, were quantified using real-time PCR. Briefly, total RNA was extracted from liver, brain, colon and spleen tissue of folate added & folate deficient mice using RNeasy Kit (Qiagen, Valencia, CA). First strand cDNA was synthesized from 1 µg RNA using ImprompII reverse transcriptase kit (Promega, Madison, WI) and purified using QIAquick PCR purification kit (Qiagen, Valencia, CA). The primer sequences used for the amplification are detailed in Table 1. External standards for all the genes were prepared by subcloning the amplicons into pGEM-T easy vector. The vectors were linearized using EcoR1 to make the standard curves. All BER gene transcripts were normalized to both GAPDH and RPLO.

Results

Analysis of DNA damage in response to folate deficiency

Folate deficiency has been associated with genomic instability and as such, folate deficiency has been observed to increase somatic mutations and chromosomal aberrations. Uracil misincorporation into DNA and DNA strand breakage has been demonstrated in folate deficient animal models [60, 71, 72] and deficient folate status has also been associated with uracil

misincorporation, increased micronuclei frequency and chromosomal instability in humans [25, 73]. In order to study the mechanism behind folate deficiency induced damages, we used C57Bl/6 mice and put them on folate adequate and folate deficient diets for 8 weeks. The folate deficient animals showed ~90% reduced folate levels in their plasma after 8 weeks. Despite the reduction in folate levels these animals did not display any significant difference in their body weight. As a first series of experiments, we measured DNA base damages such as uracil and 8-Oxo-dG levels in the liver genomic DNA. Folate metabolism plays a critical role in nucleotide synthesis as it provides one-carbon units for the conversion of dUMP to dTMP. Folate deficiency limits thymidine synthesis while increasing dUMP/dTTP ratios [25]. Since dUTP is an excellent substrate for most replicative polymerases, uracil can be readily misincorporated into the DNA under conditions of limiting folate. The resulting U:A mispairs are repaired by DNA repair enzymes leaving an abasic site that can persist if folate is continually limited. As reported previously by our lab [70] folate deficiency resulted in significant increase in uracil levels in liver genomic DNA measured using the UDG-coupled ASB assay when compared to its folate adequate counterparts (Fig. 7A).

The highly mutagenic lesion , 8-oxo-dG is seen in significant quantities in human DNA and causes G:C to T:A transitions if left unrepaired [74]. This oxidative lesion is repaired via the base excision repair pathway. Folate deficiency has been previously shown to induce oxidative stress by itself along with its other physiological and biochemical impacts through the generation of hydrogen peroxide [75]. Studies done on lymphocytes from folate deficient rats [76] and brains of folate/methyl-deficient rats [77] show increased 8-oxo-dG levels. Therefore, we wanted to determine the 8-oxo-dG levels in the liver of our folate deficient mice. In line with these previous studies, we indeed see a significant increase in 8-oxo-dG lesions (Fig 7B). Thereby,

increased levels of such DNA damages in the folate deficient condition suggest inability of BER to repair the lesions resulting in persistence and accumulation of the damaged bases. Therefore, to characterize the effect of folate deficiency on BER we wanted to determine the changes in expression of BER genes as a result of increased presence of these damages.

Analysis of expression of genes in BER pathway in response to folate deficiency

Oxidative stress induced damage is considered the most common insult affecting the genome [74] and repair of these damages is crucial to maintain the integrity of the genome [78]. Base Excision repair pathway is a simple, dynamic, environmentally responsive DNA repair pathway [79-81]. It plays an important role in repairing oxidative damages, single strand breaks and other non-helix-distorting DNA damages [82-84]. The classic BER response to DNA base damages such as uracil and alkylated bases involves a monofunctional glycosylase removing the damaged base leaving behind an abasic site. Oxidative damages such as 8-oxo-dG and thymine Glycol require bifunctional glycosylases. An endonuclease, namely, APE1/Ref-1 which also possesses 3; phosphodiesterase, 3' phosphatase and 3'-5' exonuclease activity [41], subsequently creates a single strand break adjacent to the abasic site generating a 3'-OH end. The next enzyme in the pathway, *β-pol* removes the dRP moiety left behind and generates a 5' phosphate end. Further using 3'-OH as its substrate, the enzyme inserts a new nucleotide. The dRP lyase activity of *β*-pol, serves as the rate-limiting step in this pathway [38]. Finally DNA ligase seals the nick completing the repair process. Damages to DNA caused by folate deficiency including uracil misincorporation and oxidative damages are repaired by the BER pathway. Our lab has previously reported the attenuation of BER activity during folate deficiency [42]. Therefore to analyze the mechanism of this attenuation, we looked at expression patterns of the genes involved in the BER pathway using quantitative real time PCR.

Using real time PCR, we quantified the expression levels of some of the genes involved in the BER pathway in the liver of folate adequate and folate deficient mice. These genes showed differential expression during folate deficiency. Uracil DNA glycosylase (Ung), a monofunctional glycosylase responsible for removing misincorporated uracil and oxidized cytosines from DNA show significant increase in mRNA expression suggestive of increased glycosylase activity during folate deficiency (Fig 8A). Whereas, OGG1, a bifunctional glycosylase involved in removal of 8-oxo-dG, did not show any significant difference during folate deficiency compared to the folate adequate condition (Fig 8B). The next enzyme in the pathway, APE1/Ref-1 shows an increasing trend during folate deficiency (Fig 8C). As such the pattern of expression of Ung and APE1/Ref-1 indicate coordinated repair and high efficiency to remove the damaged base and create single strand breaks. In line with our previous studies the rate limiting enzyme of the pathway, β-pol, despite being a stress response gene did not show any upregulation during folate deficiency (Fig 8D). This demonstrates the loss of damage inducibility of β-pol. Finally, the next enzymes in the BER pathway, XRCC-1, a scaffolding protein that forms a complex with LIG-3 and stimulates its activity was observed to be downregulated during folate deficiency while, lig-3 did not change significantly (Fig 8E, F). This data clearly demonstrates differential regulation of BER genes during folate deficiency.

Further, the expression pattern of *Ung* and *B-pol* was determined in other tissues such as, brain, spleen and colon. Ung, following the liver expression showed significant upregulation during folate deficiency in brain and colon (Fig.9). β-pol expression yet again followed the liver expression and showed no induction during folate deficiency in colon, spleen and brain with spleen in effect showing downregulation (Fig 10). These findings confirm that BER pathway is initiated during folate deficiency but not completed there after possibly leaving behind

unresolved toxic intermediates. This further reinforces the finding that folate deficiency impacts the BER pathway at the level of *β-pol.* Therefore, in order to determine if the mechanism of gene regulation of these two genes was due to epigenetic alterations, we next analyzed their promoter regions for methylation changes.

Promoter analysis of UNG and B-polymerase for methylation of CpG regions

DNA methylation is an epigenetic alteration that plays an important role in regulating gene expression and ultimately protein expression [85]. DNA methylation in mammals primarily occurs by the covalent modification of cytosine residues located in CpG dinucleotides [63]. And these CpG dinucleotides are concentrated in CpG islands that occur in approximately 60% of gene promoters [86]. Thus site-specific methylation changes in gene promoter regions can control gene expression. Global and gene-specific DNA hypomethylation and local regional hypermethylation are common features in tumorigenesis [17]. Epigenetic changes are one of the earliest and consistent observations in the carcinogenic process as demonstrated by extensive CpG island hypermethylation in benign colon polyps as well as advance high-grade tumors [87]. BER pathway is a damage-inducible pathway and previous study from our lab demonstrates attenuation in this inducibility during folate deficiency [42]. This study further illustrates the differential effect of folate deficiency on the expression of BER genes. In order to study the mechanism of gene expression changes in response to folate deficiency we looked at methylation status of two genes which show differential expression, namely Ung and β-pol in different tissues. Using bisulfite sequencing method, we determined the methylation profile of Ung and β-pol promoter regions. The CpG islands within the promoters of Ung and *β-pol* gene were identified using the MethPrimer software and primers were designed to amplify these CpG islands [88]. First, the methylation status of a CpG rich 262bp region (-1 to -262) of the Ung

promoter was analyzed in liver and brain tissues of folate adequate and folate deficient mice. Even though the FD animals show consistent upregulation in Ung expression in all tissues tested, our methylation analysis showed no difference in the methylation pattern between the folate adequate and folate deficient groups (Fig. 11).

To further determine if failure to upregulate *β-pol* and complete repair was a consequence of changes in the methylation status in the promoter region, we analyzed the first 300bp cis-acting region of the *β-pol* promoter and part exon 1 (+44 to -322) in three different tissues, namely, liver, brain and spleen. Yet again, there was no methylation differences between the folate adequate and folate deficient group in all the tissues tested (Fig.12). Interestingly, spleen which showed significant downregulation in *β-pol* mRNA expression did not show any difference in its methylation pattern as well. To our surprise none of the CpG sites were methylated in both the promoters under these conditions. To rule out the possibility of artifacts in our assay conditions as none of the CpG sites were methylated, we used p53 as a positive control. The methylation pattern of the region between exon 7 and exon 8 was analyzed similar to Ung and *β-pol*. Here we observed methylation at all the CpG sites within the region tested but again no difference between the folate adequate and folate deficient conditions (Fig.13). This data illustrates that differential regulation of the BER gene expression by folate deficiency is not through epigenetic alterations of the core regions of the promoters tested. Therefore, it is inviting to suggest interplay between transcription factors during folate deficiency as observed in our previous study [89].

Discussion

In this study, we show that FD animals have increased levels of DNA damage resulting in upregulation of the early repair enzymes in the BER pathway for initiation of repair. As we have

shown previously, the failure to upregulate *β-pol* under FD conditions reduces BER capacity resulting in incomplete repair and accumulation of genotoxic repair intermediates thus compromising integrity of the genome [42]. Here we show that folate deficiency promotes DNA damage as indicated by increased levels of genomic uracil, 8-oxo-G and single strand breaks (data not shown). As further evidence, expression analysis of the genes in the BER pathway does not show coordinated expression with repair activity in response to DNA damage during folate deficiency i.e., the genes involved in the initial steps of the pathway, UNG and APE1/Ref-1, show upregulation but no change is observed in expression levels of *β-pol*. In order to begin to elucidate the mechanism of gene regulation in the BER pathway we looked at methylation status of UNG and *β-pol* promoter regions. In the analysis of the UNG promoter region we saw no change in methylation of the CpG sites in either the folate adequate or folate deficient condition in liver and brain. Although *β-pol* gene expression was attenuated in the folate deficient condition, analysis of the *β-pol* promoter region as well showed no change in methylation pattern between folate adequacy or folate deficiency in all tissues tested. Interestingly, *β-pol* mRNA was significantly downregulated in spleen during folate deficiency without any changes in the methylation profile in this tissue. Hence, we find that under folate deficient conditions, the negative regulation of *β-pol* gene expression is not due to regional promoter methylation. Taken together, UNG and *β-pol* expression are not regulated by alterations in the methylation pattern of the promoter regions studied.

Folate metabolism is of central importance for one-carbon transfer reactions involved in DNA synthesis and repair mechanisms as well as SAM-dependant methylation of DNA. Folate activated one-carbon units function in de novo purine biosynthesis, thymidylate biosynthesis and ensuring the provision of SAM, the primary methyl donor for most biological methylation

reactions including DNA promoter region methylation [90] as illustrated by Fig.1. In addition to these functions folate is also involved in the transulfuration pathway leading to the formation of cystathionine, cysteine and glutathione [91]. The enzymes in the folate metabolic cycle are sensitive to redox changes and would stimulate the transulfuration pathway under pro-oxidant conditions [92]. The carcinogenic properties of folate deficiency are suggested to be associated to the role of folate in one- carbon metabolism [93]. Impaired folate metabolism can arise from primary folate deficiency, secondary B-vitamin nutrient deficiency and genetic variations that effect the accumulation and utilization of folate. Deficiency in folate metabolism might disrupt purine and thymidine synthesis resulting in abnormal DNA synthesis and repair fidelity and uracil misincorporation into DNA. Folate deficiency may also lead to alterations in DNA methylation perhaps as a function of reduced S-adenosyl methionine levels and also oxidative stress by altering the thiol switches. Although the exact mechanism for folate deficiency induced carcinogenesis is largely unknown, support for induction of cancer is evidenced by an increase in single strand break [26, 60, 71, 94, 95] micronucleus formation [61, 96], chromosomal aberrations [97, 98] and mutation frequency [99, 100] in genomic DNA during folate deficiency.

Studies conducted on BALB/c mouse models show the susceptibility of this strain of mice to the development of intestinal tumors in response to low dietary folate by itself without any influence from other environmental factors. The authors show elevated dUTP:dTTP ratios, decreased apoptosis, and increased double-strand breaks indicated by p-H2AX staining in intestinal tissue [43, 44]. Greater DNA uracil content and micronucleus frequency, resulting from chromosome damage and breakage, was demonstrated in erythrocytes of folate deficient individuals indicating a relationship between the level of uracil in DNA and double strand breaks [25]. This theoretical model is based on studies of plasmid DNA with two closely spaced uracil

within 14 base pairs of each other on opposing strands resulting in double strand breaks and linearization when transfected into cells expressing UNG [101]. Ung excision of the uracil creates an abasic site which if unresolved could cause clastogenic BER strand break intermediates. Activation of BER under folate deficient conditions can potentially induce perpetual UDG activity and uracil incorporation during repair synthesis creating a state of 'futile cycling' of BER [102]. Chemotherapeutic agents such as 5-FU and pemetrexed are inhibitors of thymidylate synthase resulting in TMP depletion and dUMP accumulation. Although the exact mechanism of cytotoxicity with these agents is not completely clear, it is known that uracil misincorporation and strand breaks are important events in the efficacy of these drugs. A study with MEF cells homozygous null for β-pol show resistance to raltitrexed, a folate inhibitor of thymidylate synthase (TS), suggesting uracil misincorporation followed by BER contributes to the cytotoxicity of TS inhibitors [103]. Under conditions of folate deficiency, the response to genomic DNA uracil accumulation by BER could elicit the futile cycling or erroneous recombination by DNA repair, cell cycle arrest or signal downstream damage responses i.e. apoptotic pathways. In line with the various studies done on folate deficiency, we show in our present study significantly elevated levels of uracil and an increase in the number of single-strand breaks in the liver DNA under folate deficient conditions (data not shown).

Folate deficiency also induces perturbations in methylation status from reduced capacity of SAM production resulting in global hypomethylation and regional hypermethylation potentially activating proto-onco genes and silencing tumor-suppressor genes. The role of DNA damage could also play a role in methylation reactions as shown in rats, maintained on folate-deficient/methyl-deficient diet, where there appears to be a high affinity for DNA methyltransferase to bind to unrepaired lesions resulting in increased methylation at those sites.

In turn, the methyltransferase enzyme is sequestered from the replication fork by the unrepaired lesions, promoting passive replication-dependant global demethylation [20]. In this case, the DNA damage caused by folate deficiency in the form of uracil misincorporation, 8-OHdG, abasic sites and strand breaks could potentially impact methyltransferase activity and alter DNA methylation. Epigenetic alterations are preneoplastic, occurring early in the carcinogenic process and persist even after genotoxic insults have been repaired indicating that epigenetic analysis is vital to understanding the biopathways of cancer initiation and progression. As our data show, the methylation pattern of two key base excision repair gene promoters is unaltered in different tissues in response to folate deficiency. In spite of the increased accumulation of the DNA damages in our folate deficient group, our data shows that none of the CpG sites in the promoters tested were methylated similar to their folate adequate counterparts. Therefore, folate deficiency does not regulate UNG and *β-pol* expression by altering its core promoter methylation. In line with this, our previous study on *β-pol* promoter provide support for the involvement of regulatory factors which affects the overall expression of the gene [89]. We demonstrated differential binding of negative regulatory elements to Folic acid response region (FARR) in the *β-pol* promoter in response to folate deficiency and oxidative stress [89].

In conclusion, accumulation of genomic insults could lead to initiation and progression of cancer or could be balanced by down-stream pathways triggering recombination or apoptosis. The response to DNA damage is a critical factor determining the cell's fate. Folate deficiency evidently impacts the BER pathway leading to the accumulation of DNA damages. As compromised DNA repair could lead to oncogenic transformation it becomes important to elucidate the mechanism by which folate deficiency causes this DNA repair deregulation. Our study provides evidence that regional DNA methylation is not the mechanism behind the

deregulation of the BER pathway, i.e., the differential expression of Ung and *β-pol* genes during folate deficiency. Therefore, further research to elucidate the involvement of other epigenetic alterations such as histone modifications and interplay of transcription factors in regulating BER gene expression during folate deficient is warranted.

Figure 6 *Folate cycle* Mechanism of one-carbon transfer reactions.

Figure 6
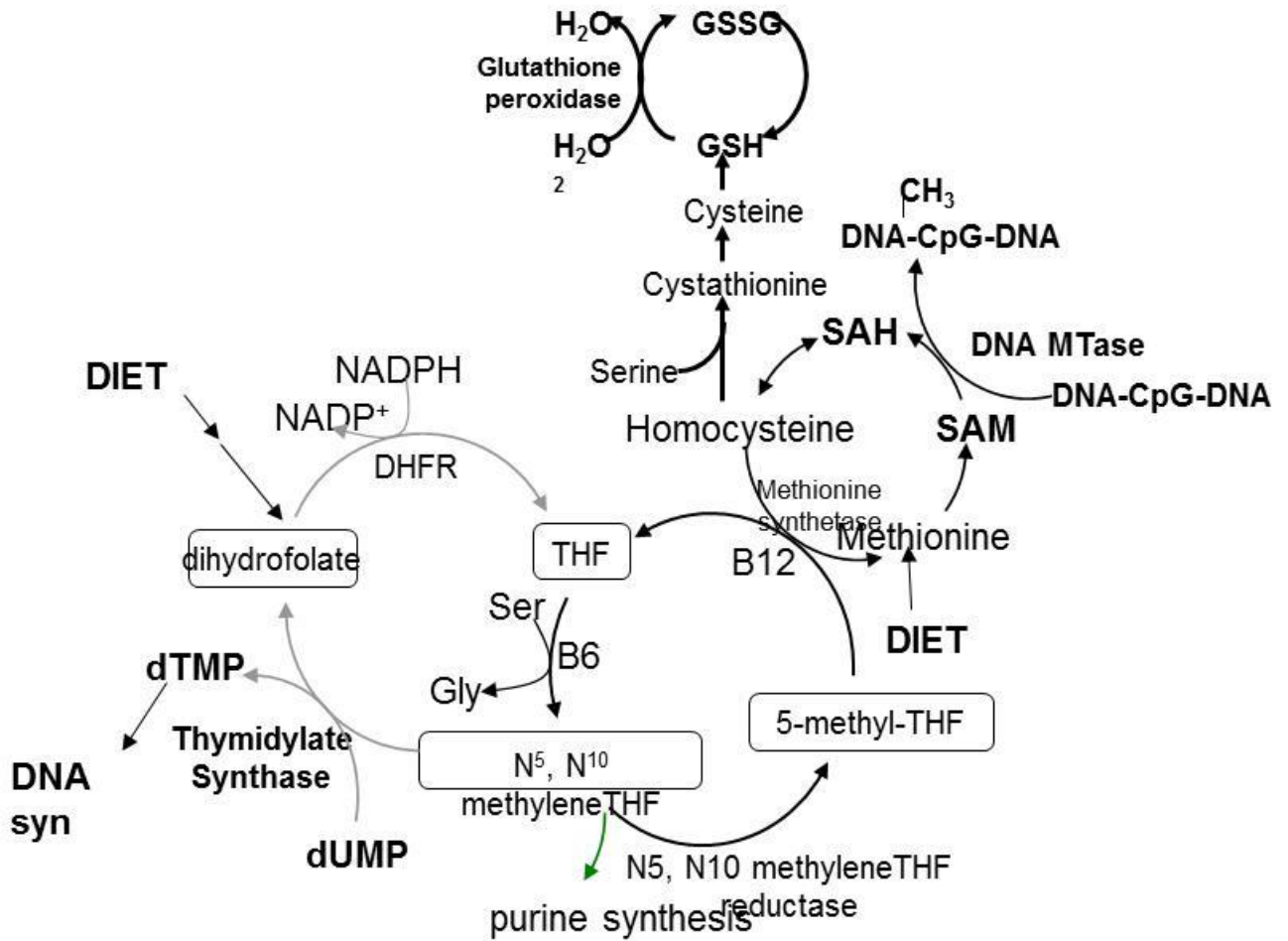
Figure 7 *Effect of folate deficiency on levels of uracil in DNA and 8-oxoG lesions in liver of mice.* (A) FA and FD (B) Relative levels of Uracil as measured by Uracil Aldehydic Slot Blot technique. (C) Relative levels of 8-oxoG. Significant differences at p<0.01.

Figure 7
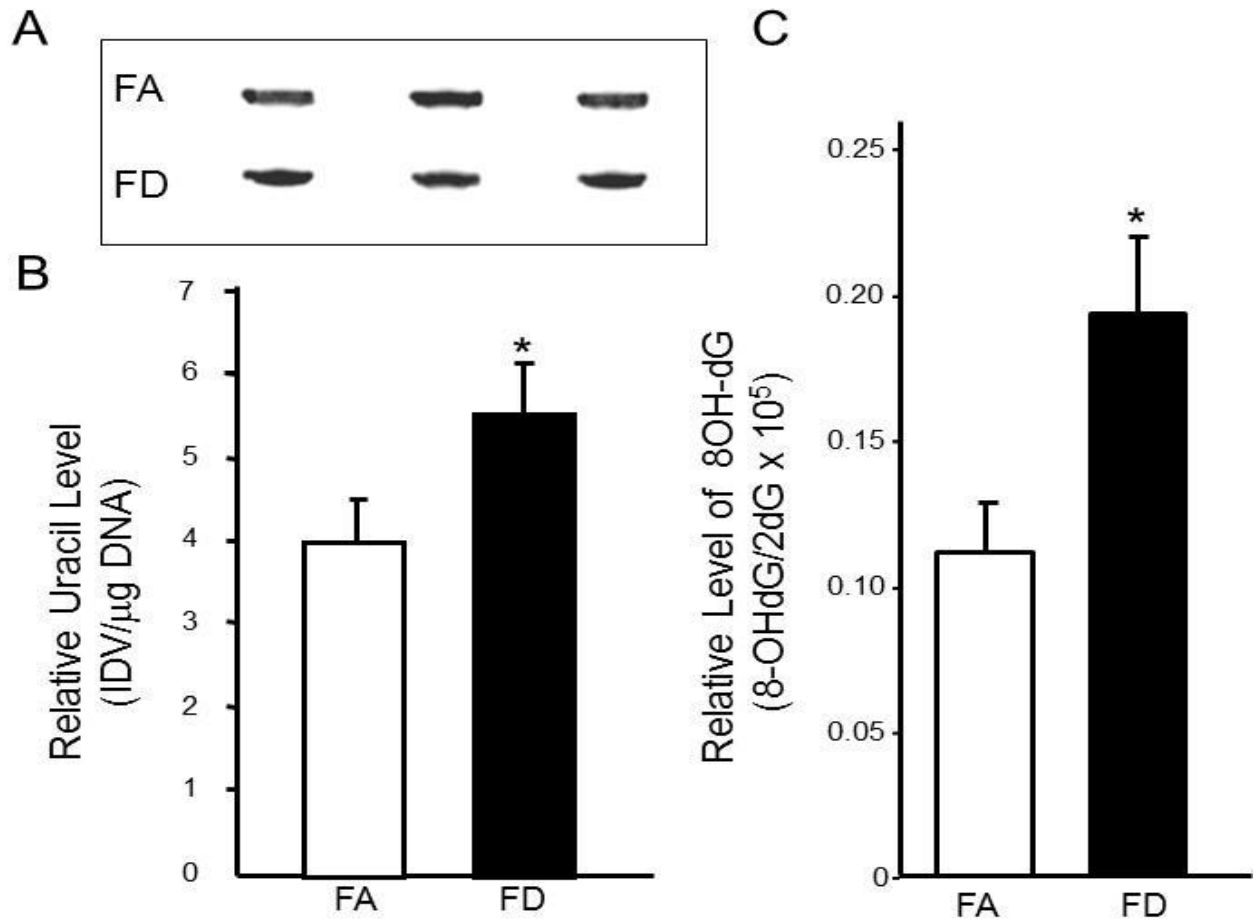
Figure 8 *Effect of folate deficiency on expression of BER genes.* mRNA expression from livers of folate-adequate and folate-deficient wild-type C57BL6 mice. Transcripts were quantified using real-time PCR and normalized to *Gapdh* or *Rplo.* (A) UNG mRNA expression normalized against *Rplo*. (B) Oxoguanine glycosylase (OGG1) mRNA expression normalized against *Rplo*. (C) Apurinic/Apyrimidinic endonuclease (APE1) mRNA expression normalized against *Rplo*. (D) DNA polymerase B (B-pol) mRNA expression normalized against *Gapdh.* (E) X-ray repair cross complementing, XRCC-1, mRNA expression normalized against *Gapdh*. (F) Ligase III, Lig-3, mRNA expression normalized against *Gapdh*. Significant differences at p<0.01

Figure 8
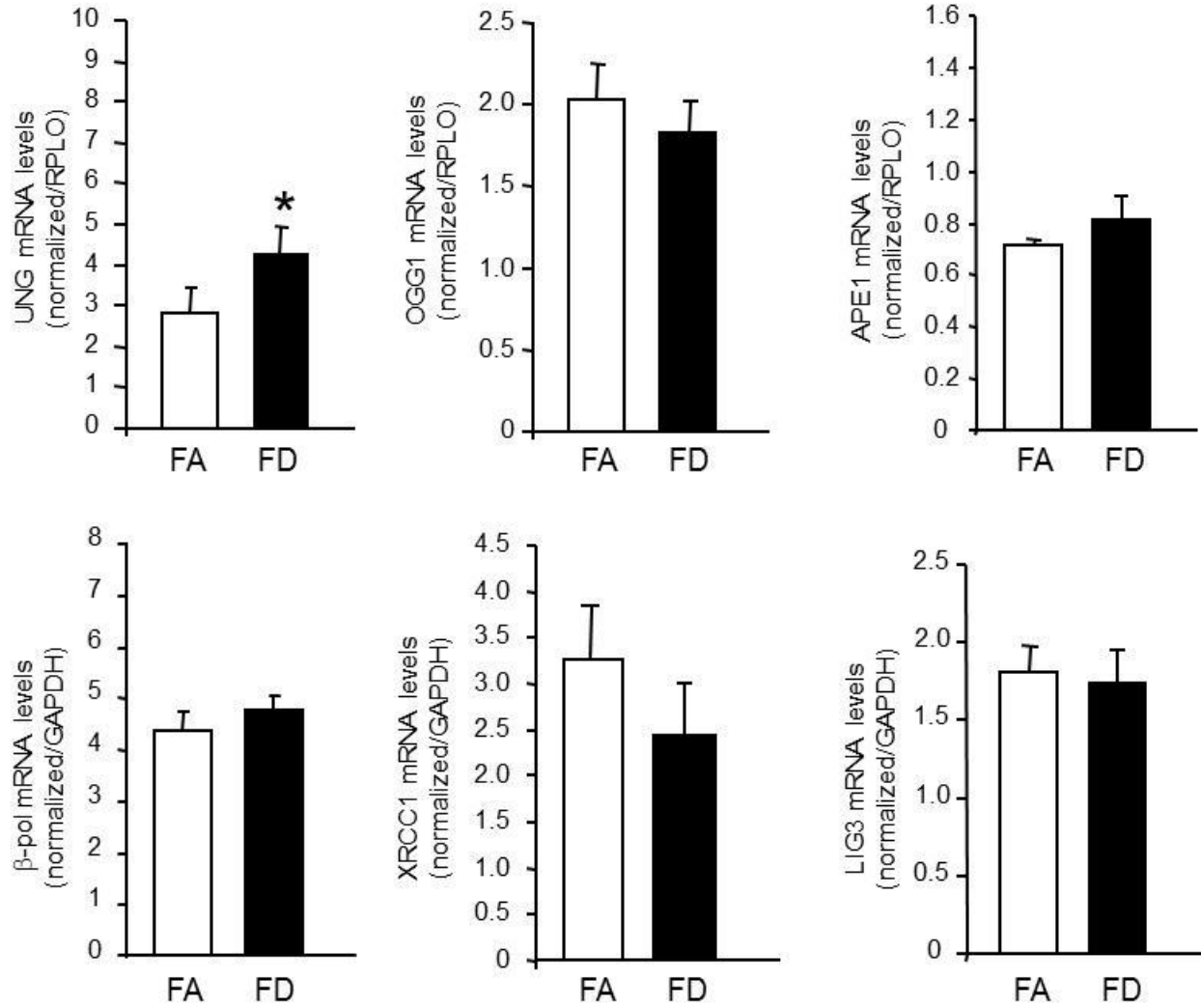
Figure 9 *Effect of folate deficiency and Ung expression in liver, brain and colon.* Uracil-DNA glycosylase mRNA expression in liver of folate-adequate and folate-deficient wild-type C57BL6 mice. Transcripts were quantified using real-time PCR and normalized to *Rplo*. Values represent an average (S.E.M) for data obtained from five animals in each group. Significant differences at $p < 0.01$.

Figure 9
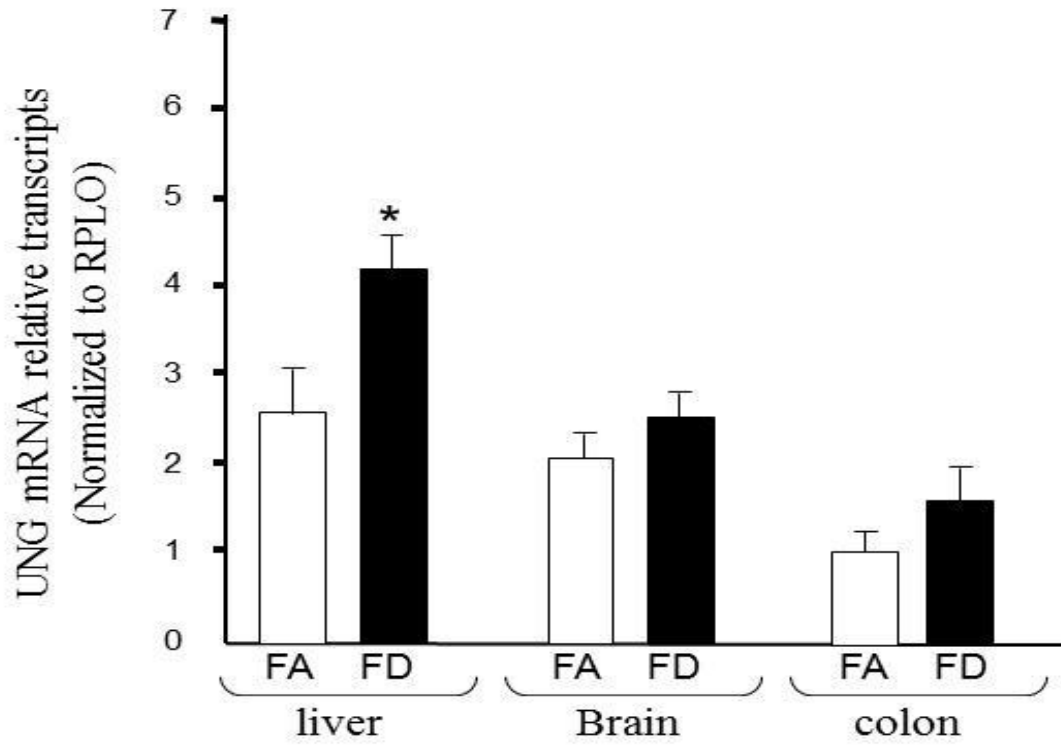
Figure 10 *Effect of folate deficiency on β-pol expression in select tissues.* DNA polymerase β mRNA expression in liver, colon, spleen and brain of folate-adequate and folate-deficient wild-type C57/Bl6 mice. Transcripts were quantified using real-time PCR and normalized to *Gapdh* and *Rplo*. Values represent an average (S.E.M) for data obtained from five animals in each group. Significant differences at $p < 0.01$.

Figure 10
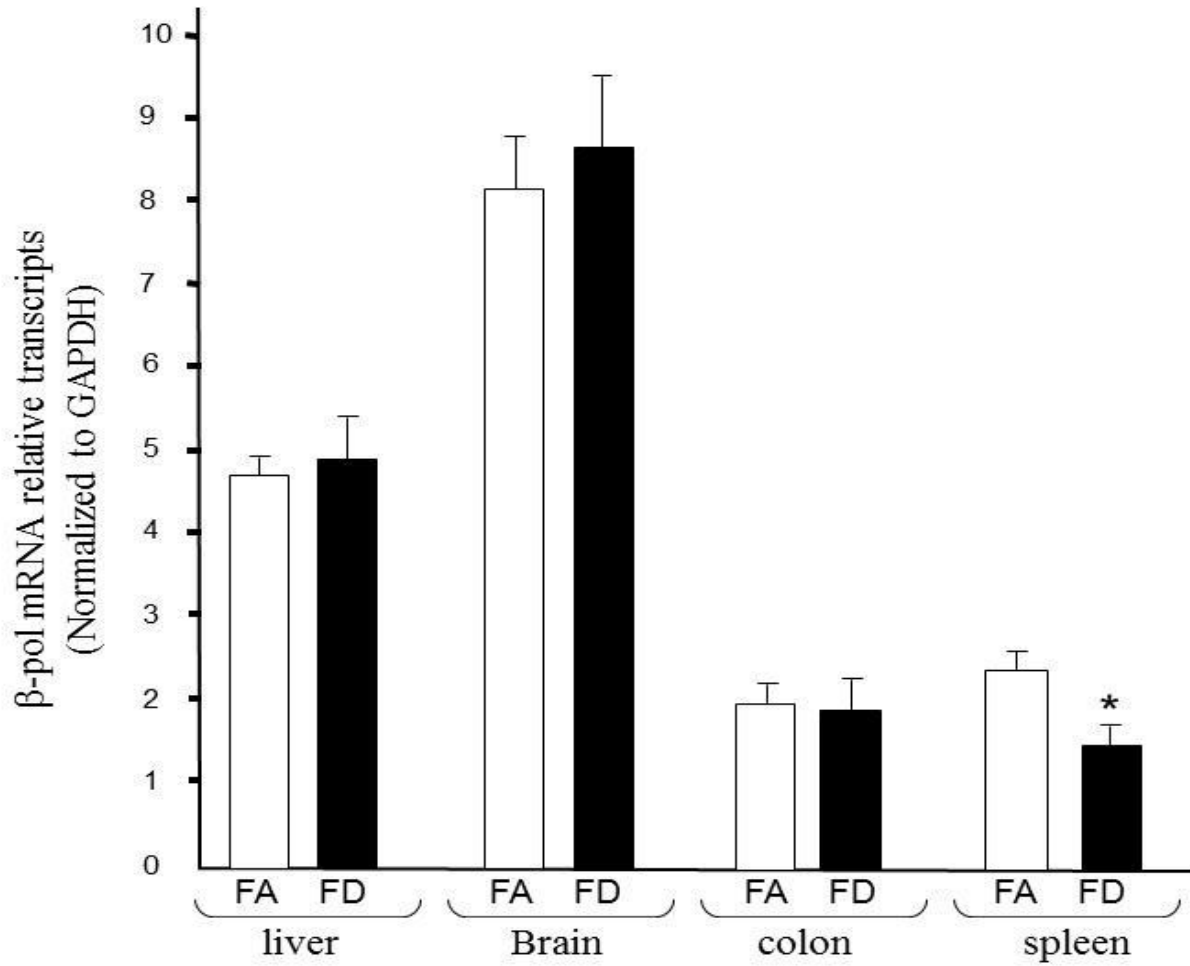
Figure 11 *Effect of folate deficiency on UNG promoter methylation in liver.* Methylation of CpG sites present within the 260bp CpG rich region in the UNG promoter using bisulfite sequencing assay. The bisulfite treated DNA was PCR amplified using primers designed around CpG islands. The resulting amplicons were cloned into pGEM-T Easy Vector

Figure 11

```
                                                                    1
                                                            ccgaggcactag
          2     3   4                                                5
-250 ccaatagggatggggcacggtcgccgcagagccaatcagtgtgcagcgtg
      6                7 8                      9              10
-200 cccgcccctgctcctcgcgtggtccaatcaaaagcggcaaggggcgggag
         11 12                13                     14 15 16
-150 ctgttttgccgcgaaaagcccacgtggaagtcttgggtgaggcgcgcggg
                  17 18          19           20      21
-100 gcagcaccaggcagcgcgagactgcggtgctgcgggtcccgggcaggaga
       22 23      24
-50  gccgcgcaccccgtttatcagccagactgggacaccttagtccaaaacaa
```

CpG Sites:	1	2	3	4	5	6	7	8	9	10	11	12	13	14	15	16	17	18	19	20	21	22	23	24
Liver FA	0	0	0	0	0	0	0	0	0	0	0	0	0	1	0	0	0	0	0	0	1	0	0	
Liver FD	0	0	0	0	0	0	0	0	0	0	0	0	0	0	0	0	0	0	0	0	0	0	0	
Brain FA	0	0	0	0	0	0	0	0	0	0	0	0	1	0	0	0	0	0	0	0	0	0	0	
Brain FD	0	0	0	0	0	0	0	0	0	0	0	0	0	0	0	0	0	0	0	0	0	1	0	

No. of colonies show methylation per seven colonies sequenced

Figure 12 *Effect of folate deficiency and 2-NP on β-pol promoter methylation in liver.*
Methylation of CpG sites present within the β-pol promoter and exon 1 was determined in liver, brain, and spleen using bisulfite sequencing assay. The bisulfite treated DNA was PCR amplified using primers designed around CpG islands. The resulting amplicons were cloned into pGEM-T Easy Vector. Plasmids from 7 colonies of each subclone were sequenced and the presence of preserved methylated cytosine residues representing methylation status was determined. FA: Folate adequate; FD: Folate deficient.

Figure 12

Figure 13 *Effect of folate deficiency on p53 promoter methylation.* As a positive control, methylation of CpG sites within p53 gene between CpG rich regions in exon 5 and exon 8 using bisulfite sequencing assay. The bisulfite treated DNA was PCR amplified using primers designed around CpG islands. The resulting amplicons were cloned into pGEM-T Easy Vector.

Figure 13

CACTGGAAGACTCCAGGTAGGAAGG***CGCG***TGGTAGGTTAGGTTAGC

                                                              3   4
CTGTTTCTTCCCCAGCTTCTGCCTGTTTCTGTTCCA***CG***AGTCC***CG***C

                    5
CCCCTACCACATGCCCAA***CG***CTCTTTGGTTCCTACCCTATCTACCT

                                                                              6
AAATGAAGTCTCCTCCTCTGTTTCCTCTTGGGCTTAGGGA***CG***TCTC

        7
TTATCTGTGGCTTCT***CG***GGGGTTCCT
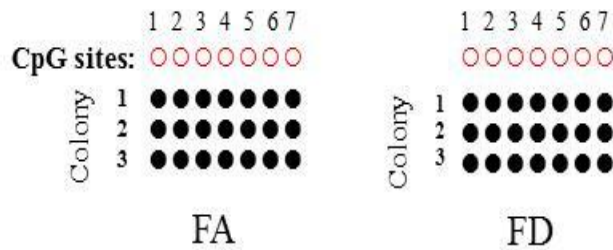
CHAPTER 3: IMPACT OF FOALTE DEFICIENCY AND *β-POL* HAPLOINSUFFICIENCY ON DNA DAMAGE AND REPAIR IN RESPONSE TO ACUTE AND LONG-TERM CARCINOGEN EXPOSURE

Introduction

Folate is a critical vitamin required for one-carbon metabolism in maintaining DNA stability through DNA synthesis, repair and methylation reactions. Folates obtained from the diet can enter the folate cycle and transfer one-carbon units in the production of purines through addition of a formyl group to 5,10-methylene tetrahydrofolate yielding adenosine and guanine, and also in the production of thymidine by conversion of dUMP to dTMP via thymidylate synthase (TS). Since the repair of DNA damage requires insertion of the correct nucleotide it is imperative that nucleotide pools are sufficient for the DNA synthesis step of DNA repair. One-carbon metabolism also includes the methionine cycle where 5-methyl THF remethylates homocysteine to methionine which is converted to SAM, the principle methyl donor in most biological reactions such as methylation of CpG sites in promoter regions [104].

Depletion of dietary folate results in an imbalance in one-carbon metabolism by limiting DNA precursors, compromising DNA repair and altering gene promoter methylation patterns. Folate deficiency has been implicated in the development of several human cancers and although the exact mechanism remains to be determined, it is the alteration in each of these processes that sets the stage for carcinogenesis. The maintenance of DNA repair fidelity is a primary concern in folate limiting conditions as depletion of thymidine results in uracil misincorporation. Initiation of repair by removal of the misincorporated base under continued folate depletion can cause DNA strand breakage, chromosomal aberrations and malignant transformation [24], [25]. The base excision repair (BER) pathway is responsible for small, non-helix distorting DNA

lesions including uracil misincorporation, 8-oxo-guanine, N-7 MeG, N-3 MeG as well as routine DNA damage mediated by ROS during normal cellular metabolism [84]. Our lab has shown that folate deficiency compromises BER by initiation repair but failure to induce *β-pol* to complete the process resulting in accumulation of toxic repair intermediates [70]. It has been reported that FD impairs excision of oxidative and alkylation damage in human lymphocytes [26]. Repair of 8-oxodG lesions is inhibited in folate-depleted rat neurons [28]and colon cells from FD rats [29]. 8-oxo-dG is a highly mutagenic base, inducing G:C to T:A transitions if left unrepaired [74]. Loss of DNA repair mechanisms can promote cancer development as observed in heritable colon cancer where mutations in mismatch repair genes are common in patients with this type of colon cancer and in xeroderma pigmentosum where individuals suffer from accelerated rates of skin cancer due to mutations in NER genes [105]. Polymorphisms in BER genes such as *β-pol*, hOGG1 and XRCC1 are being examined in conjunction with increased relative risk of certain cancers [106], [107]. However, currently there is no specific disease condition associated with loss of BER capacity. Interestingly, many human cancers express variants of *β-pol*, the rate-limiting enzyme in the BER pathway. It is estimated that approximately 30% of human tumors display amino acid changes, deletions or over-expression in the *β-pol* transcript [108-110]. Variants, depending on the type, could result in loss of repair fidelity and interference of repair due to functional-deplete variants leading to genomic instability and conferring a mutator phenotype [111, 112]. Overall, an imbalance in BER and key enzymes in the pathway (i.e. *β-pol*) can result in a functional BER deficiency promoting the onset of carcinogenesis through genomic instability.

Human exposure to DNA damaging agents occurs routinely from endogenous sources such as reactive oxygen species and exposure to exogenous sources from environmental agents

such as UV rays, ionizing radiation, chemicals and pollutants [113, 114]. Exposure to alkylating agents can be from many sources including chemotherapeutic drugs, diet, cigarette smoke, fuel combustion, and nitrosation of amines and amides mediated by enteric bacteria [115-117]. Damage to the genome must be repaired in order to maintain genomic stability and prevent persistent, heritable mutations through DNA replication.

Since folate deficiency has been demonstrated to compromise DNA repair and is a proposed driver of carcinogenesis, I investigated the mechanism of base excision repair in folate deficient animals treated with 1,2 dimethylhydrazine (DMH), a known carcinogen and SN-1 alkylating agent. In order to elucidate the in vivo response to alkylating agent, two time points were used to determine acute response (24-h) and long-term response (6-week) in both wild-type and β-pol haploinsufficient mice. Here, in the wild-type animals it is shown that folate deficiency in response to acute treatment with carcinogen shuts down BER and induces apoptosis signaling. However, after long-term treatment there is an adaptive response to DNA damage, showing initiation of repair but failure to increase overall BER resulting in clastogenic repair intermediates. This loss of initial response to DNA damage allows for accumulation of damage which persists with continued exposure to carcinogen and failure to complete repair, resulting in overall increased mutagenesis driving oncogenic progression in the FD animals.

Materials and Methods

Animals- Experiments were performed in young (4 to 6 month old) C57BL/6-specific pathogen free male mice and mice heterozygous for the DNA polymerase β gene (β-pol$^{+/-}$) and backcrossed to the C57BL/6 background.   All practices performed on animals were in agreement with the National Institutes of Health (NIH) guidelines for the care and use of

laboratory animals under a Wayne State University Animal Investigation Committee approved animal protocol. Mice were maintained on a 12-h light/dark cycle and given water *ad libitum*.

Diets and Carcinogenic Treatment- After acclimation for 7 days, wild-type (WT) and β-pol$^{+/-}$ mice were randomly assigned to two dietary groups; a folate adequate (FA) or folate deficient (FD) AIN93G-purified isoenergetic diet (Dyets, Inc., Lehigh Valley, PA) as described previously (17). The FA group received a folate adequate diet containing 2 mg/kg folic acid. The FD group received a folate-deficient diet containing 0 mg/kg folic acid. Diets were stored at −20°C. 1% succinyl sulfathiazole was added to all diets. Eight weeks after assigned feeding, randomly selected mice from both FA and FD were injected i.p. with 1,2-Dimethylhydrazine HCL (DMH, 30 mg/kg body weight) in 10mmol/L of $NaHCO_3$ (Fisher Scientific, Fair Lawn, NJ) 24-hours prior to sacrifice or for long-term treatment, animals were injected once weekly for 6 weeks and then maintained on respective diets for an additional 8 weeks until sacrifice. Euthanasia was performed by CO2 asphyxiation as approved by the animal protocol.

Gene Expression Analysis by Real-time PCR- The mRNA expression level of genes involved in BER pathway were quantified using real-time PCR. Briefly, total RNA was extracted from liver and colon tissue of folate added & folate deficient mice using RNeasy Kit (Qiagen, Valencia, CA). First strand cDNA was synthesized from 1 μg RNA using ImprompII reverse transcriptase kit (Promega, Madison, WI) and purified using QIAquick PCR purification kit (Qiagen, Valencia, CA). External standards for all the genes were prepared by subcloning the amplicons into pGEM-T easy vector. The vectors were linearized using EcoR1 to make the standard curves. All BER gene transcripts were normalized to RPLO.

Western blot analysis- Western blot analysis was performed using 100µg nuclear protein as previously described (18). Proteins were separated by 12% SDS–PAGE gel, and transferred onto nitrocellulose membrane for Western blot analysis. The gel was stained with GelCode blue stain reagent (Pierce Biotechnology) to ensure equal protein loading. Western analysis was accomplished using affinity purified polyclonal antisera developed against mouse β-pol, Ape1, and UDG. As an internal control for protein loading, membranes were reprobed with anti-Lamin B antibody (Santa Cruz Biotechnology, Santa Cruz, CA). The bands were visualized and quantified using a Biorad Molecular Imager after incubation in SuperSignal® West Pico Chemiluminescent Substrate (Pierce Biotechnology, Rockford, IL). Data are expressed as the integrated density value (I.D.V.) of the band per µg of protein loaded.

Detection of relative uracil levels- 4 ug DNA from liver was isolated as described [70] and blocked with methyoxyamine for 2 hr at 37 deg C, treated with 0.2 units of UDG (New England Biolabs) for 15 minutes at 37 deg C. DNA is then probed with 2mM biotinylated ARP (Dojindo Molecular Technologies, MD) for 15 minutes at 37 deg C. DNA is then immobilized on nitrocellulose membrane, the membrane washed in 5X SCC and baked at 80 deg C for 30 minutes then incubated with HRP-containing hybridization buffer for 45 minutes. After washing, the membrane is incubated in ECL (Thermoscientific, Rockford, IL) for 5 minutes and then visualized and exposed using Bio-Rad ChemiImaging system. The data are expressed as integrated density value (IDV) of the band per microgram loaded.

Detection of relative abasic sites- 4ug of DNA from liver was isolated as described and probed with 2mM biotinylated ARP (Dojindo Molecular Technologies, MD) for 15 minutes at 37 deg C. DNA is then immobilized on nitrocellulose membrane, the membrane washed in 5X SCC and baked at 80 deg C for 30 minutes then incubated with HRP-containing hybridization

buffer for 45 minutes. After washing, the membrane is incubated in ECL (Thermoscientific, Rockford, IL) for 5 minutes and then visualized and exposed using Bio-Rad ChemiImaging system. The data are expressed as integrated density value (IDV) of the band per microgram loaded.

UDG Activity Assay- 5ug of liver nuclear extract was incubated in a reaction mixture containing 1mM EDTA, 1mM DTT, 75mM NaCl. 0.5%BSA and 90fmol of a 5'-end labeled single-strand uracil-containing oligo with a 3'-protected end (Invitrogen). Reactions were incubated at 37 deg. C for 1 hour and then terminated by addition of 5ug proteinase K and 1uL 10% SDS for 30 min at 55 deg C. Substrate and reaction products were separated on a 20% denaturing sequencing gel. Glycosylase activity, indicated by presence of an 11-mer band, was visualized and quantified using the Biorad Molecular Imager. Negative controls consisted of a reaction mixture without nuclear extract and UDG inhibitor was added to ensure glycosylase was the result of UDG specifically and not a complementary glycosylase.

BER assay- DNA base excision repair was determined by BER assay. Biotin-end labeled 30-bp oligonucleotides (upper strand, 5'-ATATACCGCGGUCGGCCGATCAAGCTTATT-3' and lower strand, 3'-TATATGGCGCCGGCCGGCTAGTTCGAATAA-5') containing a G:U mismatch and HpaII restriction site were incubated in reaction mixture of 110mM Tris-HCl, 5mM MgCl2, 1mM DTT. 0.1 mM EDTA, 2mM ATP, 20uM dNTPs, 10 units pCPK with 50 ug liver nuclear extract for 30 minutes at 37 degrees C, followed by termination of reaction at 95 degrees C. Reannealing of the oligos for 1 hour at room temperature and then centrifuged to pellet any denatured proteins. Supernatant was treated with 20 units of HpaII RE for 1 hour at 37 degrees C and then separated on a 20% denaturing sequencing gel. Repair activity, indicated

by presence of a 16-mer band was visualized and quantified using Bio-Rad ChemiImaging system, was calculated by determining the ratio of product to substrate.

Single-strand break assay- Assessment of single-strand breaks was determined by the Fast Micromethod DNA Single Strand Break assay as described by Henderson (DNA Repair Protocols). This method is based on the ability of the specific fluorochrome Picogreen (Molecular Probes, Eugene OR) to make a stable complex with double-stranded DNA in alkaline conditions. The preferential binding of Picogreen to double-strand DNA over single-strand DNA or proteins allows detection of single-strand breaks in the DNA by following the fluorometric signal intensity. The decreasing signal intensity during denaturation is measured at Excitation/Emission of 485/538 using a fluorescence microplate reader (Genios Plus, Tecan) and is proportional to increasing single-strand break content. Results were calculated after 10 minutes in denaturing solution (1M NaOH, 20mM EDTA, 1% DMSO) and normalized to reference control sample and expressed as fluorescence units at 538 nm.

Casp-3 Assay- Casp-3 activity was measured using EnzChek (Molecular Probes, Eugene OR) to detect apoptosis in liver cell extracts. Arg-Glu-Val-Asp-AMC substrate specific proteolytic cleavage by Casp-3 is measured by fluorescence. 50uL of liver whole cell extract was used and incubated with Z-DEVD-AMC substrate for 30 minutes in the dark. Fluorescent product was monitored by a fluorescent microplate reader (Genios Plus, Tecan). Results are expressed as fluorescent units (FlU) at 440nm.

Statistical Analysis- Statistical significance between means was determined using analysis of variance, t-test where *p* values less than 0.05 were considered statistically significant.

Results

Analysis of DNA repair activities and damage resolution in response to 24-hour DMH treatment.

Analysis of UNG mRNA expression, UDG protein expression, UDG activity and uracil levels in liver from FA or FD mice treated with DMH.

Folate deficiency alters one-carbon metabolism resulting in changes in DNA synthesis and repair. Low levels of 5,10-methylene THF reduces the conversion of dUMP to dUTP resulting in misincorporation of uracil. Removal of this DNA lesion can be performed by several monofunctional glycosylases known as UDGs (uracil DNA glycosylases) and are encoded by the genes UNG and SMUG1. The majority of UDG activity is due to expression of UNG2, the nuclear isoform from the UNG gene locus [118]. I therefore determined the mRNA expression of UNG and UDG protein expression in response to 24-hour DMH treatment in FA and FD mice. The wild-type animals show a significant reduction in UNG mRNA expression in the FD condition when treated with DMH as compared to the FA condition (p = 0.001) (Fig 14A). In the β-pol$^{+/-}$ animals I observe reduced overall UNG expression with no significant change in expression between the FA and FD treated condition (Fig 14A). UDG protein immunoblot analysis shows reduced protein expression in the DMH treated wild-type FD animals compared to the FA group correlating to the mRNA expression data (Fig 14B). The UDG protein levels in the FD treated β-pol$^{+/-}$ animals, however, is increased compared to the FA animals (Fig 14C). Although the UNG mRNA expression is not upregulated in the FD treated knockout animals, the immunoblot data indicates the protein is stabilized in response to DMH treatment in the FD animals. DMH treatment in the wild-type animals failed to upregulate gene expression and increase protein expression of the critical uracil DNA glycosylase in response to FD indicating a possible abrogation of DNA repair initiation in these animals.

Folate deficiency has been shown to increase uracil levels in DNA through reduced thymine synthesis and increased dUMP/dTTP ratios [25]. Since dUTP is an excellent substrate for most replicative polymerases it can be readily misincorporated into DNA under folate limiting conditions. To assess the level of uracil misincorporation, the uracil-ASB assay was performed on DNA isolated from livers of wild-type and β-pol $^{-/+}$ mice in the indicated treatment groups. In wild-type animals, a significant reduction in uracil levels is observed in FD treated as compared to FA treated. The knockout FD treated animals show reduction in uracil levels although this is not significant (Fig 15A). As shown previously, uracil misincorporation was significantly increased in wild-type folate deficient animals yet here I see reduced levels of uracil while UDG is also reduced. This finding could indicate possible attenuation in DNA synthesis due to increased damage burden, i.e. cell cycle checkpoint for decision to mediate repair or undergo apoptosis. Uracil excision was determined by the UDG activity assay which measures the glycosylase activity of liver nuclear extract by ability to excise uracil from a 30-mer oligo substrate. The wild-type animals show significant reduced glycosylase activity in the FD treated condition (Fig 15B), consistent with the reduced UNG mRNA expression and UDG protein expression. In the β-pol$^{+/-}$ mice, UDG activity is higher in the FA control and FA treated conditions compared to FD control and FD treated, with significance observed between FD untreated and FA treated (Fig 15C). These differences could perhaps be due to reduced coordination of repair initiation in the β-pol haploinsufficient animals. A UDG inhibitor was used in one reaction to demonstrate glycosylase activity was the result of UDG specifically, and not another uracil-specific glycosylase such as SMUG1, further indicating that the FD wild-type treated animals fail to initiate DNA repair.

Analysis of β-Pol gene expression, β-Pol protein expression and level of BER activity in liver from FA or FD mice treated with DMH.

β-polymerase is a key enzyme in the BER pathway possessing both nucleotide transferase activity and dRP lyase activity essential for completion of single-nucleotide repair. After Ape/Ref-1 hydrolyzes the abasic site leaving behind a 5'-deoxyribose phosphate (dRP), *β-pol* fills the gap of the excised nucleotide and removes the dRP group [41]. β-pol is a 39 kDa DNA polymerase where the 31 kDa domain contains the nucleotidyl transferase activity and the 8 kDa domain has the dRP lyase activity [38, 39]. It has been determined that the dRP lyase activity is essential and rate-limiting during BER initiated by monofunctional glycosylases [41]. The high level of sequence conservation of *β-pol* among species indicates high probability that it is essential for animal survival [119]. BER is attenuated in the absence of β-pol leading to hypersensitivity to genotoxins; *β-pol* null cells are hypersensitive to MMS [120], [121],[122]and *β-pol* gene deletions in KO mice display reduced DNA damage threshold and increased genomic instability [123] [124].

In this study, *β-pol* mRNA expression was not significantly different between groups in the wild-type animals showing no increase in response to DMH treatment in either the FA or FD groups (Fig 16A). In the knockout animals, overall mRNA β-pol expression is reduced by close to 50% compared to the wild-type counterparts as our lab has previously shown [125]. In response to DMH both the FA and FD knockout animals show upregulation of *β-pol* (Fig 16A). *β-pol* protein expression, as determined by western blot analysis, shows a significant increase in expression in both the FD wild-type and *β-pol*$^{+/-}$ treated animals (Fig 16B,C), however this increase failed to reach statistical significance in the wild-type animals. The higher protein expression in comparison to mRNA levels in the wild-type animals could indicate the cellular feedback to turn off gene expression in the presence of abundant protein. However, the protein

expression is several fold higher in the FD DMH compared to one FD control animal (data not shown). As shown for the knockout animals, the protein is stabilized significantly in the FD DMH group compared to the controls showing a similar trend to the mRNA expression data. To directly look at the effect of folate deficiency and acute impact of DMH on BER, I performed the BER activity assay on liver nuclear extracts from wild-type and β-$pol^{+/-}$ animals in the indicated groups. Interestingly, FD wild-type animals treated with DMH show a significant (p=0.04) increase in BER (Fig 16D) while glycosylase expression and activity is not induced as shown above. Seeing as β-pol protein expression is stabilized in these animals, this could be an indication of dysregulation within the typical tightly-coordinated BER pathway. Our lab has previously shown that imbalanced BER by lack of increased β-pol expression and BER activity results in accumulation of toxic repair intermediates [70]. However, imbalance created by increased β-pol expression and BER activity can also lead to functional deficiency of the BER pathway and promote genomic instability [126]. The β-pol knockout animals show no significant increase in BER activity in the FD DMH treated condition (Fig 16D). The knockout animals showed increased UDG and APE/Ref1 expression indicating initiation of the pathway with failure to increase BER activity to complete repair. To continue to elucidate the mechanism of DNA repair I investigated expression levels of other important genes and proteins in the BER pathway.

Analysis of base excision repair pathway genes and Ape/Ref-1 protein levels in liver from FA or FD mice treated with DMH.

The base excision repair pathway is an efficiently coordinated process in which the product of one reaction is passed on to the next reaction while keeping the toxic repair intermediates from accumulating and initiating downstream signaling effects. The process is initiated by glycosylase damage recognition and removal of the offending base, creating an

abasic site. From there, Ape/Ref-1 incises the phosphate backbone leaving behind a dRP moiety (in the case of a monofunctional glycosylase), and β-pol inserts the new base and removes the dRP group followed by ligation of the strand by Ligase-III [41].

To further investigate the repair mechanisms in response to FD and acute DMH treatment I compared mRNA expression of genes in the BER pathway. As shown above, the UNG glycosylase mRNA expression shows significant reduction in the FD wild-type treated animals compared to FA treated (Fig 17A). The highest UNG expression in the knockout animals is observed in FA control, with overall expression lower than FA treated wild-type (Fig 17A).

MBD-4 (Methyl Binding Domain protein 4) acts as a uracil and thymine glycosylase that recognizes and removes G:T and G:U mismatches caused from spontaneous deamination at CpG sites [127]. If left unrepaired, these mismatches would result in transition mutations at promoter methylation sites [128], [129], [130], [131]. The mRNA expression of MBD-4 in the wild-type animals shows significant (p=0.002) loss of expression in FD DMH compared to FA DMH, and no significant induction of expression vs. FD control (Fig 17B). The $β\text{-}pol^{+/-}$ FD and treated animals show significantly reduced expression compared to FA control animals (Fig 17B). Although we don't expect to see increased cytosine deamination with DMH treatment, it has been shown that some carcinogenic agents can preferentially alkylate CpG sites in promoter regions resulting in mutational hot spots [132], [133]. The severely reduced expression of MBD-4 in the knockout animals could indicate failure to initiate additional glycosylase activity above that of UNG.

As shown above, $β\text{-}pol$ mRNA is not significantly increased in response to DMH in the FD wild-type animals with the $β\text{-}pol^{+/-}$ showing a 50% reduction in mRNA expression (Fig 17C). The completion of BER requires ligation of the DNA strand by DNA Lig-III. mRNA expression

of Lig-III in wild-type animals shows significantly increased expression in the FA DMH treated compared to the FD DMH treated animals indicating Lig-III available to complete repair (Fig 4D). In the β-$pol^{+/-}$ animals, a significant reduction in Lig-III expression is seen in the FD and DMH treated animals compared to the FA untreated (Fig 17D). Both the FA wild-type and FA knockout mice demonstrate increased Lig-III expression correlating to the increased glycosylase expression and completion of repair.

Poly (ADP-ribose) polymerase-1, or PARP-1 has been identified as a critical protein in BER as it binds to AP sites and single-strand breaks (SSBs), protecting these sites from cellular nucleases [134] while recruiting BER machinery to the site [135], [136]. PARP-1 has been described as a BER sensor and functions as a regulatory molecule in response to DNA damage [137], [138]. Parp-1 mRNA expression in the wild-type mice is significantly upregulated in the FA DMH treated condition compared to control and DMH treated FD animals indicating presence of PARP-1 with increased repair capacity (Fig 17E). In conjunction with increased expression of the other enzymes in the BER pathway shown above, the FA untreated β-$pol^{+/-}$ animals show significantly elevated expression of PARP-1 (p=0.0001) (Fig 17F). The severe reduction in PARP-1 expression in the FD DMH treated β-$pol^{+/-}$ animals also indicates that Parp-1 is not available for protection of SSB as well as for activation and signaling of cell death. Parp1 has been shown to prevent the conversion of excessive SSBs to DSBs by binding to the SSB and providing protection until repair proteins are sufficient [139]. Parp1 has also been implicated as a sensor of BER, functioning to monitor the status of BER and to initiate cell death in the event of BER failure [138]. In the case of DMH treated β-$pol^{+/-}$, absence of Parp1could have dual detrimental effects: i.) reduced protection of SSB repair intermediates providing opportunity for formation of DSBs and chromosomal damage and ii) reduced sensing of

inadequate BER to initiate cell death and prevent accumulation of damage leading to further genomic instability.

Monofunctional glycosylases require an AP endonuclease to incise the DNA backbone at the 5'end of the AP site leaving a SSB with a 5'dRP and a 3'OH group. Expression of Ape/Ref-1 protein, as determined by western blot analysis, is shown to be reduced in FD DMH treated wild-type animals compared to the FA DMH treated group (Fig 18A). This is consistent with the lack of repair initiation observed in the FD animals. In the *β-pol*+/- animals, expression of Ape/Ref1 is reduced in the FD untreated compared to FA untreated, consistent with higher glycosylase expression and activity as well as *β-pol* expression observed in the FA untreated animals. Interestingly, the FD knockout animals show significant increase in Ape/Ref-1 expression in response to DMH treatment (Fig 18B). This correlates to the increased UDG expression seen in these animals indicating processing of the AP site induced by the glycosylase.

Analysis of gene expression in response to alkylation damage in liver from FA or FD mice treated with DMH.

Dimethylhydrazine is a chemical alkylating agent shown to induce methyl adducts to DNA bases in the form of O^6Me-G and N-7 MeA [140]. Repair of alkylation damage by the BER pathway is initiated by methyl-purine glycosylase (MPG) and recognizes such damages as N-7 MeA and N-3 MeA. The base lesion O^6MeG is a stable adduct and can persist in DNA in the absence of the DNA repair protein, MGMT [141], [142]. The O^6MeG lesion is repaired by a one-step mechanism in which the alkyl group is transferred from the oxygen in the guanine to a cysteine residue on MGMT irreversibly, thereby inactivating MGMT [143]. This lesion is highly mutagenic if not repaired resulting in A:T transition mutations. In this study, the mRNA expression of both MPG and MGMT in response to folate deficiency and DMH was determined. In the wild-type animals, FD eliminated response of MPG to DMH treatment and no increase in

expression is shown in FD or DMH treated *β-pol*^{+/-} animals (Fig 19A). This finding indicates failure to initiate BER in response to alkylation damage in the FD condition. The expression of MGMT is even more dramatically reduced in wild-type FD animals (p=0.001) in response to DMH and the knockout animals showing no significant upregulation of gene expression in response to DMH treatment (Fig 19B). Loss of repair mechanisms to remove the highly mutagenic lesion O^{6}MeG and persistence of alkylation damage such as N-7 MeG and N-3 MeA can result in mutations in onco genes such as Kras which is shown to be a potent driver in carcinogenesis.

Analysis of DNA damage in response to acute DMH treatment in liver from FA or FD mice.

Damaged or misincorporated bases are removed by a lesion-specific glycosylase resulting in an abasic site that is then recognized by apurinic/apyrimidinic endonuclease, APE1/Ref-1. Abasic sites are considered intermediates in the BER pathway and can be formed spontaneously by hydrolysis of the N-glycosidic bond or following chemical modification of by DNA-damaging agents and removal by DNA glycosylases [144]. In this study, the level of abasic sites were quantified using the adehydic-reactive probe slot-blot (ASB) method [145]. As shown, the number of abasic sites was reduced in DMH-treated FD wild-type animals as compared to the FA counterparts (Fig 20A). The glycosylase activity, as shown above, is not increased in these animals further indicating failure to initiate repair of the damage and subsequent persistence of the lesions. In the *β-pol*^{+/-} animals, the level of abasic sites in DMH-treated animals is increased with significant increase in the DMH-treated FD condition versus untreated animals (Fig 20A). Given that the DMH-treated FD knockout animals showed increased UDG levels, elevated UDG activity, and increased Ape/Ref-1 protein expression, repair of damage is initiated but persistence of AP sites indicates a block in completion of repair.

To look further into the level of DNA damage induced with 24 hour treatment of DMH in the FD condition, I determined the level of single-strand breaks using the Fast-micromethod for detection of single-strand breaks [146]. Single-strand breaks are a DNA repair intermediate where the DNA backbone has been incised but not polymerized by β-pol and subsequent ligation completed. Interestingly, the level of SSBs in the wild-type FD DMH-treated animals is increased significantly (p= 0.004) compared to the FD control animals (Fig 20B). This is inconsistent with previous findings where initiation of BER with failure to complete repair (i.e. loss of β-pol) resulted in an increase in SSBs [70]. Here, perhaps the imbalance of increased β-pol protein expression is creating a signaling cascade that results in SSBs. In the knockout animals, the FD DMH-treated show slightly elevated SSBs, although this finding is not significant (Fig 20B). This is consistent with increased glycosylase activity and abasic sites shown in these animals. Loss of PARP-1 recognition and protection of these sites can make them vulnerable to nuclease attack. Determining the resolution of this damage will aid in elucidating the fate of the cell in terms of cell killing or selection of a transformed population, initiating carcinogenesis.

Analysis of apoptosis signaling in response to acute DMH treatment in liver from FA or FD mice.

During cell cycle progression, transition from G1 to S phase requires CHK1 signaling to determine the level of DNA damage before the cell undergoes replication and mitosis. If the signaling determines the DNA damage to be too severe to be repaired, the cell will undergo apoptosis to prevent propagation of transformed progeny. Having determined BER activity and level of DNA damage in the form of abasic sites and SSBs, I then characterized the apoptotic response to acute DMH treatment under the condition of folate deficiency. The wild-type DMH-treated FD animals show significant induction of CASP-3 mRNA expression compared to FD

control (p= 0.01) and FA DMH (p= 0.007) demonstrating increased apoptosis signaling in response to DNA damage and failure to repair (Fig 21A). In the *β-pol^{+/-}* animals, overall CASP-3 expression is reduced with non-significant increase in FD DMH treated versus FD control (p= 0.26) (Fig 21A). Loss of apoptosis signaling in the presence of accumulation of damage and increased damage tolerance can lead to increased mutagenicity. To further confirm presence of apoptotic signaling, the Enz-chek Casp-3 activity assay was used to detect enzymatic cleavage by Casp-3 and Casp-7. As shown in Fig 21B, in the wild-type animals, Casp-3 activity was indeed increased in the FD DMH treated compared to FD control and FA DMH-treated and this was significant (p= 0.01 and 0.03, respectively). This shows that the activity of Casp-3 correlates to the mRNA expression for the wild-type animals. In the *β-pol^{+/-}* animals, the FA untreated show slightly increased Casp-3 activity although this was not significant. Interestingly, the wild-type FD treated animals showed increased Casp-3 activity compared to the knockout counterparts, and this result was significant (p=0.008) (Fig 21B).

Overall, the acute response to DMH treatment in folate deficient wild-type animals demonstrates a reduced capacity to upregulate glycosylases in order to initiate repair, reduced APE/Ref-1 to process damage, and shows upregulation of β-pol indicating a possible imbalance in BER signaling. The increased level of damage and failure to remove and repair the damage in these animals appears to result in increased SSBs and signaling of the apoptosis cascade. The *β-pol^{+/-}* FD DMH-treated animals, however display an attempt to initiate repair and process the damage but failure to complete BER. Although the number of SSBs is increased in these animals, Casp-3 expression and activity is not induced indicating tolerance of DNA damage. In order to understand how these initiating events progress, I studied the effect of 6-week treatment of DMH (long-term) on folate deficient animals.

Analysis of DNA repair activities and damage resolution in response to 6-week DMH treatment.

Analysis of UNG mRNA expression, UDG activity and uracil levels in liver from FA or FD mice treated with 6-week course of DMH.

In the condition of folate deficiency, the altered dUMP:dTMP ratios result in increased uracil misincorporation requiring a uracil DNA glycosylase to recognize and remove the damage. As our lab has previously shown, UNG expression is increased in response to folate deficiency and expression is further induced in response to FD and oxidative stress from animals treated with 2-NP (data not shown). In this study, a similar trend is observed showing increased UNG mRNA expression in response to FD in both the wild-type and *β-pol*^{+/-} animals and the expression is further increased with treatment of DMH (Fig 22). To assess the level of uracil misincorporation, the uracil-ASB assay was performed on DNA isolated from livers of wild-type and *β-pol*^{-/+} mice in this long-term treatment group. In the wild-type animals, the uracil levels were decreased in both the FA and FD DMH-treated groups compared to the untreated controls, as well as in the DMH-treated knockout animals (Fig 23A). This could indicate adapted glycosylase response to damage and efficient removal of the misincorporated uracil. However, when UDG activity was measured, the glycosylase activity in the FD treated animals was reduced compared to the FA counterparts (Fig 23B). The reason for increased UNG expression but reduced glycosylase activity in these animals is unclear, but perhaps indicative of an imbalance between gene expression and enzyme activity.

Analysis of β-Pol gene expression and level of BER activity in liver from FA or FD mice treated with a 6-week course of DMH.

To further characterize the BER pathway in FD long-term DMH-treated animals, I looked at mRNA expression levels of β-pol. β-pol gene expression was not induced in response to FD and DMH (Fig 24A). This has been demonstrated previously, failure to upregulate β-pol

in response to folate deficiency and DNA damage. Analysis of BER activity revealed no significant increase in activity in response to FD and DMH in the wild-type animals (Fig 24B), displaying a reduction in activity in the FD DMH-treated group. This is in line with previous studies showing failure to upregulate repair in FD conditions in response to DNA damage.

Analysis of gene expression in response to alkylation damage in liver from FA or FD mice treated with 6-week course of DMH.

As previously discussed, the removal of alkylating agent-induced lesions is critical to the integrity of DNA. In this study, the mRNA expression of both MPG and MGMT in response to folate deficiency and DMH was determined. In the wild-type animals, increased MPG mRNA expression was observed in the FD DMH-treated condition and down-regulation of MPG was observed in the knock-out animals compared to the wild-type counterparts (Fig 25A). The expression of MGMT was also upregulated in the wild-type FD DMH-treated animals with reduced expression in the β-pol$^{+/-}$ animals (Fig 25B). The increased glycosylase expression in the wild-type FD animals again indicates initiation of repair and upregulation of MGMT shows response to treatment with the alkylating agent DMH.

Analysis of DNA damage in response to 6-week DMH treatment in liver from FA or FD mice.

In the FD DMH-treated wild-type animals, there is an increased induction of AP sites and this increase nears significance compared to the FD untreated group (p=0.07). The increase in monofunctional glycosylase activity (UNG, MPG) with loss of subsequent processing of the site can lead to accumulation of abasic sites. In the β-pol$^{+/-}$ animals, the level of AP sites is reduced in the FD condition compared to FA and this result is significant (p=0.03) (Fig 26A). Analysis of the level of SSBs revealed a significantly reduced number of SSBs in the FD wild-type animals versus the FD untreated (p=0.002) (Fig 26B). It is interesting to note the dramatic induction of SSBS in the FA DMH-treated wild-type animals. The β-pol$^{+/-}$ animals displayed

overall reduced number of SSBs compared to untreated wild-type, but FD knockout showing near significant (p=0.056) increase compared to FA knockout.

Analysis of DNA apoptosis signaling in response to 6-week DMH treatment in liver from FA or FD mice.

Casp-3 mRNA levels were measured by real-time PCR and normalized to RPLO. The mRNA expression is not significantly reduced in FD treated wild-type animals compared to either FA or FD untreated, however FA treated animals showed significant reduction in Casp-3 mRNA expression (p=0.04) (Fig 27A). In the β-$pol^{+/-}$ animals, Casp-3 mRNA was reduced in FD treated, although this result did not reach significance (p=0.058). Activity of Casp-3 was measured using the Enz-Chek assay as described in "Materials and Methods". Induction of Casp-3 activity was observed in both wild-type treated FA and FD animals compared to untreated controls (p=0.001 and p=0.02 respectively) (Fig 27B). The FD β-$pol^{+/-}$ animals displayed reduced casp-3 activity compared to FA counterparts, and this result was significant (p=0.005) correlating to the Casp-3 mRNA data shown above.

Analysis of gene expression in mucosa in response to DMH treatment

Investigation of mRNA expression of DNA repair genes in mucosa from 24-h treated wild-type and knockout animals revealed overall upregulation in the folate deficient animals with a pattern of high expression in the FD knockout control animals (Fig 28). Interestingly, the CASP-3 expression in these untreated animals is reduced compared to DMH treated animals following the pattern of upregulation of genes to repair damaged DNA and inhibition of apoptosis. However, the CASP-3 expression is still significantly above control untreated and observing the trend in these mucosa data is upregulation in response to FD, it is possible that overall gene expression is increased. Mucosal cells have a high rate of DNA synthesis and a

turnover time of 24-48 hours which may explain higher response to damage by increasing gene expression in the FD untreated and DMH treated animals.

Under long-term DMH treatment, there are no significant differences in UNG mRNA expression between FA and FD or untreated controls (Fig 29A). In response to alkylation damage however, there is a decrease in MPG expression in the FD treated wild-type animals and this decrease is consistent in the knockout groups (Fig 29B). MGMT expression (Fig 29C), is induced in the FA DMH-treated but attenuated in FD treated and the knockout animals indicated compromised repair of alkylation damage in the mucosa of these animals. CASP-3 mRNA expression was determined and shows induction in the FA DMH-treated wild-type animals and in the FD knockout animals (Fig 29D), consistent with microarray data from these animals.

Discussion

This study compares the initial DNA repair response and damage resolution in folate adequate and folate deficient animals acutely treated with carcinogen (24-h) to the DNA repair and damage response after long-term (6-week) exposure. As shown in the 24-h treatment, FD wild-type animals demonstrate an overall reduction in repair initiation in response to DMH treatment by failure to upregulate UNG mRNA expression, UDG protein levels and activity. APE1 expression is reduced consistent with loss of repair initiation and processing. Interestingly, *β-pol* protein expression is induced in these animals and BER activity is induced. One explanation for this is an imbalance in BER by upregulation of *β-pol*. Elevated expression has been observed in several human cancers caused by deletions and amino-acid substitutions [147-149]. Altered *β-pol* transcripts result in dysfunctional protein leading to erroneous blocked repair [150]. Another possible explanation for elevated protein expression in these animals is left-over stabilized expression prior to DMH exposure. As indicated by failure to increase *β-pol*

mRNA levels, it is possible that in the short-term treatment, mRNA expression hasn't caught up to protein exp. A look at gene expression of enzymes in the BER pathway shows loss of expression throughout the pathway in the FD wild-type animals. Whereas the FA animals demonstrate increased glycosylase expression, increased PARP-1 expression and increased Lig-3 expression in response to DMH. Analysis of the level of abasic sites reveals significant reduction in the FD animals exposed to DMH. Since APE1 expression is not increased in these animals, one would expect to see an accumulation of AP sites in response to DNA damage. However, since glycosylase expression fails to be induced, it is probable that the damaged bases are not being removed, resulting in persistent lesions. It has been shown in b-pol null cells treated with MMS failed to induce AP sites allowing stable lesions such as N7-MeG and N3-MeA to persist in the DNA [40]. Further analysis of DNA damage includes determining the number of SSBs using the fast micromethod of SSB detection. Here, an increase in the number of SSBs is seen in the FD wild-type animals versus FA animals. Accumulation of excessive base lesions could explain this increase. Apoptosis signaling is also increased in the FD wild-type animals in response to DMH as indicated by increased Casp-3 mRNA expression and activity.

The β-pol$^{+/-}$ animals present a different response to acute DMH treatment than the wild-type counterparts. In these animals, FD induces expression of UNG and APE1 but no significant increase in BER activity. Parp-1 gene expression is reduced significantly in the knockout animals, with the lowest expression observed in the FD β-pol$^{+/-}$ animals indicating Parp-1 is not available for protection of SSBs and recruitment of late-stage BER enzymes. Interestingly, the level of AP sites is increased in the FD knockout animals even with increased APE1 expression to process the abasic site. AP sites can arise spontaneously as well and give rise to point

mutations and SNPs if DNA replication is not blocked [151]. In response to DMH treatment, Casp-3 mRNA expression and activity is not significantly increased in the FD knockout animals.

After prolonged treatment with DMH, the folate deficient wild type animals demonstrate an adapted response to DNA damage by inducing UNG, MPG and MGMT mRNA expression. However, *β-pol* gene expression is not induced in these animals and the level of BER activity is not significantly higher than the FD untreated animals. The number of abasic sites in the FD treated animals is significantly higher than FA or untreated control, corresponding to increased glycosylase removal of the damaged base but loss of sequential repair resulting in accumulation of BER intermediates. The level of SSBs in the FD treated animals is also higher than FD control animals (p=0.003) indicating further accumulation of DNA damage. Analysis of apoptosis signaling shows no significant increase in Casp-3 mRNA expression in the FD treated animals compared to controls, however the Casp-3 activity is higher in these animals and this result is significant (p=0.01).

Interestingly, the FA treated wild-type animals show very high levels of SSBs compared to controls and the FD animals. This could be a temporary artifact induced with increased overall repair in these animals, also explained by lack of apoptosis signaling (Casp-3 mRNA expression) in response to these breaks. However the possibility that folate supplementation after initiation of carcinogenesis could accelerate proliferation of cells with accumulated DNA damage is inviting to explore. There is emerging evidence that folate supplementation could be detrimental depending on the stage of carcinogenic transformation. As noted previously, Kras mutations are found in 30% of all cancers [152], and has been shown to be associated with increased expression of DHFR and TS, allowing Kras mutated cell to utilize the folate salvage pathway for DNA synthesis and oncogenic progression.

Clinical relevance from this study is the demonstration profound loss of DNA repair mechanisms in the folate deficient wild-type animals in response to acute treatment with alkylating agent. Many biological and chemo therapies used in the treatment of cancer require dual-agent regimens: one agent to induce cytotoxic DNA damage and another agent to inhibit the repair of the damaging lesion and promote cell killing. BER inhibitors targeting PARP-1, *β-pol*, and APE1 are being investigated in clinical trials to improve efficacy of chemotherapies. One such chemotherapy is temozolomide (TMZ) an alkylating agent used in the treatment of several cancers. This agent induces a spectrum of DNA lesions including O^6MeG, N7-MeG and N3-MeA [153], most of which is alkylation damage that can repair by the base excision repair pathway. Resistance to treatment with TMZ is associated with high levels of expression of DNA repair genes, rendering targeting of DNA repair pathways an attractive option in combinatorial therapies. As shown in this study, there is reduced BER response under FD conditions with acute DMH treatment. It is inviting to suggest that temporary folate deficiency could be used as an alternative mechanism to inhibit DNA repair and improve efficacy of TMZ. In this way, the clinical treatment plan would involve only a single-agent chemotherapy, therefore reducing toxicity and enhancing tolerability in patients.

This extensive investigation of DNA repair mechanisms and apoptosis signaling showed inhibited repair during acute carcinogen treatment followed by upregulation in apoptosis signaling. These studies were performed in liver, a tissue with comparatively slow cell turnover. However, excessive cellular loss due to injury, necrosis, or apoptosis, triggers rapid hepatocyte proliferation in order to regenerate the tissue. Since we observe induced apoptosis signaling in the livers of FD wild-type treated animals, this does not generally confer protection of oncogenic initiation through programmed cell death. The loss of repair and tolerance of damage in cells

could lead to selection of those initiated cells and proliferation of a cell population with a mutator phenotype. In future studies, it would be valuable to assess the amount and type of lesions present in the DNA and examine markers of cell proliferation in this tissue.

Figure 14 *Effect of folate deficiency and 24-h DMH on UNG mRNA expression and UDG protein levels in liver of wild type and β-pol haploinsufficient mice. A*, UNG mRNA expression from livers of C57Bl/6 wild type and *β-pol* haploinsufficient mice as determined by real-time PCR and normalized to RPLO. *B*, The level of UDG protein in liver nuclear extract from wild type or *C*, *β-pol* haploinsufficient mice on folate adequate or folate deficient diets treated with DMH was determined by Western blot analysis. The level of UDG protein was normalized based on the amount of protein loaded on each gel. The I.D.V. (integrated density value) corresponding to the level of UDG protein was quantified by the BioRad Molecular Imager® System. FA: Folate adequate; FD: folate deficient.
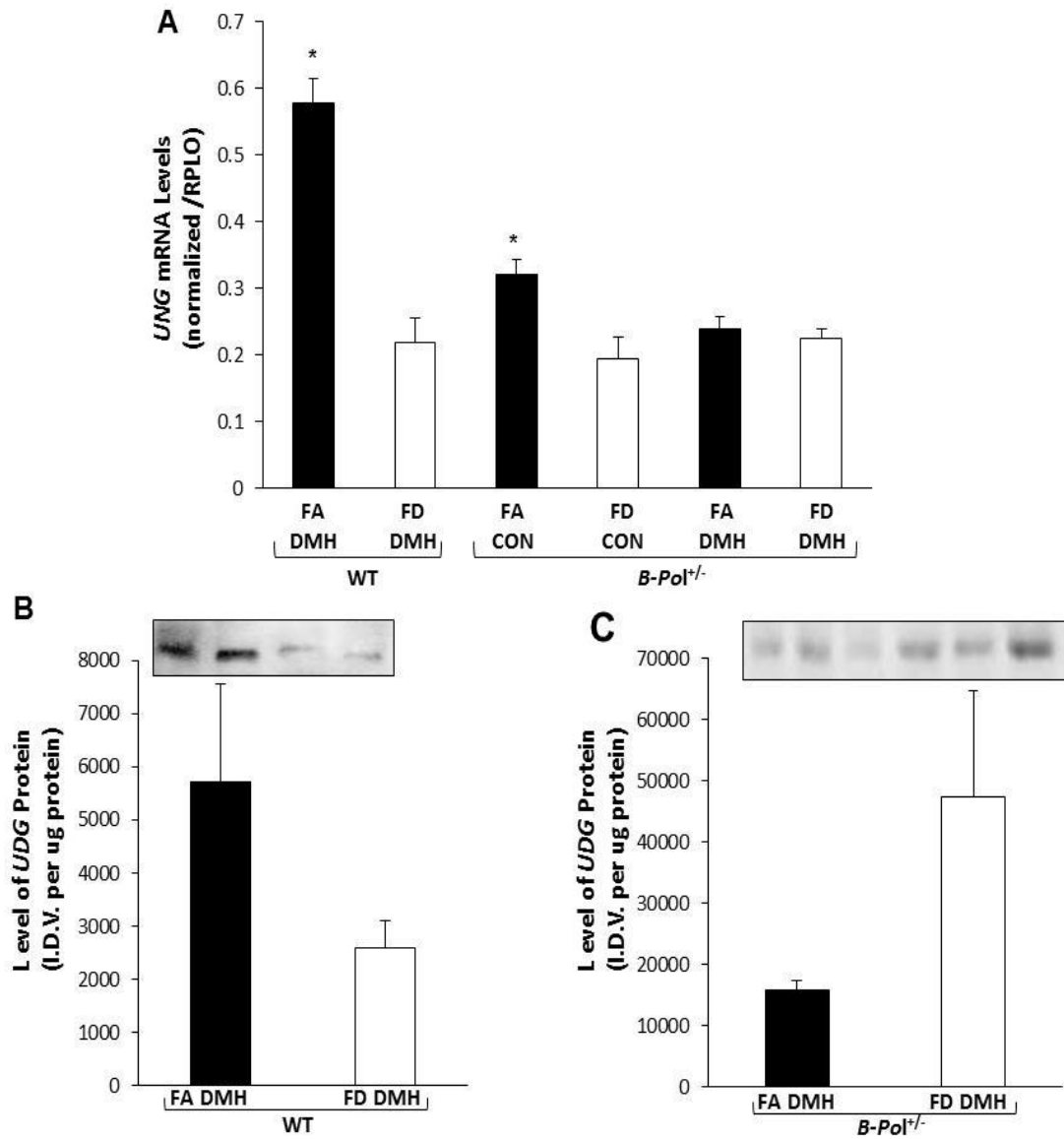
Figure 14

Figure 15 *Effect of folate deficiency and 24-hDMH treatment on Uracil levels and UDG activity in liver from wild type and β-pol haploinsufficient mice. A*, DNA from liver was isolated as described in "Materials and Methods". DNA was blocked with methoxyamine, treated with UDG, probed with biotinylated ARP, and immobilized via vacuum filtration onto a nitrocellulose membrane. Bands were visualized and quantified using the BioRad Molecular Imager® System and data are expressed as I.D.V. per ug DNA used. *B*, Assessment of UDG activity by ability to excise uracil in liver from wild type and *C*, β-pol haploinsufficient mice was performed as described in "Materials and Methods". 5'-end labeled uracil-containing oligo was incubated in 5ug liver extract and separation of substrate and reaction products were separated on a 20% denaturing sequencing gel. Glycosylase activity, indicated by presence of an 11-mer band, was visualized and quantified using the BioRad Molecular Imager® System and calculating the relative amount of the 11-mer oligonucleotide product with the unreacted 30-mer substrate (product/product + substrate). Results are expressed as I.D.V. per ug protein. FA: Folate adequate; FD: folate deficient. Significant differences at $p < 0.05$.
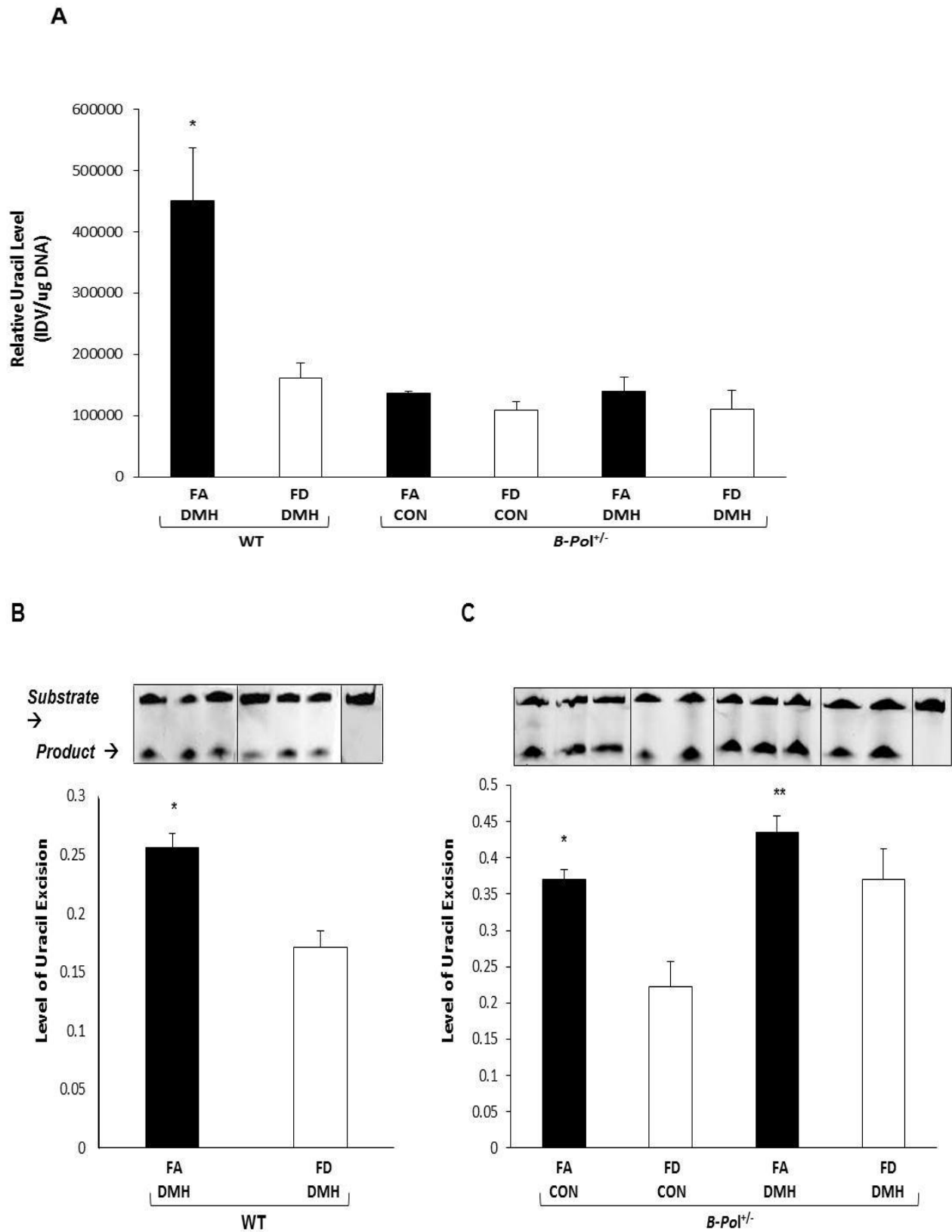
Figure 15

Figure 16 *Effect of folate deficiency and 24-h DMH treatment on β-pol mRNA expression and β-pol protein levels and base excision repair capacity in liver from wild type and β-pol haploinsufficient mice.* *A*, *β-pol* mRNA expression from livers of C57Bl/6 wild type and *β-pol* haploinsufficient mice as determined by real-time PCR and normalized to RPLO. *B*, The level of *β-pol* protein in liver nuclear extract from wild type or *C*, β-pol haploinsufficient mice on folate adequate or folate deficient diets treated with DMH was determined by Western blot analysis. The level of *β-pol* protein was normalized based on the amount of protein loaded on each gel. The I.D.V (integrated density value) corresponding to the level of *β-pol* protein was quantified by the BioRad Molecular Imager® System. *D*, Repair activity was analyzed by incubation of nuclear liver extract with G:U mismatch oligo and treatment with HpaII restriction endonuclease. Substrate and reaction products were separated on a sequencing gel and visualized and quantified with BioRad Molecular Imager® System and repair activity was assessed by appearance of a 16-mer fragment. Results are expressed as I.D.V per ug protein. FA: Folate adequate; FD: folate deficient. Significant differences at $p < 0.05$.
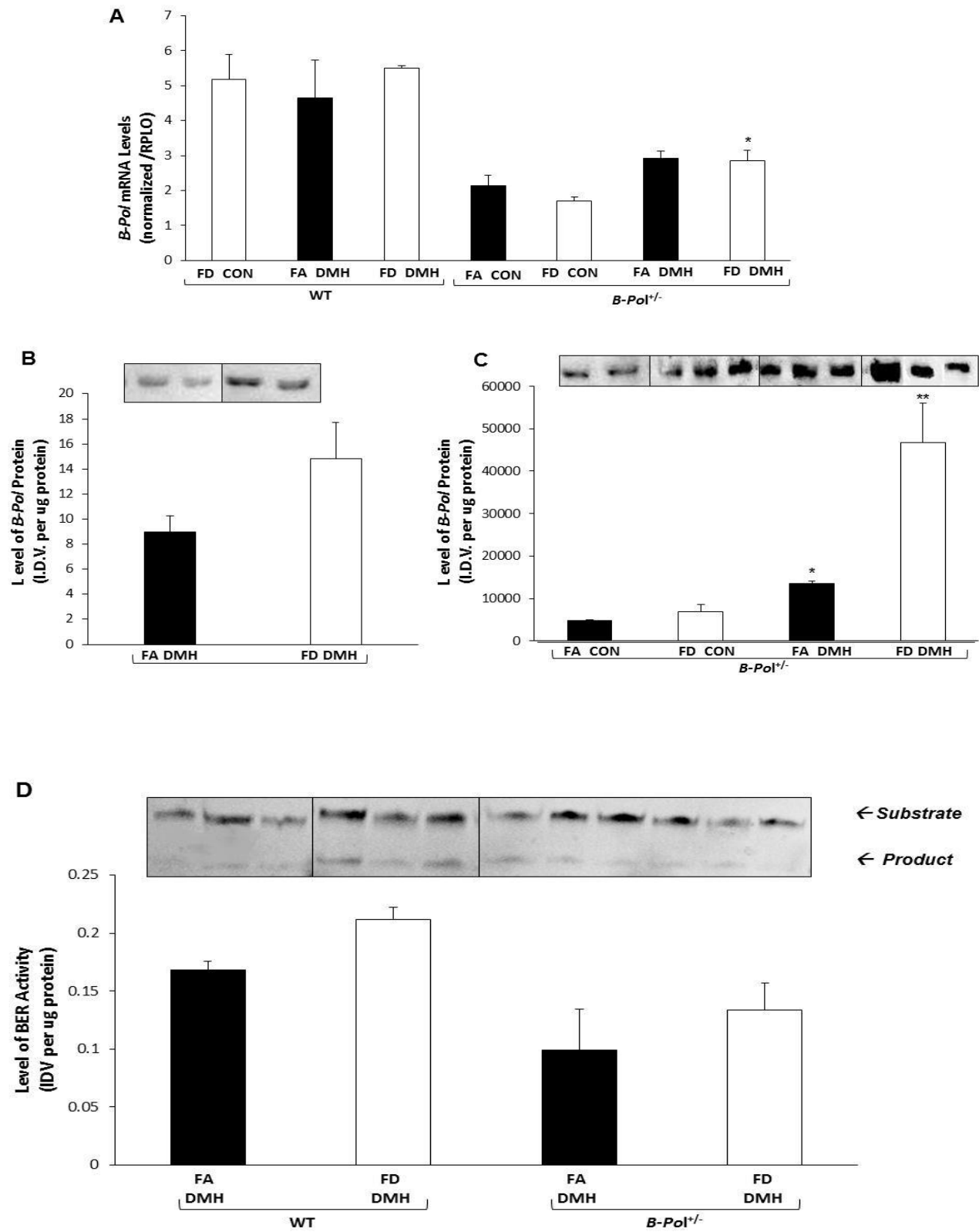
Figure 16

Figure 17 *Effect of folate deficiency and 24-h DMH treatment on expression of BER genes in liver of wild type and β-pol haploinsufficient mice.* Transcripts were quantified using real-time PCR and normalized to *Rplo*. *A*, *UNG* mRNA expression normalized against *Rplo*. *B, MBD-4* mRNA expression normalized to *Rplo*. *C*, *β-pol* mRNA expression normalized to *Rplo*. *D*, *Lig-3* mRNA expression normalized to *Rplo*. *E*-F, *Parp*-1 mRNA expression normalized to *Rplo*. *E*, wild-type. *F*, knockout. FA: Folate adequate; FD: folate deficient. Significant differences at $p < 0.05$

Figure 17
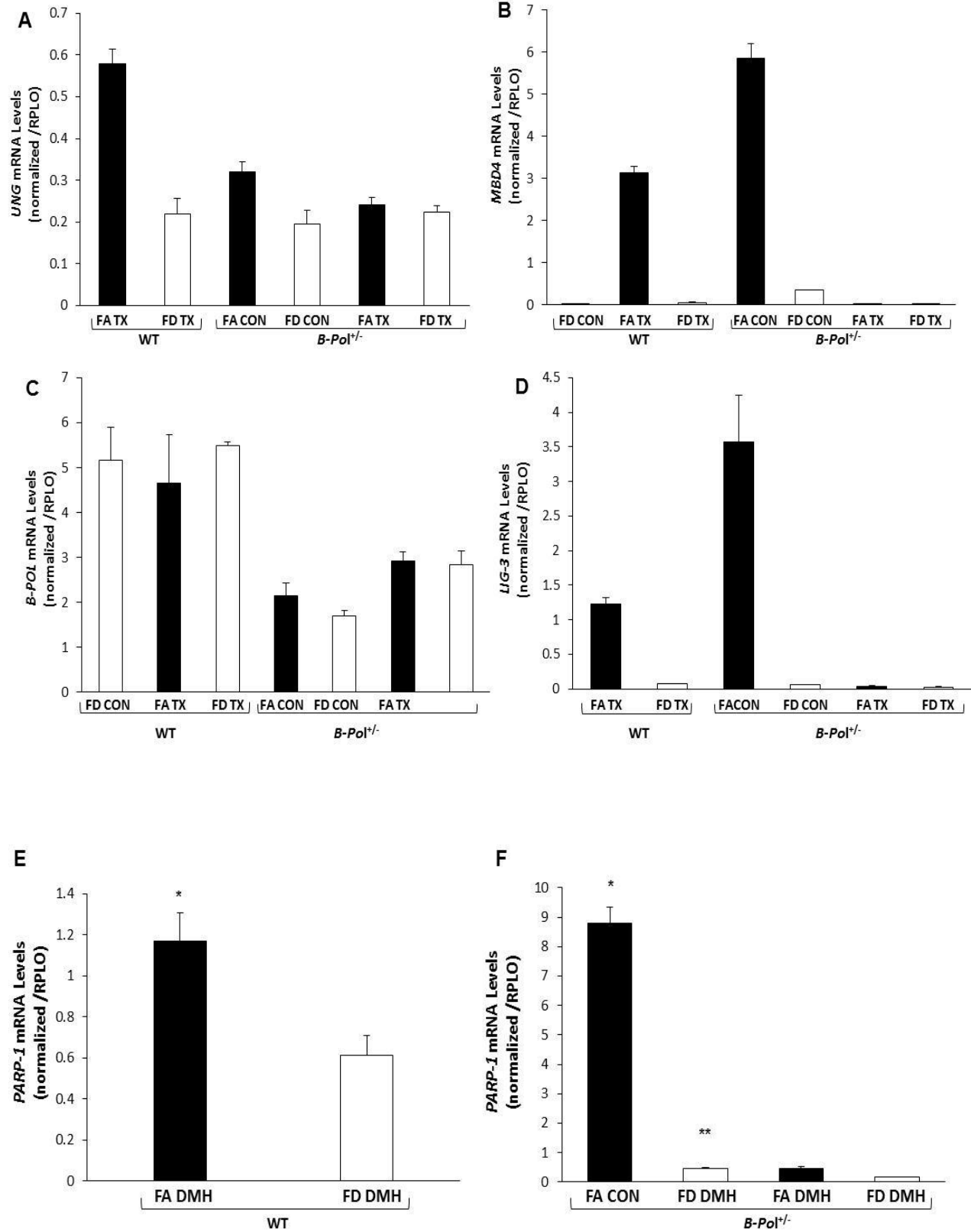
Figure 18 *The level of APE/Ref-1 protein in liver nuclear extract from wild type or β-pol haploinsufficient mice on folate adequate or folate deficient diets treated 24-h with DMH.* Protein expression was determined by Western blot analysis. The level of APE/Ref-1 protein was normalized based on the amount of protein loaded on each gel. The I.D.V. (integrated density value) corresponding to the level of APE/Ref-1 protein was quantified by the BioRad Molecular Imager® System. *A,* wild-type. *B, β-pol$^{+/-}$* animals. Significant differences at $p < 0.05$.

Figure 18

A

Level of *Ape/Ref-1* Protein (I.D.V. per ug protein)

FA DMH   FD DMH

WT

B

Level of *Ape/Ref-1* Protein (I.D.V. per ug protein)

FA CON   FD CON   FA DMH   FD DMH

B-Pol^{+/-}

Figure 19 *Effect of folate deficiency on gene expression in liver in response to alkylation damage in 24-h DMH-treatment in wild type and β-pol haploinsufficient mice.* Transcripts were quantified using real-time PCR and normalized to *Rplo*. *A*, MPG mRNA expression. *B*, MGMT mRNA expression. FA: Folate adequate; FD: folate deficient. Significant differences at $p < 0.05$.
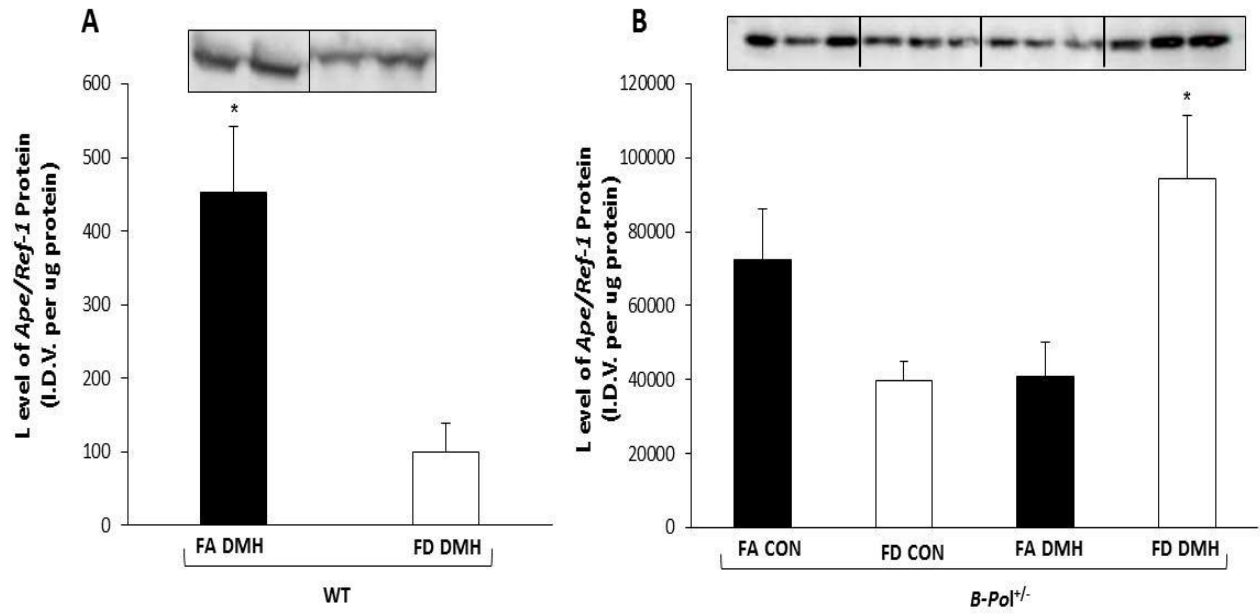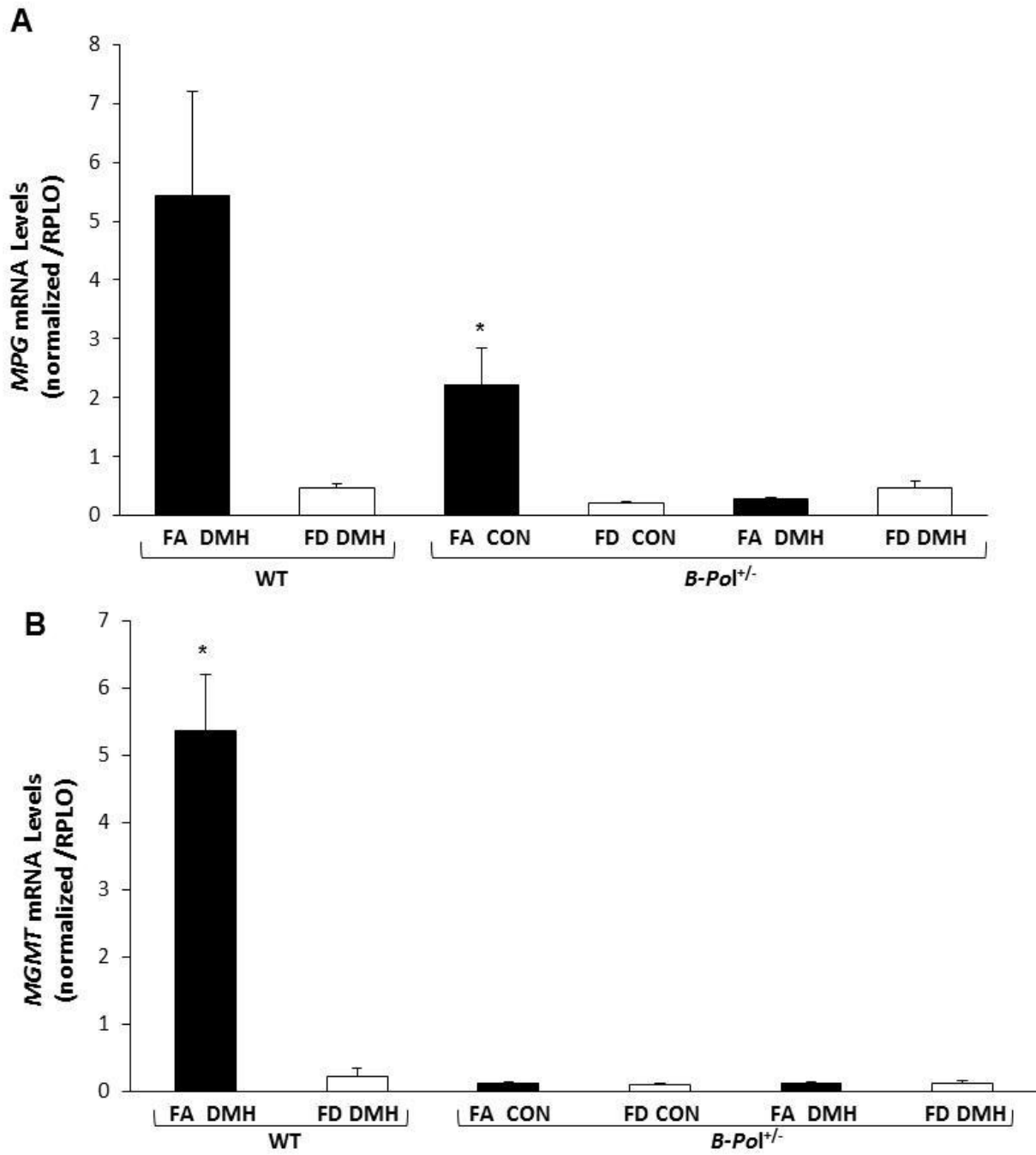
Figure 19

Figure 20 *Analysis of DNA damage in response to folate deficiency and 24-h DMH treatment in liver of wild type and β-pol haploinsufficient mice.* *A*, Levels of AP sites as determined by the ASB assay. DNA was isolated from liver extracts and the levels of aldehydic DNA lesion (ADLs) was measured by the ASB assay as described in "Materials and Methods". DNA was blocked with methoxyamine, probed with biotinylated ARP, and immobilized via vacuum filtration onto a nitrocellulose membrane. Bands were visualized and quantified using the BioRad Molecular Imager® System and data are expressed as I.D.V. per ug DNA loaded. *B*, Level of single-strand breaks (SSBs) was determined using the Fast micromethod of SSB detection as described in materials and methods. Significant differences at $p < 0.05$.

Figure 20

A

B

Figure 21 *Effect of folate deficiency and 24-h DMH on apoptosis pathways in liver of wild type and β-pol haploinsufficient mice.* *A*, Casp-3 mRNA expression. Transcripts were quantified using real-time PCR and normalized to *Rplo*. *B,* Casp-3 activity assay by EnzChek Molecular Probes was used to detect apoptosis in liver cell extracts in folate adequate and folate deficient wild type and *β-pol* haploinsufficient mice. Arg-Glu-Val-Asp-AMC substrate specific proteolytic cleavage by Casp-3 is measured by fluorescence. Fluorescent product is monitored by a fluorescent microplate reader. Results are expressed as fluorescent units (FlU) at 440nm. Significant differences at $p<0.05$.

Figure 21

Figure 22 *Effect of folate deficiency and long-term DMH treatment on UNG mRNA expression in wild type and β-pol haploinsufficient mice.* UNG mRNA expression from livers of C57Bl/6 wild type and *β-pol* haploinsufficient mice as determined by real-time PCR and normalized to RPLO. FA: Folate adequate; FD: folate deficient. Significant differences at p<0.05.
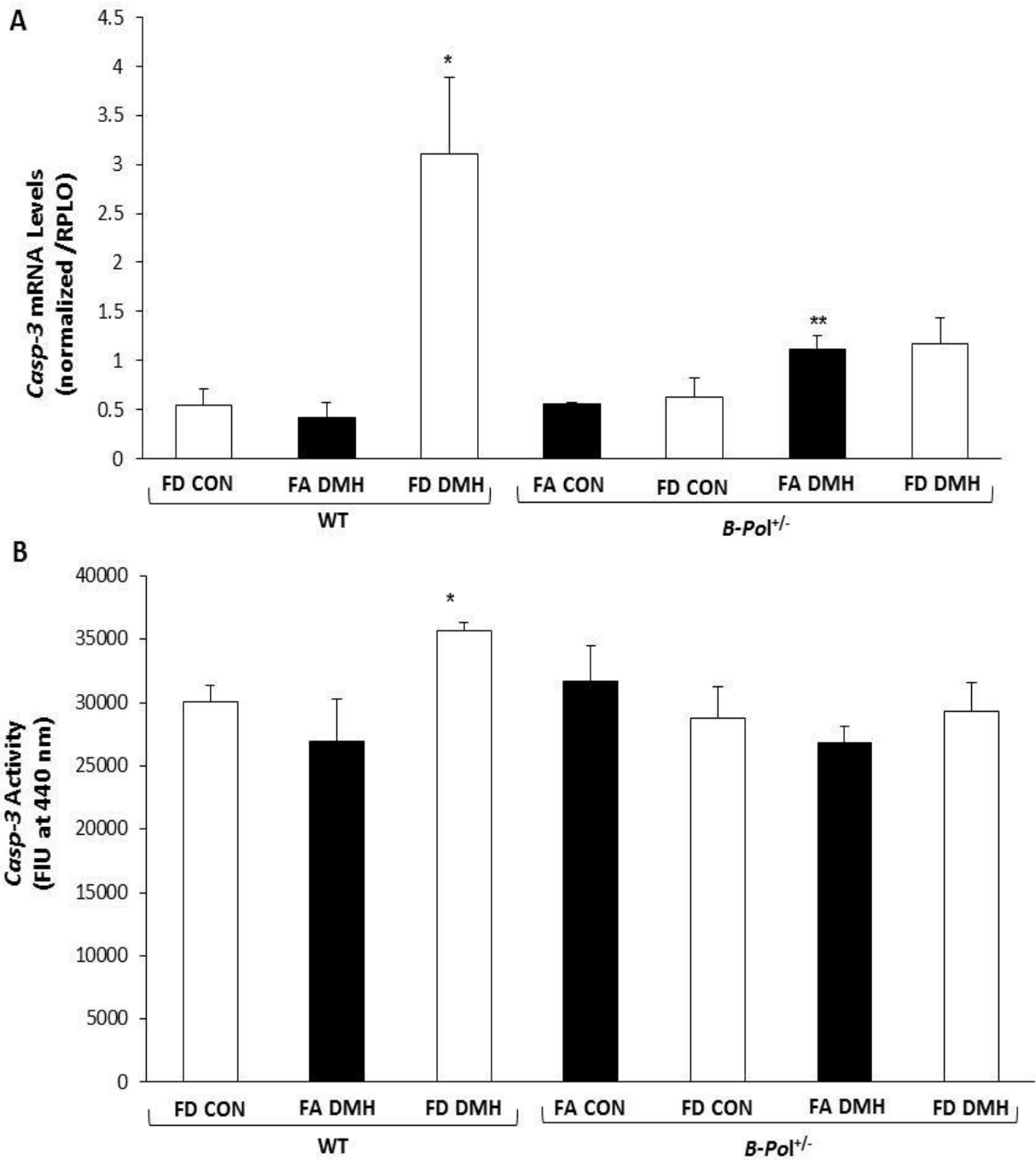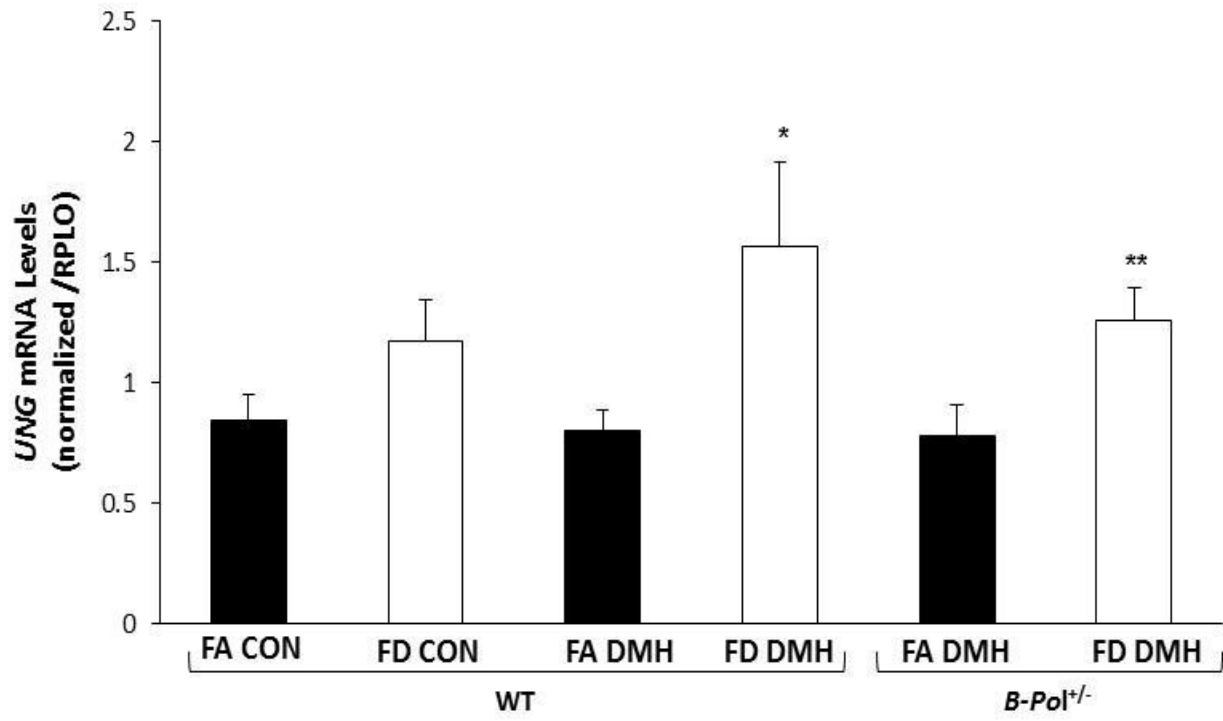
Figure 22

Figure 23 *Effect of folate deficiency and long-term DMH treatment on Uracil levels and UDG activity in liver from wild type and β-pol haploinsufficient mice.* *A*, DNA from liver was isolated as described in "Materials and Methods". DNA was blocked with methoxyamine, treated with UDG, probed with biotinylated ARP, and immobilized via vacuum filtration onto a nitrocellulose membrane. Bands were visualized and quantified using the BioRad Molecular Imager® System and data are expressed as I.D.V. per ug DNA used. *B*, Assessment of UDG activity by ability to excise uracil was performed as described in "Materials and Methods". 5'-end labeled uracil-containing oligo was incubated in 5ug liver extract and separation of substrate and reaction products were separated on a 20% denaturing sequencing gel. Glycosylase activity, indicated by presence of an 11-mer band, was visualized and quantified using the BioRad Molecular Imager® System and calculating the relative amount of the 11-mer oligonucleotide product with the unreacted 30-mer substrate (product/product + substrate). Results are expressed as I.D.V. per ug protein. FA: Folate adequate; FD: folate deficient. Significant differences at $p < 0.05$.

Figure 23

A
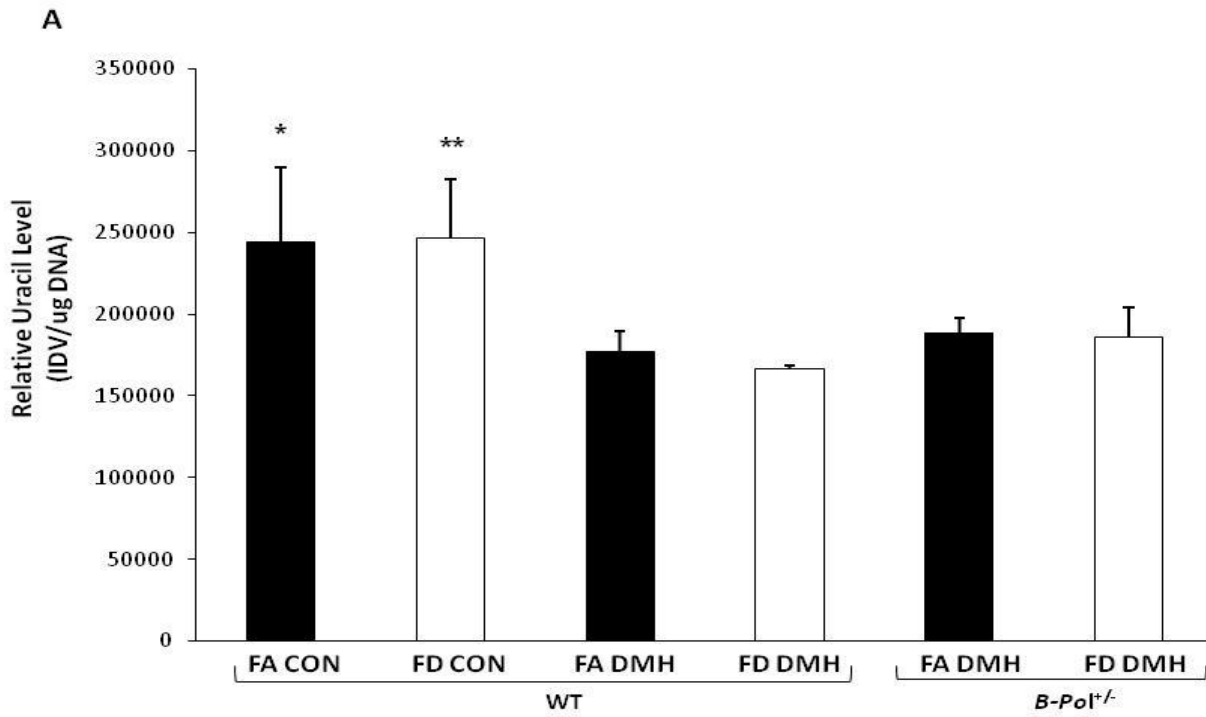
B
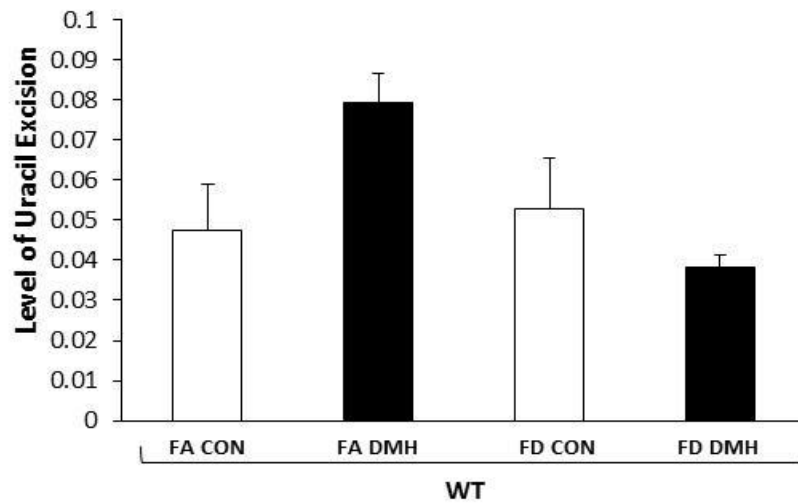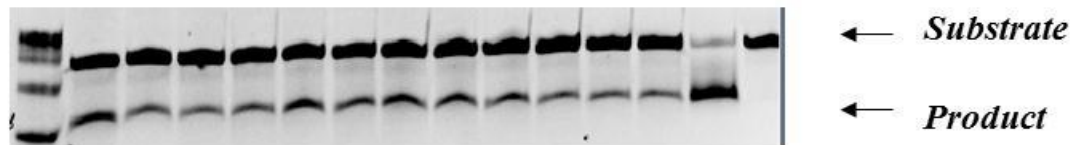
Figure 24 *Effect of folate deficiency and long-term DMH treatment on β-pol mRNA expression and base excision repair capacity in liver from wild type mice*. *A*, *β-pol* mRNA expression from livers of C57Bl/6 wild-type mice as determined by real-time PCR and normalized to RPLO. *B*, Repair activity was analyzed by incubation of nuclear liver extract with G:U mismatch oligo and treatment with HpaII restriction endonuclease. Substrate and reaction products were separated on a sequencing gel and visualized and quantified with BioRad Molecular Imager® System and repair activity was assessed by appearance of a 16-mer fragment. Results are expressed as I.D.V per ug protein. FA: Folate adequate; FD: folate deficient.

Figure 24
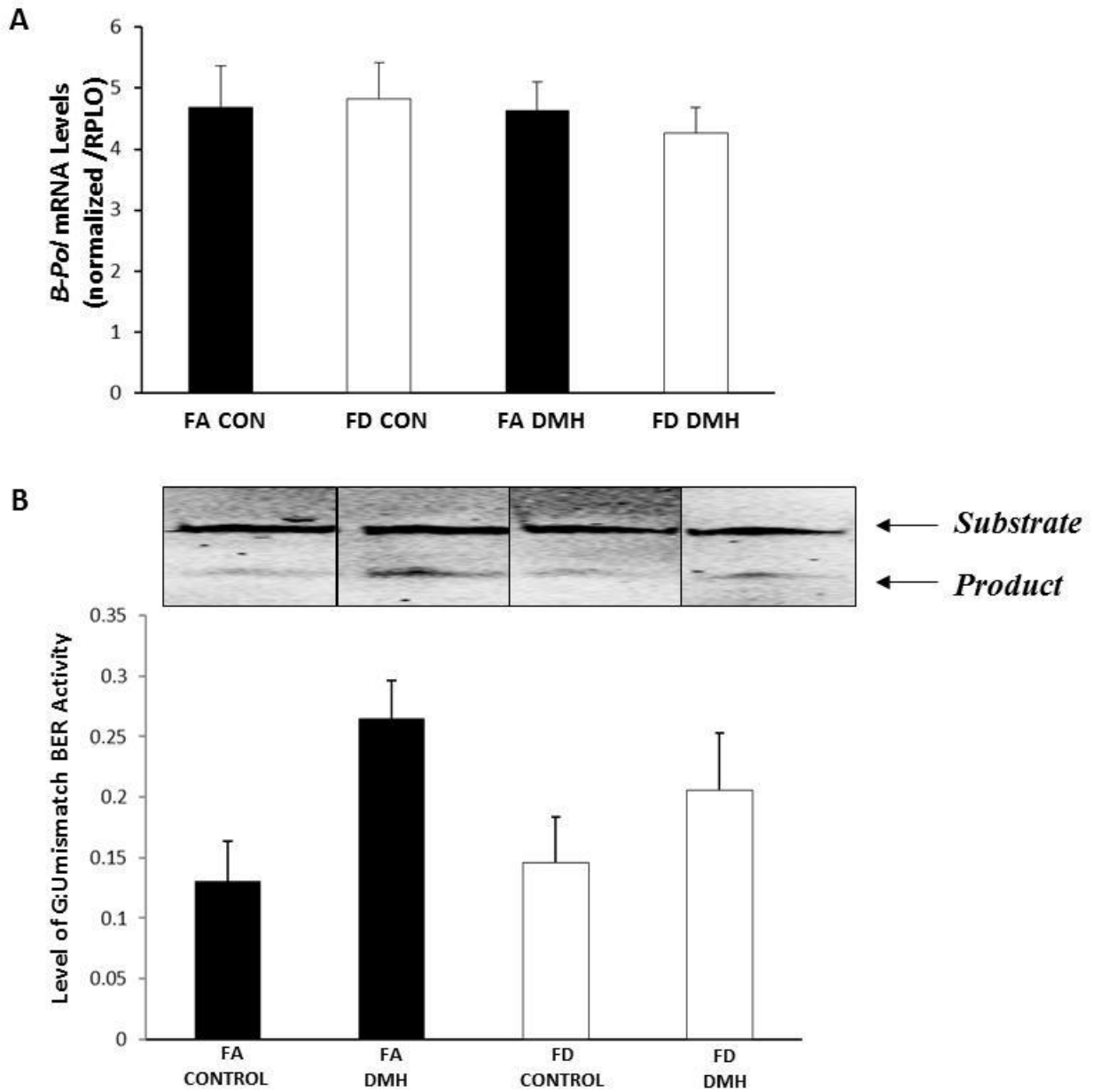
Figure 25 *Effect of folate deficiency on gene expression in response to alkylation damage in long-term DMH-treated wild type and β-pol haploinsufficient mice.* Transcripts were quantified using real-time PCR and normalized to *Rplo.* *A*, MPG mRNA expression. *B*, MGMT mRNA expression. FA: Folate adequate; FD: folate deficient.

Figure 25

A

B
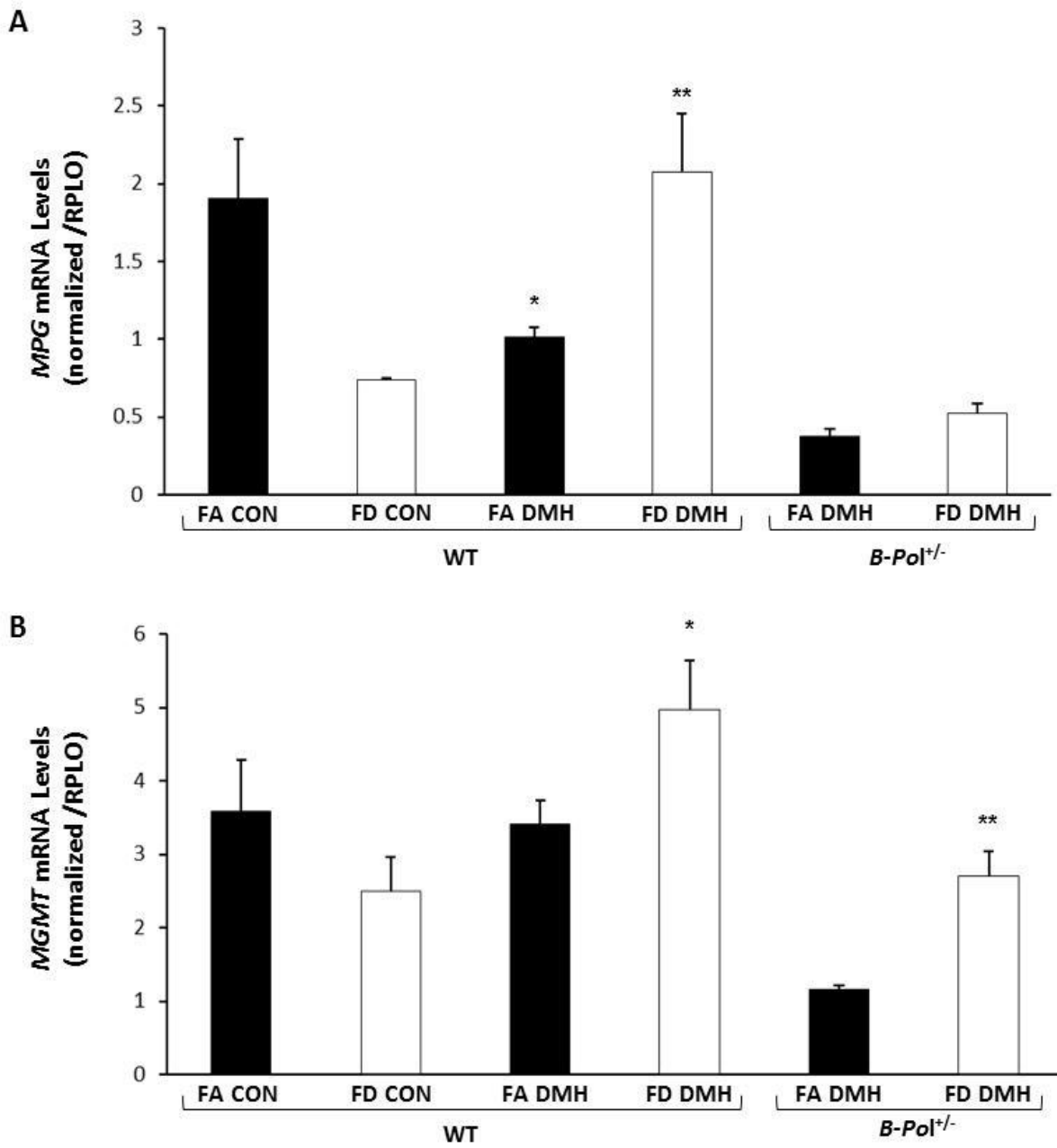
Figure 26 *Analysis of DNA damage in response to folate deficiency and long-term DMH treatment in liver of wild type and β-pol haploinsufficient mice*. *A*, Levels of AP sites as determined by the ASB assay. DNA was isolated from liver extracts and the levels of aldehydic DNA lesion (ADLs) was measured by the ASB assay as described in "Materials and Methods". DNA was blocked with methoxyamine, probed with biotinylated ARP, and immobilized via vacuum filtration onto a nitrocellulose membrane. Bands were visualized and quantified using the BioRad Molecular Imager® System and data are expressed as I.D.V. per ug DNA loaded. *B*, Level of single-strand breaks (SSBs) was determined using the Fast micromethod of SSB detection as described in materials and methods. Significant differences at $p < 0.05$.

Figure 26

A

B

Figure 27 Effect *of folate deficiency and long-term DMH treatment on apoptosis pathways in liver of wild type and β-pol haploinsufficient mice. A*, Casp-3 mRNA expression. Transcripts were quantified using real-time PCR and normalized to *Rplo. B,* Casp-3 activity assay by EnzChek Molecular Probes was used to detect apoptosis in liver cell extracts in folate adequate and folate deficient wild type and *β-pol* haploinsufficient mice. Arg-Glu-Val-Asp-AMC substrate specific proteolytic cleavage by Casp-3 is measured by fluorescence. Fluorescent product is monitored by a fluorescent microplate reader. Results are expressed as fluorescent units (FlU) at 440nm. FA: Folate adequate; FD: folate deficient. Significant differences at p<0.05.

Figure 27
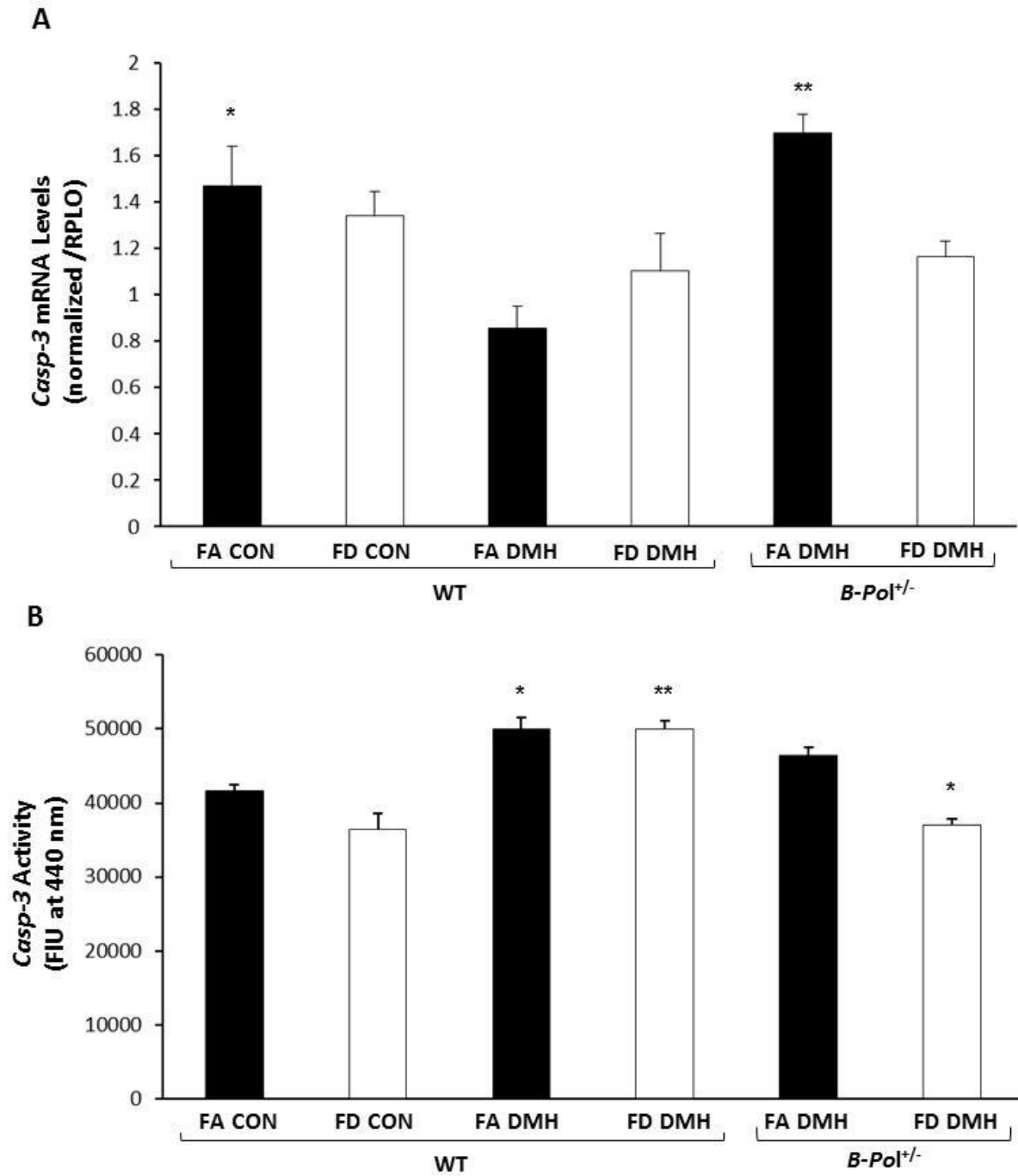
Figure 28 *Effect of folate deficiency and 24-h DMH treatment on expression of BER and DNA repair genes in mucosa of wild type and β-pol haploinsufficient mice.* Transcripts were quantified using real-time PCR and normalized to *Rplo*. A, *UNG* mRNA expression normalized against *Rplo*. B, *MBD-4* mRNA expression normalized to *Rplo*. C, *MPG* mRNA expression normalized to *Rplo*. D, *MGMT* mRNA expression normalized to *Rplo*. E, *LIG-3* mRNA expression normalized to *Rplo*. F, *PARP-1* mRNA expression normalized to *Rplo*. G, *CASP-3* mRNA expression normalized to *Rplo*. FA: Folate adequate; FD: folate deficient. Significant differences at $p < 0.05$.

Figure 28

Figure 29 *Effect of folate deficiency and long-term DMH treatment on expression of BER and DNA repair genes in mucosa of wild type and β-pol haploinsufficient mice.* Transcripts were quantified using real-time PCR and normalized to *Rplo*. A, *UNG* mRNA expression normalized against *Rplo*. B, *MPG* mRNA expression normalized to *Rplo*. C, *MGMT* mRNA expression normalized to *Rplo*. D, *CASP-3* mRNA expression normalized to *Rplo*. FA: Folate adequate; FD: folate deficient. Significant differences at p<0.05.

Figure 29
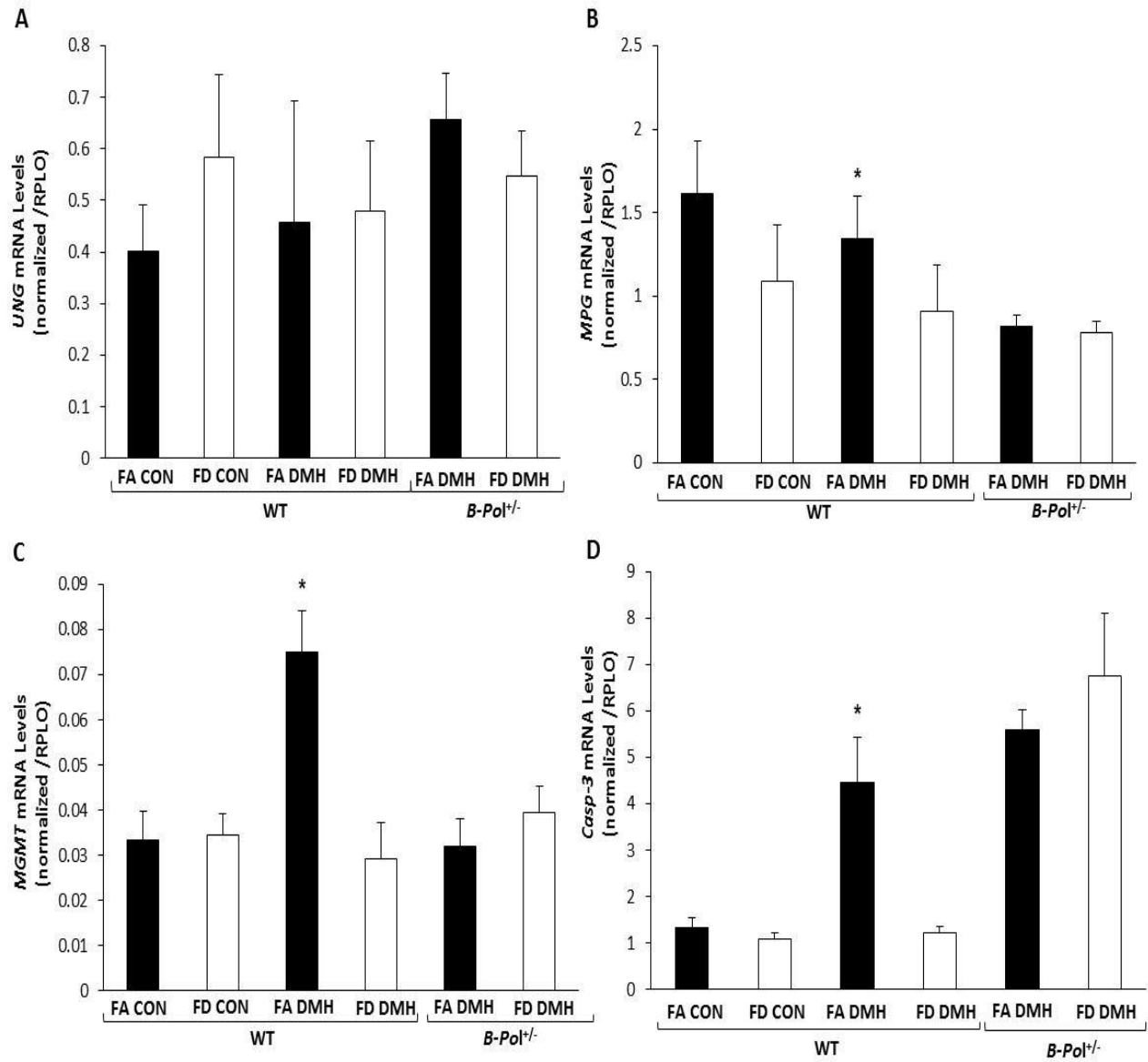
CHAPTER 4: SUMMARY AND FUTURE DIRECTIONS

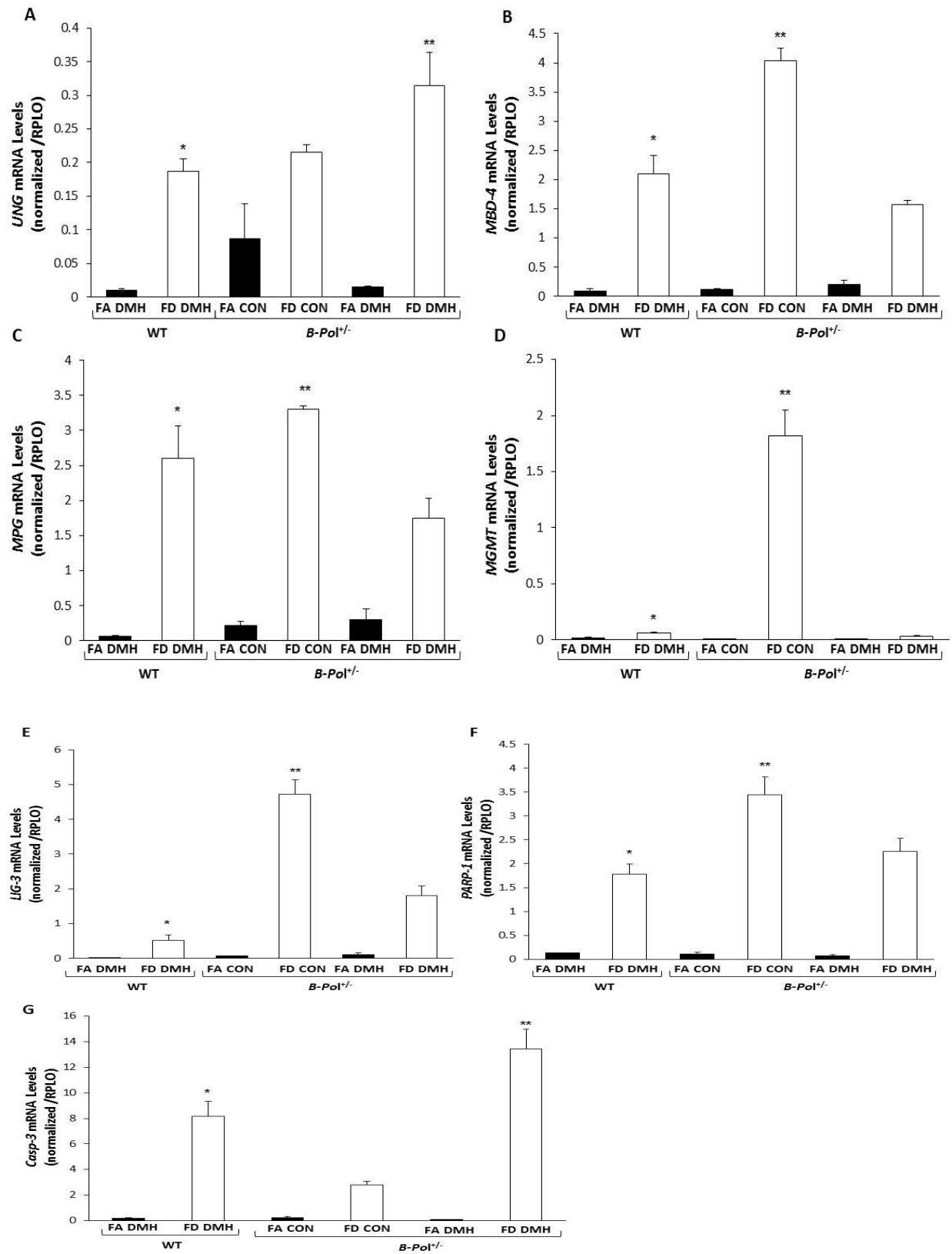Folate deficiency has been implicated in the etiologies of many cancers as described previously. The mechanism of carcinogenesis under folate deficiency is yet undetermined but many studies have shown altered methylation patterns in the promoter regions of proto-oncogenes and tumor suppressor genes resulting in an adverse gene expression profile leading to the initiation and onset of cancer. The pathway in which folate provides precursors for DNA repair and synthesis is another mechanism that could drive an oncogenic phenotype if deregulated by loss of folate substrates entering the cycle. DNA repair mechanisms will also be altered under conditions of reduced purine and thymidine synthesis as occurs with folate deficiency.

In this study, I demonstrate altered gene expression of critical base excision repair genes and DNA repair capacity under folate deficient conditions and this response is exacerbated with treatment of carcinogen. The changes in gene expression appear to be tissue-specific, showing loss of initiation and resolution of repair in liver with acute treatment whereas in mucosa, BER gene expression is induced in response to FD and DMH. One interesting finding is the severe attenuation of MGMT expression observed consistently under FD DMH-treated conditions in liver and colon. The DNA adduct O^6MeG is produced by SN1-type alkylating agents and is a stable lesion causing base mispairing and subsequent point mutations [154]. It is considered a major mutagenic and carcinogenic DNA adduct induced by alkylating agents [155]. The critical function of MGMT in removing O^6MeG lesions has been demonstrated in mice transgenic for human MGMT displaying reduced liver tumors after treatment with MNU [156], protection from lung carcinogenesis [157] and formation of aberrant crypt foci and K-ras mutations in colons of AOM-treated mice [158], [159]. Furthermore, MGMT has been suggested to be a key enzyme

in protection of human sporadic colon cancer, as expression of MGMT is lost in nearly 50% of these cancers [160]. Although the O^6MeG lesion is repaired by separate DNA repair mechanism of direct reversal, BER is responsible for repairing the N-methylation lesions induced by alkylating agents. It has been demonstrated in BER-compromised mice (MPG-null) that N-methyl lesions can persist unrepaired in the DNA [161] and these lesions can give rise to accelerated colon cancer upon treatment with AOM [155].

Given that loss of MGMT expression results in point mutations, commonly occurring in Kras, and that constitutive activation of Ras is a potent driver in cancer cell growth and proliferation, it is important to investigate the downstream effects of this activation. As mentioned, over 30% of cancers have mutant Kras and has recently been shown that these cancers have upregulated expression of DHFR and TS, thereby using the folate pathway and one-carbon metabolism for accelerated DNA synthesis and proliferation. Taking recent evidence that folate supplementation may promote carcinogenesis in conditions of initiated transformation, it is imperative to investigate this mechanism and determine the level of supplementation which results in an adverse effect. The data presented here and from our lab are using folate concentrations of 2mg/kg which is not a level translating to over-supplementation in human subjects. In order to see the effect at levels more closely matching that of the currently folate-supplemented US population, the dose would require 8mg/kg translating to 6-fold of RDA commonly seen in the population [53]. It is also concerning in terms of the routine practice of oncologists prescribing folic acid supplements in conjunction with chemotherapy.

The role of folate in synthesis of DNA precursors is also implicated in growth factor signaling through the Akt-mTOR pathway. mTOR is a serine/threonine protein kinase that regulates cellular anabolic and catabolic processes by sensing nutrient, energy and oxygen

availability [162]. mTOR is present as two distinct complexes called mTOR complex 1 (mTORC1) and mTOR complex 2 (mTOR2) [163]. mTORC1 regulates cell growth and protein synthesis as well as autophagy for utilization of breakdown products. The activity of all translational as well as specifically targeted translation of mRNAs involved in cell growth and proliferation is regulated by mTORC1 and requires high levels of ATP for completion of protein synthesis [162]. As a sensor of nutrient and growth factor levels, mTORC1 also regulates autophagy, the cellular breakdown of proteins and organelles for availability during periods of starvation or limited growth factors [164].

Activation of mTORC1 signaling includes influx of growth factors and amino acids, glucose, oxygen and constitutive signaling from upstream growth factor kinases. Inhibition of mTORC1 signaling occurs in response to nutrient deprivation, depletion of cellular ATP and DNA damage and can trigger autophagy and altered nucleotide metabolism mechanisms [165]. Decreased ATP levels and subsequent increase in AMP/ATP ratios activates AMPK which then suppresses mTORC1kinase activity through phosphorylation of Raptor (regulatory associated protein of mTOR) [166].

Pemetrexed is an anti-folate drug used in the treatment of epithelial cancers that inhibits thymidylate synthase (TS) and also purine synthesis through the enzyme AICART [167, 168]. Upon treatment with pemetrexed, AICART is inhibited resulting in accumulation of an AMP-like intermediate in purine synthesis, ZMP. This in turn triggers activation of AMPK which senses ATP levels for proliferation and cell growth and inhibit mTORC1when energy levels are not sufficient. It has been shown that in addition to inhibiting TS, pemetrexed inhibits purine synthesis, activating AMPK and thus suppressing mTOR signaling [169].

Since folate deficiency also inhibits the *de novo* synthesis of purines our lab did a preliminary investigation of mTOR signaling in response to folate deficiency and DMH treatment. As shown in Figure 30, both mTOR and Raptor protein levels are reduced in response to FD (Fig 30A, B). However, when treated with DMH, a DNA damaging agent, mTOR and Raptor protein expression is induced in FD animals (Fig 30C, D) and in β-*pol*$^{+/-}$ animals the expression of these proteins is further increased (data not shown). These expression analysis were done using total mTOR and Raptor antibodies, as such the phosphorylation of these proteins should be studied to elucidate the activation/inhibition cascade as well as look at targets downstream such as those involved in initiation of protein synthesis.

PARP1 activation requires cellular ATP and it has been demonstrated that activation of PARP1 in response to DNA damage results in cell death due to depletion of ATP [170]. Our labs microarray data from the long-term DMH treated animals showed upregulation of PARP1 mRNA expression in the FD β-*pol*$^{+/-}$ animals, consistent with the finding of increased apoptosis in these animals. However in the acute-treated animals PARP-1 expression is down-regulated in response to DMH in the FD wild-type animals, and even further reduced in the FD knockouts. The mechanism of energy depletion, AMPK activation and modulation of mTOR signaling under the condition of folate deficiency requires further investigation. Additional studies will provide an opportunity to discover molecular regulators in the mTOR pathway and how this is implicated in response to DNA damage and oncogenic transformation.

Figure 30 *The level of mTOR and Raptor protein in liver nuclear extract from wild type mice on folate adequate or folate deficient diets with long-term DMH treatment.* Protein expression was determined by Western blot analysis. *A,* mTOR wild-type untreated. *B,* Raptor wild-type untreated. *C,* mTOR wild-type FA untreated vs. FD DMH treated. *D,* Raptor wild-type FA untreated vs. FD DMH treated. The level of mTOR and Raptor protein was normalized based on the amount of protein loaded on each gel. The I.D.V. (integrated density value) corresponding to the level of protein was quantified by the BioRad Molecular Imager® System.

Figure 30
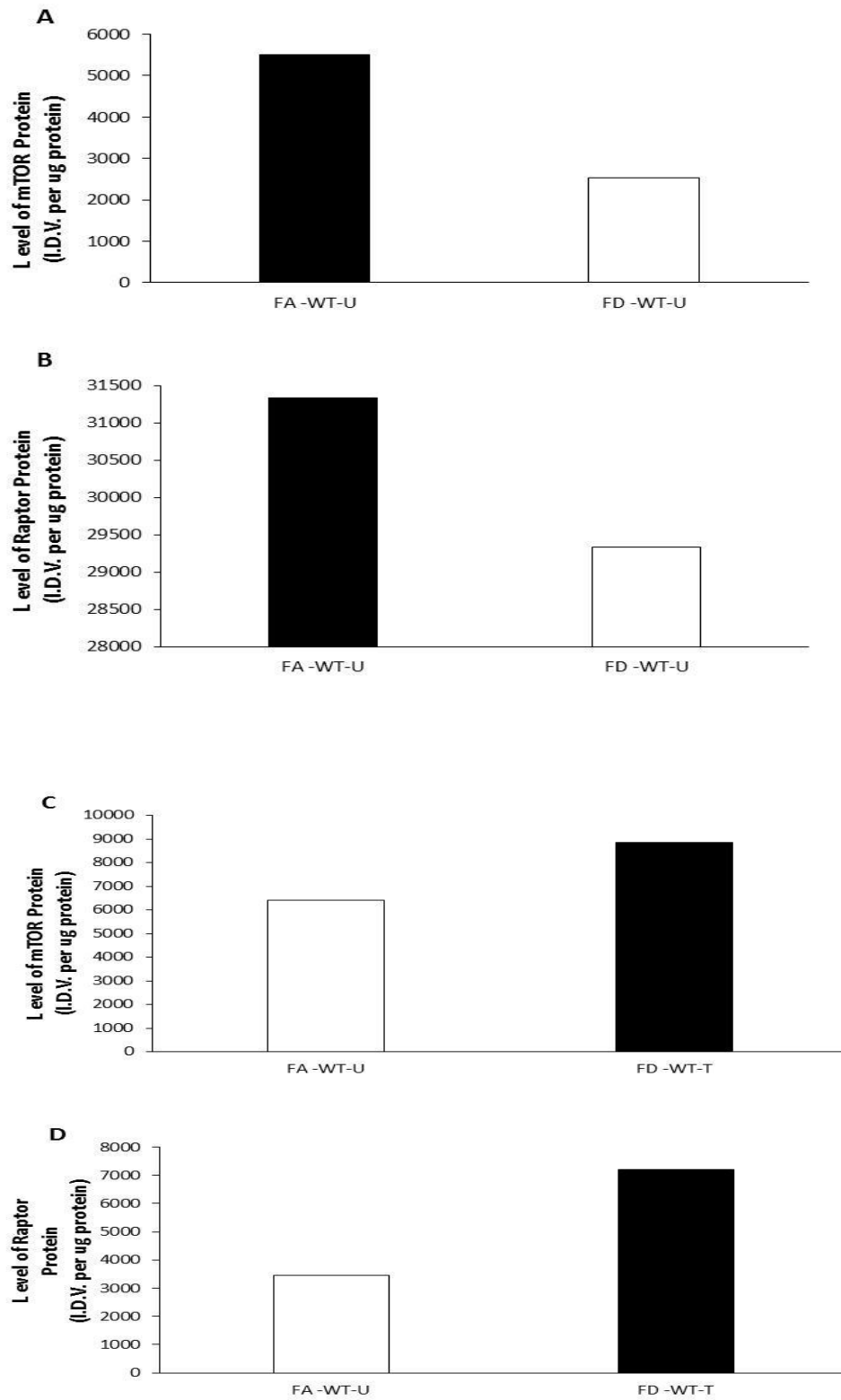
REFERENCES

1.   Lin PH, Appel LJ, Funk K, Craddick S, Chen C, Elmer P, McBurnie MA, Champagne C: **The PREMIER intervention helps participants follow the Dietary Approaches to Stop Hypertension dietary pattern and the current Dietary Reference Intakes recommendations**. *J Am Diet Assoc* 2007, **107**(9):1541-1551.

2.   Esposito K, Maiorino MI, Ceriello A, Giugliano D: **Prevention and control of type 2 diabetes by Mediterranean diet: a systematic review**. *Diabetes Res Clin Pract* 2010, **89**(2):97-102.

3.   Milner JA: **Diet and cancer: facts and controversies**. *Nutr Cancer* 2006, **56**(2):216-224.

4.   Erdmann K, Cheung BW, Schroder H: **The possible roles of food-derived bioactive peptides in reducing the risk of cardiovascular disease**. *J Nutr Biochem* 2008, **19**(10):643-654.

5.   Guil S, Esteller M: **DNA methylomes, histone codes and miRNAs: tying it all together**. *Int J Biochem Cell Biol* 2009, **41**(1):87-95.

6.   Chi P, Allis CD, Wang GG: **Covalent histone modifications--miswritten, misinterpreted and mis-erased in human cancers**. *Nat Rev Cancer* 2010, **10**(7):457-469.

7.   Lee BM, Mahadevan LC: **Stability of histone modifications across mammalian genomes: implications for 'epigenetic' marking**. *J Cell Biochem* 2009, **108**(1):22-34.

8.   vel Szic KS, Ndlovu MN, Haegeman G, Vanden Berghe W: **Nature or nurture: let food be your epigenetic medicine in chronic inflammatory disorders**. *Biochem Pharmacol* 2010, **80**(12):1816-1832.

9.   Kussmann M, Affolter M: **Proteomics at the center of nutrigenomics: comprehensive molecular understanding of dietary health effects**. *Nutrition* 2009, **25**(11-12):1085-1093.

10.   Morton NE: **Into the post-HapMap era**. *Adv Genet* 2008, **60**:727-742.

11.   Davis CD, Milner JA: **Biomarkers for diet and cancer prevention research: potentials and challenges**. *Acta Pharmacol Sin* 2007, **28**(9):1262-1273.

12.   Pogribny IP, Ross SA, Wise C, Pogribna M, Jones EA, Tryndyak VP, James SJ, Dragan YP, Poirier LA: **Irreversible global DNA hypomethylation as a key step in hepatocarcinogenesis induced by dietary methyl deficiency**. *Mutat Res* 2006, **593**(1-2):80-87.

13.   Ross SA: **Evidence for the relationship between diet and cancer**. *Exp Oncol* 2010, **32**(3):137-142.

14.   Xu X, Chen J: **One-carbon metabolism and breast cancer: an epidemiological perspective**. *J Genet Genomics* 2009, **36**(4):203-214.

15.   Giovannucci E, Stampfer MJ, Colditz GA, Hunter DJ, Fuchs C, Rosner BA, Speizer FE, Willett WC: **Multivitamin use, folate, and colon cancer in women in the Nurses' Health Study**. *Ann Intern Med* 1998, **129**(7):517-524.

16.   Sohn KJ, Jang H, Campan M, Weisenberger DJ, Dickhout J, Wang YC, Cho RC, Yates Z, Lucock M, Chiang EP *et al*: **The methylenetetrahydrofolate reductase C677T mutation induces cell-specific changes in genomic DNA methylation and uracil misincorporation: a possible molecular basis for the site-specific cancer risk modification**. *Int J Cancer* 2009, **124**(9):1999-2005.

17.   Arasaradnam RP, Commane DM, Bradburn D, Mathers JC: **A review of dietary factors and its influence on DNA methylation in colorectal carcinogenesis**. *Epigenetics* 2008, **3**(4):193-198.

18.   Turek-Plewa J, Jagodzinski PP: **The role of mammalian DNA methyltransferases in the regulation of gene expression**. *Cell Mol Biol Lett* 2005, **10**(4):631-647.

19.   Balaghi M, Wagner C: **DNA methylation in folate deficiency: use of CpG methylase**. *Biochem Biophys Res Commun* 1993, **193**(3):1184-1190.

20.   James SJ, Pogribny IP, Pogribna M, Miller BJ, Jernigan S, Melnyk S: **Mechanisms of DNA damage, DNA hypomethylation, and tumor progression in the folate/methyl-deficient rat model of hepatocarcinogenesis**. *J Nutr* 2003, **133**(11 Suppl 1):3740S-3747S.

21. Jacob RA, Gretz DM, Taylor PC, James SJ, Pogribny IP, Miller BJ, Henning SM, Swendseid ME: **Moderate folate depletion increases plasma homocysteine and decreases lymphocyte DNA methylation in postmenopausal women**. *J Nutr* 1998, **128**(7):1204-1212.

22. Rampersaud GC, Kauwell GP, Hutson AD, Cerda JJ, Bailey LB: **Genomic DNA methylation decreases in response to moderate folate depletion in elderly women**. *Am J Clin Nutr* 2000, **72**(4):998-1003.

23. Hervouet E, Debien E, Campion L, Charbord J, Menanteau J, Vallette FM, Cartron PF: **Folate supplementation limits the aggressiveness of glioma via the remethylation of DNA repeats element and genes governing apoptosis and proliferation**. *Clin Cancer Res* 2009, **15**(10):3519-3529.

24. Reidy JA: **Role of deoxyuridine incorporation and DNA repair in the expression of human chromosomal fragile sites**. *Mutat Res* 1988, **200**(1-2):215-220.

25. Blount BC, Mack MM, Wehr CM, MacGregor JT, Hiatt RA, Wang G, Wickramasinghe SN, Everson RB, Ames BN: **Folate deficiency causes uracil misincorporation into human DNA and chromosome breakage: implications for cancer and neuronal damage**. *Proc Natl Acad Sci U S A* 1997, **94**(7):3290-3295.

26. Duthie SJ, Hawdon A: **DNA instability (strand breakage, uracil misincorporation, and defective repair) is increased by folic acid depletion in human lymphocytes in vitro**. *FASEB J* 1998, **12**(14):1491-1497.

27. Duthie SJ, Mavrommatis Y, Rucklidge G, Reid M, Duncan G, Moyer MP, Pirie LP, Bestwick CS: **The response of human colonocytes to folate deficiency in vitro: functional and proteomic analyses**. *J Proteome Res* 2008, **7**(8):3254-3266.

28. Kruman, II, Kumaravel TS, Lohani A, Pedersen WA, Cutler RG, Kruman Y, Haughey N, Lee J, Evans M, Mattson MP: **Folic acid deficiency and homocysteine impair DNA repair in hippocampal**

neurons and sensitize them to amyloid toxicity in experimental models of Alzheimer's disease.
J Neurosci 2002, **22**(5):1752-1762.

29.   Choi SW, Kim YI, Weitzel JN, Mason JB: **Folate depletion impairs DNA excision repair in the colon of the rat**. *Gut* 1998, **43**(1):93-99.

30.   Wilson DM, 3rd, Bohr VA: **The mechanics of base excision repair, and its relationship to aging and disease**. *DNA Repair (Amst)* 2007, **6**(4):544-559.

31.   Seeberg E, Eide L, Bjoras M: **The base excision repair pathway**. *Trends Biochem Sci* 1995, **20**(10):391-397.

32.   Dizdaroglu M: **Base-excision repair of oxidative DNA damage by DNA glycosylases**. *Mutat Res* 2005, **591**(1-2):45-59.

33.   Wood RD, Mitchell M, Sgouros J, Lindahl T: **Human DNA repair genes**. *Science* 2001, **291**(5507):1284-1289.

34.   Maynard S, Schurman SH, Harboe C, de Souza-Pinto NC, Bohr VA: **Base excision repair of oxidative DNA damage and association with cancer and aging**. *Carcinogenesis* 2009, **30**(1):2-10.

35.   Marsin S, Vidal AE, Sossou M, Menissier-de Murcia J, Le Page F, Boiteux S, de Murcia G, Radicella JP: **Role of XRCC1 in the coordination and stimulation of oxidative DNA damage repair initiated by the DNA glycosylase hOGG1**. *J Biol Chem* 2003, **278**(45):44068-44074.

36.   Caldecott KW: **Mammalian single-strand break repair: mechanisms and links with chromatin**. *DNA Repair (Amst)* 2007, **6**(4):443-453.

37.   D'Amours D, Desnoyers S, D'Silva I, Poirier GG: **Poly(ADP-ribosyl)ation reactions in the regulation of nuclear functions**. *Biochem J* 1999, **342 (Pt 2)**:249-268.

38.   Piersen CE, Prasad R, Wilson SH, Lloyd RS: **Evidence for an imino intermediate in the DNA polymerase beta deoxyribose phosphate excision reaction**. *J Biol Chem* 1996, **271**(30):17811-17815.

39. Prasad R, Beard WA, Chyan JY, Maciejewski MW, Mullen GP, Wilson SH: **Functional analysis of the amino-terminal 8-kDa domain of DNA polymerase beta as revealed by site-directed mutagenesis. DNA binding and 5'-deoxyribose phosphate lyase activities**. *J Biol Chem* 1998, **273**(18):11121-11126.

40. Sobol RW, Wilson SH: **Mammalian DNA beta-polymerase in base excision repair of alkylation damage**. *Prog Nucleic Acid Res Mol Biol* 2001, **68**:57-74.

41. Srivastava DK, Berg BJ, Prasad R, Molina JT, Beard WA, Tomkinson AE, Wilson SH: **Mammalian abasic site base excision repair. Identification of the reaction sequence and rate-determining steps**. *J Biol Chem* 1998, **273**(33):21203-21209.

42. Cabelof DC, Raffoul JJ, Nakamura J, Kapoor D, Abdalla H, Heydari AR: **Imbalanced base excision repair in response to folate deficiency is accelerated by polymerase beta haploinsufficiency**. *J Biol Chem* 2004, **279**(35):36504-36513.

43. Knock E, Deng L, Wu Q, Lawrance AK, Wang XL, Rozen R: **Strain differences in mice highlight the role of DNA damage in neoplasia induced by low dietary folate**. *J Nutr* 2008, **138**(4):653-658.

44. Garcia-Crespo D, Knock E, Jabado N, Rozen R: **Intestinal neoplasia induced by low dietary folate is associated with altered tumor expression profiles and decreased apoptosis in mouse normal intestine**. *J Nutr* 2009, **139**(3):488-494.

45. Sanjoaquin MA, Allen N, Couto E, Roddam AW, Key TJ: **Folate intake and colorectal cancer risk: a meta-analytical approach**. *Int J Cancer* 2005, **113**(5):825-828.

46. Kim YI: **Folate and colorectal cancer: an evidence-based critical review**. *Mol Nutr Food Res* 2007, **51**(3):267-292.

47. Van Guelpen B, Hultdin J, Johansson I, Hallmans G, Stenling R, Riboli E, Winkvist A, Palmqvist R: **Low folate levels may protect against colorectal cancer**. *Gut* 2006, **55**(10):1461-1466.

48. Cole BF, Baron JA, Sandler RS, Haile RW, Ahnen DJ, Bresalier RS, McKeown-Eyssen G, Summers RW, Rothstein RI, Burke CA *et al*: **Folic acid for the prevention of colorectal adenomas: a randomized clinical trial**. *JAMA* 2007, **297**(21):2351-2359.

49. Camidge DR, Kono SA, Lu X, Okuyama S, Baron AE, Oton AB, Davies AM, Varella-Garcia M, Franklin W, Doebele RC: **Anaplastic Lymphoma Kinase Gene Rearrangements in Non-small Cell Lung Cancer are Associated with Prolonged Progression-Free Survival on Pemetrexed**. *J Thorac Oncol* 2011, **6**(4):774-780.

50. Pfeiffer CM, Caudill SP, Gunter EW, Osterloh J, Sampson EJ: **Biochemical indicators of B vitamin status in the US population after folic acid fortification: results from the National Health and Nutrition Examination Survey 1999-2000**. *Am J Clin Nutr* 2005, **82**(2):442-450.

51. Pfeiffer CM, Johnson CL, Jain RB, Yetley EA, Picciano MF, Rader JI, Fisher KD, Mulinare J, Osterloh JD: **Trends in blood folate and vitamin B-12 concentrations in the United States, 1988 2004**. *Am J Clin Nutr* 2007, **86**(3):718-727.

52. Mason JB, Dickstein A, Jacques PF, Haggarty P, Selhub J, Dallal G, Rosenberg IH: **A temporal association between folic acid fortification and an increase in colorectal cancer rates may be illuminating important biological principles: a hypothesis**. *Cancer Epidemiol Biomarkers Prev* 2007, **16**(7):1325-1329.

53. Lindzon GM, Medline A, Sohn KJ, Depeint F, Croxford R, Kim YI: **Effect of folic acid supplementation on the progression of colorectal aberrant crypt foci**. *Carcinogenesis* 2009, **30**(9):1536-1543.

54. Song J, Sohn KJ, Medline A, Ash C, Gallinger S, Kim YI: **Chemopreventive effects of dietary folate on intestinal polyps in Apc+/-Msh2-/- mice**. *Cancer Res* 2000, **60**(12):3191-3199.

55. Bird RP: **Role of aberrant crypt foci in understanding the pathogenesis of colon cancer**. *Cancer Lett* 1995, **93**(1):55-71.

56. Choi SW, Mason JB: **Folate and carcinogenesis: an integrated scheme**. *J Nutr* 2000, **130**(2):129-132.

57. Mattson MP, Kruman, II, Duan W: **Folic acid and homocysteine in age-related disease**. *Ageing Res Rev* 2002, **1**(1):95-111.

58. Moat SJ, Lang D, McDowell IF, Clarke ZL, Madhavan AK, Lewis MJ, Goodfellow J: **Folate, homocysteine, endothelial function and cardiovascular disease**. *J Nutr Biochem* 2004, **15**(2):64-79.

59. Giovannucci E: **Epidemiologic studies of folate and colorectal neoplasia: a review**. *J Nutr* 2002, **132**(8 Suppl):2350S-2355S.

60. Duthie SJ, Grant G, Narayanan S: **Increased uracil misincorporation in lymphocytes from folate-deficient rats**. *Br J Cancer* 2000, **83**(11):1532-1537.

61. Libbus BL, Borman LS, Ventrone CH, Branda RF: **Nutritional folate-deficiency in Chinese hamster ovary cells. Chromosomal abnormalities associated with perturbations in nucleic acid precursors**. *Cancer Genet Cytogenet* 1990, **46**(2):231-242.

62. Powers HJ: **Interaction among folate, riboflavin, genotype, and cancer, with reference to colorectal and cervical cancer**. *J Nutr* 2005, **135**(12 Suppl):2960S-2966S.

63. Sharma S, Kelly TK, Jones PA: **Epigenetics in cancer**. *Carcinogenesis* 2010, **31**(1):27-36.

64. Tost J: **DNA methylation: an introduction to the biology and the disease-associated changes of a promising biomarker**. *Mol Biotechnol* 2010, **44**(1):71-81.

65. Holmquist GP: **Endogenous lesions, S-phase-independent spontaneous mutations, and evolutionary strategies for base excision repair**. *Mutat Res* 1998, **400**(1-2):59-68.

66. Hamilton ML, Guo Z, Fuller CD, Van Remmen H, Ward WF, Austad SN, Troyer DA, Thompson I, Richardson A: **A reliable assessment of 8-oxo-2-deoxyguanosine levels in nuclear and**

mitochondrial DNA using the sodium iodide method to isolate DNA. *Nucleic Acids Res* 2001, **29**(10):2117-2126.

67.   Nakae D, Mizumoto Y, Kobayashi E, Noguchi O, Konishi Y: **Improved genomic/nuclear DNA extraction for 8-hydroxydeoxyguanosine analysis of small amounts of rat liver tissue**. *Cancer Lett* 1995, **97**(2):233-239.

68.   Shigenaga MK, Aboujaoude EN, Chen Q, Ames BN: **Assays of oxidative DNA damage biomarkers 8-oxo-2'-deoxyguanosine and 8-oxoguanine in nuclear DNA and biological fluids by high-performance liquid chromatography with electrochemical detection**. *Methods Enzymol* 1994, **234**:16-33.

69.   Adachi S, Zeisig M, Moller L: **Improvements in the analytical method for 8-hydroxydeoxyguanosine in nuclear DNA**. *Carcinogenesis* 1995, **16**(2):253-258.

70.   Cabelof DC, Nakamura J, Heydari AR: **A sensitive biochemical assay for the detection of uracil**. *Environ Mol Mutagen* 2006, **47**(1):31-37.

71.   Kim YI, Shirwadkar S, Choi SW, Puchyr M, Wang Y, Mason JB: **Effects of dietary folate on DNA strand breaks within mutation-prone exons of the p53 gene in rat colon**. *Gastroenterology* 2000, **119**(1):151-161.

72.   Pogribny IP, Muskhelishvili L, Miller BJ, James SJ: **Presence and consequence of uracil in preneoplastic DNA from folate/methyl-deficient rats**. *Carcinogenesis* 1997, **18**(11):2071-2076.

73.   Crott JW, Liu Z, Choi SW, Mason JB: **Folate depletion in human lymphocytes up-regulates p53 expression despite marked induction of strand breaks in exons 5-8 of the gene**. *Mutat Res* 2007, **626**(1-2):171-179.

74.   Fortini P, Pascucci B, Parlanti E, D'Errico M, Simonelli V, Dogliotti E: **8-Oxoguanine DNA damage: at the crossroad of alternative repair pathways**. *Mutat Res* 2003, **531**(1-2):127-139.

75. Chern CL, Huang RF, Chen YH, Cheng JT, Liu TZ: **Folate deficiency-induced oxidative stress and apoptosis are mediated via homocysteine-dependent overproduction of hydrogen peroxide and enhanced activation of NF-kappaB in human Hep G2 cells**. *Biomed Pharmacother* 2001, **55**(8):434-442.

76. Duthie SJ, Grant G, Pirie LP, Watson AJ, Margison GP: **Folate deficiency alters hepatic and colon MGMT and OGG-1 DNA repair protein expression in rats but has no effect on genome-wide DNA methylation**. *Cancer Prev Res (Phila)* 2010, **3**(1):92-100.

77. Bagnyukova TV, Powell CL, Pavliv O, Tryndyak VP, Pogribny IP: **Induction of oxidative stress and DNA damage in rat brain by a folate/methyl-deficient diet**. *Brain Res* 2008, **1237**:44-51.

78. Wilson DM, 3rd, McNeill DR: **Base excision repair and the central nervous system**. *Neuroscience* 2007, **145**(4):1187-1200.

79. Lindahl T: **Keynote: past, present, and future aspects of base excision repair**. *Prog Nucleic Acid Res Mol Biol* 2001, **68**:xvii-xxx.

80. Parikh SS, Mol CD, Hosfield DJ, Tainer JA: **Envisioning the molecular choreography of DNA base excision repair**. *Curr Opin Struct Biol* 1999, **9**(1):37-47.

81. Wilson SH, Kunkel TA: **Passing the baton in base excision repair**. *Nat Struct Biol* 2000, **7**(3):176-178.

82. Sancar A, Lindsey-Boltz LA, Unsal-Kacmaz K, Linn S: **Molecular mechanisms of mammalian DNA repair and the DNA damage checkpoints**. *Annu Rev Biochem* 2004, **73**:39-85.

83. Slupphaug G, Kavli B, Krokan HE: **The interacting pathways for prevention and repair of oxidative DNA damage**. *Mutat Res* 2003, **531**(1-2):231-251.

84. Friedberg (ed.): **DNA Repair and Mutagenesis**, 2 edn. Washington: ASM press; 2006.

85. Costello JF, Plass C: **Methylation matters**. *J Med Genet* 2001, **38**(5):285-303.

86.   Wang Y, Leung FC: **An evaluation of new criteria for CpG islands in the human genome as gene markers**. *Bioinformatics* 2004, **20**(7):1170-1177.

87.   Costello JF, Fruhwald MC, Smiraglia DJ, Rush LJ, Robertson GP, Gao X, Wright FA, Feramisco JD, Peltomaki P, Lang JC *et al*: **Aberrant CpG-island methylation has non-random and tumour-type-specific patterns**. *Nat Genet* 2000, **24**(2):132-138.

88.   Li LC, Dahiya R: **MethPrimer: designing primers for methylation PCRs**. *Bioinformatics* 2002, **18**(11):1427-1431.

89.   Unnikrishnan A, Prychitko TM, Patel HV, Chowdhury ME, Pilling AB, Ventrella-Lucente LF, Papakonstantinou EV, Cabelof DC, Heydari AR: **Folate deficiency regulates expression of DNA polymerase beta in response to oxidative stress**. *Free Radic Biol Med* 2011, **50**(2):270-280.

90.   Hayashi I, Sohn KJ, Stempak JM, Croxford R, Kim YI: **Folate deficiency induces cell-specific changes in the steady-state transcript levels of genes involved in folate metabolism and 1-carbon transfer reactions in human colonic epithelial cells**. *J Nutr* 2007, **137**(3):607-613.

91.   Hitchler MJ, Domann FE: **Metabolic defects provide a spark for the epigenetic switch in cancer**. *Free Radic Biol Med* 2009, **47**(2):115-127.

92.   Mosharov E, Cranford MR, Banerjee R: **The quantitatively important relationship between homocysteine metabolism and glutathione synthesis by the transsulfuration pathway and its regulation by redox changes**. *Biochemistry* 2000, **39**(42):13005-13011.

93.   Duthie SJ, Narayanan S, Sharp L, Little J, Basten G, Powers H: **Folate, DNA stability and colo-rectal neoplasia**. *Proc Nutr Soc* 2004, **63**(4):571-578.

94.   Duthie SJ, Narayanan S, Blum S, Pirie L, Brand GM: **Folate deficiency in vitro induces uracil misincorporation and DNA hypomethylation and inhibits DNA excision repair in immortalized normal human colon epithelial cells**. *Nutr Cancer* 2000, **37**(2):245-251.

95. Melnyk S, Pogribna M, Miller BJ, Basnakian AG, Pogribny IP, James SJ: **Uracil misincorporation, DNA strand breaks, and gene amplification are associated with tumorigenic cell transformation in folate deficient/repleted Chinese hamster ovary cells**. *Cancer Lett* 1999, **146**(1):35-44.

96. Everson RB, Wehr CM, Erexson GL, MacGregor JT: **Association of marginal folate depletion with increased human chromosomal damage in vivo: demonstration by analysis of micronucleated erythrocytes**. *J Natl Cancer Inst* 1988, **80**(7):525-529.

97. Duthie SJ, Narayanan S, Brand GM, Pirie L, Grant G: **Impact of folate deficiency on DNA stability**. *J Nutr* 2002, **132**(8 Suppl):2444S-2449S.

98. Lindahl T: **Suppression of spontaneous mutagenesis in human cells by DNA base excision-repair**. *Mutat Res* 2000, **462**(2-3):129-135.

99. Branda RF, Hacker M, Lafayette A, Nigels E, Sullivan L, Nicklas JA, O'Neill JP: **Nutritional folate deficiency augments the in vivo mutagenic and lymphocytotoxic activities of alkylating agents**. *Environ Mol Mutagen* 1998, **32**(1):33-38.

100. Branda RF, Lafayette AR, O'Neill JP, Nicklas JA: **The effect of folate deficiency on the hprt mutational spectrum in Chinese hamster ovary cells treated with monofunctional alkylating agents**. *Mutat Res* 1999, **427**(2):79-87.

101. Dianov GL, Timchenko TV, Sinitsina OI, Kuzminov AV, Medvedev OA, Salganik RI: **Repair of uracil residues closely spaced on the opposite strands of plasmid DNA results in double-strand break and deletion formation**. *Mol Gen Genet* 1991, **225**(3):448-452.

102. Berger SH, Pittman DL, Wyatt MD: **Uracil in DNA: consequences for carcinogenesis and chemotherapy**. *Biochem Pharmacol* 2008, **76**(6):697-706.

103. Li L, Berger SH, Wyatt MD: **Involvement of base excision repair in response to therapy targeted at thymidylate synthase**. *Mol Cancer Ther* 2004, **3**(6):747-753.

104. Duthie SJ: **Folate and cancer: how DNA damage, repair and methylation impact on colon carcinogenesis**. *J Inherit Metab Dis* 2010.

105. de Boer J, Hoeijmakers JH: **Nucleotide excision repair and human syndromes**. *Carcinogenesis* 2000, **21**(3):453-460.

106. Kowalski M, Przybylowska K, Rusin P, Olszewski J, Morawiec-Sztandera A, Bielecka-Kowalska A, Pietruszewska W, Mlynarski W, Janusz S, Majsterek I: **Genetic polymorphisms in DNA base excision repair gene XRCC1 and the risk of squamous cell carcinoma of the head and neck**. *J Exp Clin Cancer Res* 2009, **28**:37.

107. Duell EJ, Millikan RC, Pittman GS, Winkel S, Lunn RM, Tse CK, Eaton A, Mohrenweiser HW, Newman B, Bell DA: **Polymorphisms in the DNA repair gene XRCC1 and breast cancer**. *Cancer Epidemiol Biomarkers Prev* 2001, **10**(3):217-222.

108. Iwanaga A, Ouchida M, Miyazaki K, Hori K, Mukai T: **Functional mutation of DNA polymerase beta found in human gastric cancer--inability of the base excision repair in vitro**. *Mutat Res* 1999, **435**(2):121-128.

109. Matsuzaki J, Dobashi Y, Miyamoto H, Ikeda I, Fujinami K, Shuin T, Kubota Y: **DNA polymerase beta gene mutations in human bladder cancer**. *Mol Carcinog* 1996, **15**(1):38-43.

110. Dong Z, Zhao G, Zhao Q, Yang H, Xue L, Tan X, Zheng N: **[A study of DNA polymerase beta mutation in human esophageal cancer]**. *Zhonghua Yi Xue Za Zhi* 2002, **82**(13):899-902.

111. Sobol RW, Kartalou M, Almeida KH, Joyce DF, Engelward BP, Horton JK, Prasad R, Samson LD, Wilson SH: **Base excision repair intermediates induce p53-independent cytotoxic and genotoxic responses**. *J Biol Chem* 2003, **278**(41):39951-39959.

112. Sobol RW, Watson DE, Nakamura J, Yakes FM, Hou E, Horton JK, Ladapo J, Van Houten B, Swenberg JA, Tindall KR *et al*: **Mutations associated with base excision repair deficiency and methylation-induced genotoxic stress**. *Proc Natl Acad Sci U S A* 2002, **99**(10):6860-6865.

113. Fry RC, Begley TJ, Samson LD: **Genome-wide responses to DNA-damaging agents**. *Annu Rev Microbiol* 2005, **59**:357-377.

114. Norbury CJ, Hickson ID: **Cellular responses to DNA damage**. *Annu Rev Pharmacol Toxicol* 2001, **41**:367-401.

115. Lewin MH, Bailey N, Bandaletova T, Bowman R, Cross AJ, Pollock J, Shuker DE, Bingham SA: **Red meat enhances the colonic formation of the DNA adduct O6-carboxymethyl guanine: implications for colorectal cancer risk**. *Cancer Res* 2006, **66**(3):1859-1865.

116. Sedgwick B: **Nitrosated peptides and polyamines as endogenous mutagens in O6-alkylguanine-DNA alkyltransferase deficient cells**. *Carcinogenesis* 1997, **18**(8):1561-1567.

117. Hecht SS: **DNA adduct formation from tobacco-specific N-nitrosamines**. *Mutat Res* 1999, **424**(1-2):127-142.

118. Krokan HE, Drablos F, Slupphaug G: **Uracil in DNA--occurrence, consequences and repair**. *Oncogene* 2002, **21**(58):8935-8948.

119. Wilson S, Abbotts J, Widen S: **Progress toward molecular biology of DNA polymerase beta**. *Biochim Biophys Acta* 1988, **949**(2):149-157.

120. Sobol RW, Horton JK, Kuhn R, Gu H, Singhal RK, Prasad R, Rajewsky K, Wilson SH: **Requirement of mammalian DNA polymerase-beta in base-excision repair**. *Nature* 1996, **379**(6561):183-186.

121. Sobol RW, Prasad R, Evenski A, Baker A, Yang XP, Horton JK, Wilson SH: **The lyase activity of the DNA repair protein beta-polymerase protects from DNA-damage-induced cytotoxicity**. *Nature* 2000, **405**(6788):807-810.

122. Trivedi RN, Wang XH, Jelezcova E, Goellner EM, Tang JB, Sobol RW: **Human methyl purine DNA glycosylase and DNA polymerase beta expression collectively predict sensitivity to temozolomide**. *Mol Pharmacol* 2008, **74**(2):505-516.

123. Allen D, Herbert DC, McMahan CA, Rotrekl V, Sobol RW, Wilson SH, Walter CA: **Mutagenesis is elevated in male germ cells obtained from DNA polymerase-beta heterozygous mice**. *Biol Reprod* 2008, **79**(5):824-831.

124. Cabelof DC, Guo Z, Raffoul JJ, Sobol RW, Wilson SH, Richardson A, Heydari AR: **Base excision repair deficiency caused by polymerase beta haploinsufficiency: accelerated DNA damage and increased mutational response to carcinogens**. *Cancer Res* 2003, **63**(18):5799-5807.

125. Ventrella-Lucente LF, Unnikrishnan A, Pilling AB, Patel HV, Kushwaha D, Dombkowski AA, Schmelz EM, Cabelof DC, Heydari AR: **Folate deficiency provides protection against colon carcinogenesis in DNA polymerase beta haploinsufficient mice**. *J Biol Chem* 2010, **285**(25):19246-19258.

126. Srivastava DK, Husain I, Arteaga CL, Wilson SH: **DNA polymerase beta expression differences in selected human tumors and cell lines**. *Carcinogenesis* 1999, **20**(6):1049-1054.

127. Petronzelli F, Riccio A, Markham GD, Seeholzer SH, Stoerker J, Genuardi M, Yeung AT, Matsumoto Y, Bellacosa A: **Biphasic kinetics of the human DNA repair protein MED1 (MBD4), a mismatch-specific DNA N-glycosylase**. *J Biol Chem* 2000, **275**(42):32422-32429.

128. Parsons BL: **MED1: a central molecule for maintenance of genome integrity and response to DNA damage**. *Proc Natl Acad Sci U S A* 2003, **100**(25):14601-14602.

129. Bellacosa A: **Role of MED1 (MBD4) Gene in DNA repair and human cancer**. *J Cell Physiol* 2001, **187**(2):137-144.

130. Millar CB, Guy J, Sansom OJ, Selfridge J, MacDougall E, Hendrich B, Keightley PD, Bishop SM, Clarke AR, Bird A: **Enhanced CpG mutability and tumorigenesis in MBD4-deficient mice**. *Science* 2002, **297**(5580):403-405.

131. Wong E, Yang K, Kuraguchi M, Werling U, Avdievich E, Fan K, Fazzari M, Jin B, Brown AM, Lipkin M *et al*: **Mbd4 inactivation increases Cright-arrowT transition mutations and promotes gastrointestinal tumor formation**. *Proc Natl Acad Sci U S A* 2002, **99**(23):14937-14942.

132. Chen JX, Zheng Y, West M, Tang MS: **Carcinogens preferentially bind at methylated CpG in the p53 mutational hot spots**. *Cancer Res* 1998, **58**(10):2070-2075.

133. Evison BJ, Bilardi RA, Chiu FC, Pezzoni G, Phillips DR, Cutts SM: **CpG methylation potentiates pixantrone and doxorubicin-induced DNA damage and is a marker of drug sensitivity**. *Nucleic Acids Res* 2009, **37**(19):6355-6370.

134. Parsons JL, Dianova, II, Allinson SL, Dianov GL: **Poly(ADP-ribose) polymerase-1 protects excessive DNA strand breaks from deterioration during repair in human cell extracts**. *FEBS J* 2005, **272**(8):2012-2021.

135. Pleschke JM, Kleczkowska HE, Strohm M, Althaus FR: **Poly(ADP-ribose) binds to specific domains in DNA damage checkpoint proteins**. *J Biol Chem* 2000, **275**(52):40974-40980.

136. El-Khamisy SF, Masutani M, Suzuki H, Caldecott KW: **A requirement for PARP-1 for the assembly or stability of XRCC1 nuclear foci at sites of oxidative DNA damage**. *Nucleic Acids Res* 2003, **31**(19):5526-5533.

137. Wilson SH, Beard WA, Shock DD, Batra VK, Cavanaugh NA, Prasad R, Hou EW, Liu Y, Asagoshi K, Horton JK *et al*: **Base excision repair and design of small molecule inhibitors of human DNA polymerase beta**. *Cell Mol Life Sci* 2010, **67**(21):3633-3647.

138. Jelezcova E, Trivedi RN, Wang XH, Tang JB, Brown AR, Goellner EM, Schamus S, Fornsaglio JL, Sobol RW: **Parp1 activation in mouse embryonic fibroblasts promotes Pol beta-dependent cellular hypersensitivity to alkylation damage**. *Mutat Res* 2010, **686**(1-2):57-67.

139. Woodhouse BC, Dianova, II, Parsons JL, Dianov GL: **Poly(ADP-ribose) polymerase-1 modulates DNA repair capacity and prevents formation of DNA double strand breaks**. *DNA Repair (Amst)* 2008, **7**(6):932-940.

140. Choudhary G, Hansen H: **Human health perspective on environmental exposure to hydrazines: a review**. *Chemosphere* 1998, **37**(5):801-843.

141. Goth R, Rajewsky MF: **Persistence of O6-ethylguanine in rat-brain DNA: correlation with nervous system-specific carcinogenesis by ethylnitrosourea**. *Proc Natl Acad Sci U S A* 1974, **71**(3):639-643.

142. Kaina B, van Zeeland AA, de Groot A, Natarajan AT: **DNA repair and chromosomal stability in the alkylating agent-hypersensitive Chinese hamster cell line 27-1**. *Mutat Res* 1990, **243**(3):219-224.

143. Kaina B, Christmann M, Naumann S, Roos WP: **MGMT: key node in the battle against genotoxicity, carcinogenicity and apoptosis induced by alkylating agents**. *DNA Repair (Amst)* 2007, **6**(8):1079-1099.

144. Frosina G, Fortini P, Rossi O, Carrozzino F, Abbondandolo A, Dogliotti E: **Repair of abasic sites by mammalian cell extracts**. *Biochem J* 1994, **304 (Pt 3)**:699-705.

145. Nakamura J, Walker VE, Upton PB, Chiang SY, Kow YW, Swenberg JA: **Highly sensitive apurinic/apyrimidinic site assay can detect spontaneous and chemically induced depurination under physiological conditions**. *Cancer Res* 1998, **58**(2):222-225.

146. Henderson DS: **DNA repair protocols : mammalian systems**, 2nd edn. Totowa, N.J.: Humana Press; 2006.

147. Bergoglio V, Canitrot Y, Hogarth L, Minto L, Howell SB, Cazaux C, Hoffmann JS: **Enhanced expression and activity of DNA polymerase beta in human ovarian tumor cells: impact on sensitivity towards antitumor agents**. *Oncogene* 2001, **20**(43):6181-6187.

148. Bergoglio V, Pillaire MJ, Lacroix-Triki M, Raynaud-Messina B, Canitrot Y, Bieth A, Gares M, Wright M, Delsol G, Loeb LA *et al*: **Deregulated DNA polymerase beta induces chromosome instability and tumorigenesis**. *Cancer Res* 2002, **62**(12):3511-3514.

149. Servant L, Bieth A, Hayakawa H, Cazaux C, Hoffmann JS: **Involvement of DNA polymerase beta in DNA replication and mutagenic consequences**. *J Mol Biol* 2002, **315**(5):1039-1047.

150. Starcevic D, Dalal S, Sweasy JB: **Is there a link between DNA polymerase beta and cancer?** *Cell Cycle* 2004, **3**(8):998-1001.

151. Hegde ML, Hazra TK, Mitra S: **Early steps in the DNA base excision/single-strand interruption repair pathway in mammalian cells**. *Cell Res* 2008, **18**(1):27-47.

152. Castagnola P, Giaretti W: **Mutant KRAS, chromosomal instability and prognosis in colorectal cancer**. *Biochim Biophys Acta* 2005, **1756**(2):115-125.

153. Goellner EM, Grimme B, Brown AR, Lin YC, Wang XH, Sugrue KF, Mitchell L, Trivedi RN, Tang JB, Sobol RW: **Overcoming temozolomide resistance in glioblastoma via dual inhibition of NAD+ biosynthesis and base excision repair**. *Cancer Res* 2011, **71**(6):2308-2317.

154. Swann PF: **Why do O6-alkylguanine and O4-alkylthymine miscode? The relationship between the structure of DNA containing O6-alkylguanine and O4-alkylthymine and the mutagenic properties of these bases**. *Mutat Res* 1990, **233**(1-2):81-94.

155. Wirtz S, Nagel G, Eshkind L, Neurath MF, Samson LD, Kaina B: **Both base excision repair and O6-methylguanine-DNA methyltransferase protect against methylation-induced colon carcinogenesis**. *Carcinogenesis* 2010, **31**(12):2111-2117.

156. Nakatsuru Y, Matsukuma S, Nemoto N, Sugano H, Sekiguchi M, Ishikawa T: **O6-methylguanine-DNA methyltransferase protects against nitrosamine-induced hepatocarcinogenesis**. *Proc Natl Acad Sci U S A* 1993, **90**(14):6468-6472.

157. Liu L, Qin X, Gerson SL: **Reduced lung tumorigenesis in human methylguanine DNA-- methyltransferase transgenic mice achieved by expression of transgene within the target cell**. *Carcinogenesis* 1999, **20**(2):279-284.

158. Zaidi NH, Pretlow TP, O'Riordan MA, Dumenco LL, Allay E, Gerson SL: **Transgenic expression of human MGMT protects against azoxymethane-induced aberrant crypt foci and G to A mutations in the K-ras oncogene of mouse colon**. *Carcinogenesis* 1995, **16**(3):451-456.

159. Wali RK, Skarosi S, Hart J, Zhang Y, Dolan ME, Moschel RC, Nguyen L, Mustafi R, Brasitus TA, Bissonnette M: **Inhibition of O(6)-methylguanine-DNA methyltransferase increases azoxymethane-induced colonic tumors in rats**. *Carcinogenesis* 1999, **20**(12):2355-2360.

160. Lind GE, Thorstensen L, Lovig T, Meling GI, Hamelin R, Rognum TO, Esteller M, Lothe RA: **A CpG island hypermethylation profile of primary colorectal carcinomas and colon cancer cell lines**. *Mol Cancer* 2004, **3**:28.

161. Meira LB, Moroski-Erkul CA, Green SL, Calvo JA, Bronson RT, Shah D, Samson LD: **Aag-initiated base excision repair drives alkylation-induced retinal degeneration in mice**. *Proc Natl Acad Sci U S A* 2009, **106**(3):888-893.

162. Sengupta S, Peterson TR, Sabatini DM: **Regulation of the mTOR complex 1 pathway by nutrients, growth factors, and stress**. *Mol Cell* 2010, **40**(2):310-322.

163. Guertin DA, Sabatini DM: **Defining the role of mTOR in cancer**. *Cancer Cell* 2007, **12**(1):9-22.

164. Klionsky DJ, Cuervo AM, Seglen PO: **Methods for monitoring autophagy from yeast to human**. *Autophagy* 2007, **3**(3):181-206.

165. Peng T, Golub TR, Sabatini DM: **The immunosuppressant rapamycin mimics a starvation-like signal distinct from amino acid and glucose deprivation**. *Mol Cell Biol* 2002, **22**(15):5575-5584.

166. Gwinn DM, Shackelford DB, Egan DF, Mihaylova MM, Mery A, Vasquez DS, Turk BE, Shaw RJ: **AMPK phosphorylation of raptor mediates a metabolic checkpoint**. *Mol Cell* 2008, **30**(2):214-226.

167. Taylor EC, Kuhnt D, Shih C, Rinzel SM, Grindey GB, Barredo J, Jannatipour M, Moran RG: **A dideazatetrahydrofolate analogue lacking a chiral center at C-6, N-[4-[2-(2-amino-3,4-dihydro-4-oxo-7H-pyrrolo[2,3-d]pyrimidin-5- yl)ethyl]benzoyl]-L-glutamic acid, is an inhibitor of thymidylate synthase**. *J Med Chem* 1992, **35**(23):4450-4454.

168. Shih C, Chen VJ, Gossett LS, Gates SB, MacKellar WC, Habeck LL, Shackelford KA, Mendelsohn LG, Soose DJ, Patel VF *et al*: **LY231514, a pyrrolo[2,3-d]pyrimidine-based antifolate that inhibits multiple folate-requiring enzymes**. *Cancer Res* 1997, **57**(6):1116-1123.

169. Rothbart SB, Racanelli AC, Moran RG: **Pemetrexed indirectly activates the metabolic kinase AMPK in human carcinomas**. *Cancer Res* 2010, **70**(24):10299-10309.

170. Tang JB, Goellner EM, Wang XH, Trivedi RN, St Croix CM, Jelezcova E, Svilar D, Brown AR, Sobol RW: **Bioenergetic metabolites regulate base excision repair-dependent cell death in response to DNA damage**. *Mol Cancer Res* 2010, **8**(1):67-79.

ABSTRACT

THE IMPACT OF FOLATE DEFICIENCY ON THE BASE EXCISION REPAIR PATHWAY: ANALYSIS OF ENZYME COORDINATION IN RESPONSE TO DNA DAMAGE AND IMBALANCED REPAIR

by

AMANDA B. PILLING

August 2011

Advisor: Dr. Ahmad R. Heydari

Major: Nutrition and Food Science

Degree: Doctor of Philosophy

The condition of folate deficiency has been implicated in carcinogenesis, with the strongest evidence formulated in colon cancer. The role of folate in DNA repair, DNA synthesis and methylation reactions renders this nutrient an valuable target for studying the onset and progression of cancer. Using molecular techniques to determine gene and protein expression, enzyme activity and methylation status elucidates the mechanism of DNA repair and damage in folic acid deficient animals in response to carcinogen. The findings presented in this study indicate failure to remove and repair damage in the condition of folate deficiency and suggest that the accumulation of DNA base lesions and damage can result in clonogenic selection of initiated cells, driving carcinogenesis.

AUTOBIOGRAPHICAL STATEMENT

In 2000, I received my Bachelors of Science degree majoring in microbiology from Michigan State University. Upon graduation I began working at the University of Michigan Medical School in the Department of Research Pathology. In 2005 I began my graduate work as a Master's student at Wayne State University in the Department of Nutrition and Food Science. I soon changed my status to earn a PhD under the mentorship of Dr. Ahmad Heydari studying the base excision repair pathway and cancer. I am currently in my first year as a post-doctoral fellow at the University of Colorado in Denver in the Department of Medical Oncology.